

# Solar Total Energy Test Facility Project Semiannual Report October 1976 - March 1977

Ben Patterson, Jr., Editor

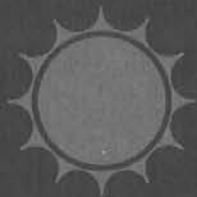
Prepared by Sandia Laboratories, Albuquerque, New Mexico 87115  
and Livermore, California 94550 for the United States Energy Research  
and Development Administration under Contract AT(29-1)-789

Printed August 1977

***When printing a copy of any digitized SAND  
Report, you are required to update the  
markings to current standards.***



Sandia Laboratories  
energy report



Issued by Sandia Laboratories, operated for the United States Energy Research & Development Administration by Sandia Corporation.

---

#### NOTICE

This report was prepared as an account of work sponsored by the United States Government. Neither the United States nor the United States Energy Research & Development Administration, nor any of their employees, nor any of their contractors, subcontractors, or their employees, makes any warranty, express or implied, or assumes any legal liability or responsibility for the accuracy, completeness or usefulness of any information, apparatus, product or process disclosed, or represents that its use would not infringe privately owned rights.

Printed in the United States of America

Available from  
National Technical Information Service  
U. S. Department of Commerce  
5285 Port Royal Road  
Springfield, VA 22161

Price: Printed Copy \$5.50; Microfiche \$3.00

SAND77-0738  
Unlimited Release  
Printed August 1977

SOLAR TOTAL ENERGY TEST FACILITY PROJECT  
SEMIANNUAL REPORT  
October 1976 - March 1977

Edited by  
Ben Petterson, Jr.  
Solar Total Energy Test Facility Division 5712  
Sandia Laboratories  
Albuquerque, NM 87115

ABSTRACT

This report describes the activities of the Sandia Laboratories Solar Total Energy Test Facility Project during the 6-month period, October 1976 through March 1977. Included are highlights of the period, descriptions of the system and its components, including recent modifications, and the results of systems analyses and component testing.

## CONTENTS

	<u>Page</u>
Section I. Introduction	9
Section II. Overview of Activities	15
Highlights	15
Publications and Presentations	18
Section III. Program Description and Status	19
Task 1. Program Management	19
Task 2. System Management	23
2.1 Systems Engineering	23
2.2 Systems Analysis	25
2.3 Test Management	25
Task 3. Collector Subsystems	28
3.1 Operation and Testing	29
3.2 Component and Subsystem Development	38
Task 4. Collector Subsystems Contracted	57
Task 5. High-Temperature Storage Subsystem	79
5.1 Development	79
5.2 Operations	85
Task 6. Turbine/Generator Subsystem	90
Task 7. Heating and Cooling Subsystems	93
Task 8. Collector Module Test Facility	94
8.1 Development and Modification	95
8.2 Operations	98

## FIGURES

<u>Figure</u>		<u>Page</u>
1	Cascaded Solar Total Energy System Schematic	10
2	Projected Solar Total Energy Test Facility	10
3	Solar Total Energy Test Facility Schedule and Milestones	11
4	Solar Total Energy Program Milestones	12
5	Distributed Collector Systems Component and Subsystem Development Project Near Term Milestones	13
6	Project Milestones Through FY77	20
7	Parabolic Trough Solar Thermal/Photovoltaic Bicentennial Display	21
8	Project Staffing	22
9	Solar Total Energy Test Facility with Sandia Collectors	29
10	Sandia Phase IV-B Receiver Design	40
11	Effects of Pressure on Receiver Tube Heat Loss	41
12	Sandwich Structures	45
13	Specular Reflectance of Silver-Plated Brass Samples at 500 nm	48
14	Solar Reflectance Properties of Special Aluminum and Alzak Reflectors	49
15	Specular Reflectance Properties of Aluminized FEP Reflectors	51
16	Hemispherical Reflectance of 3M Scotchcal 5400	53
17	Specular Reflectance Properties of 3M Scotchcal 5400 at 500 nm	55
18	In-Situ Laser Ray Trace Tester	56
19	General Atomic Fixed Mirror Solar Collector	58
20	Annual Movement of Receiver on General Atomic Collector	59
21	Cross-Section of General Atomic Receiver Design	60
22	General Atomic Receiver Tracking Control Schematic	61
23	General Atomic Fluid System Model	61
24	General Atomic Multivariable Control Schematic	62
25	Fluid Temperatures for Purged System with Recirculation and Variable Minimum Flow (60-gal. Buffer Tank)	63
26	Raytheon Parabolic Dish Collector	64
27	Toric Parabola Collector	65
28	Reflector Mirror Mounting Details	65
29	Raytheon Receiver Design	66
30	Sheldahl Solar Linear Array Thermal System (SLATS)	67
31	Pressure vs. Saturation Temperatures for Water	68
32	SLATS Receiver, Plan View and Cross Section	69

FIGURES (cont)

<u>Figure</u>		<u>Page</u>
33	Reflector Bonded to Plywood	70
34	Reflector and Substrate Assembled to Galvanized Sheet Support	71
35	Field Control Logic Flow Chart	72
36	Module Control Logic Flow Chart	74
37	Fluid Loop Schematic	75
38	Fresnel Solar Collector Test Model	76
39	Fresnel Distributed Collector Housing	76
40	Flow Rates to and from Storage	80
41	Status of Multiple Tank Storage at Selected Times of Day	80
42	Thermal Storage Tank Insulation Cost Comparison, Winter Day Cycle, Three Tanks	82
43	Calculated Heat Loss Through Insulation, Intermediate Service Fiberglass Board, Three Tanks, Leg Loss not Included	83
44	Estimated Cost of Multiple-Tank, High-Temperature Storage System	83
45	Percentage Heat Loss vs. Insulation Thickness for a Large System	84
46	Percentage of Heat Lost Through Tank Bases vs. Insulation Thickness Over Walls and Tops	84
47	High Temperature Thermocline Storage Subsystem	85
48	Effect of Pressure on Thermal Conductivity	87
49	Thermocline Scale Model	88
50	Gross Cycle Efficiency vs. Turbine Inlet Pressure	91
51	Gross Cycle Efficiency vs. Condenser Pressure	91
52	Turbine Efficiency vs. Toluene Superheater Out Temperature	93
53	Collector Module Test Facility	94
54	Flow Meter Calibration Container	96
55	Predicted Temperature Gradient in an Asymmetrically Heated Receiver Carrying Therminol	97
56	Test Loop Foundation Work	98
57	Test Modules on Loop No. 1	99
58	Sheldahl Collector Module on Barber Nichols Test Loop	100
59	Simulated Raytheon Receiver Under Test on Sandia Collector	102
60	Acurex-Aerotherm Collector	102
61	CY1977 CMTF Test Schedule	103

TABLES

<u>Table</u>		<u>Page</u>
I	Mechanical Properties of Mirror Support Structures	44
II	Effects of Environmental Exposure on Parabolic Concentrator Structures	46
III	Specular Reflectance Properties at 500 nm	48
IV	Reflectance Properties of Special Alcoa Aluminum Reflectors and Alzak	50
V	Specular Reflectance Values at 10 mrad for the Al-FEP Mirrors	50
VI	Specular Reflectance at 10 mrad Angular Aperture	54
VII	Projected Characteristics of Solar Total Energy System Test Facility	57
VIII	Comparison of Collector Features	78

## SECTION I. INTRODUCTION

The primary objective of the Sandia Solar Total Energy Test Facility Project is to determine and demonstrate the technical and economic feasibility of solar total energy systems for a variety of sites and loads. The following goals have been established to support this primary objective: (1) Construct a solar total energy system which is sufficiently versatile to be used as an engineering evaluation center or test bed for further development of individual components or other solar energy subsystems, (2) Encourage private sector participation in the program and in the development of components and subsystems for solar total energy application, (3) Determine those areas of research and development that offer the greatest payoffs, and (4) Develop and refine analytical techniques capable of evaluating the great number of possible combinations of total energy system configurations.

The Solar Total Energy System, depicted in the block diagram in Figure 1 and as an artist's concept in Figure 2, will operate as follows: A heat transfer fluid (Therminol 66) is heated in the receiver tubes of the solar collectors by reflected and focused solar radiation. This fluid is pumped to the high-temperature storage subsystem. Fluid is extracted from this storage on a demand basis and pumped to the heat exchanger which produces superheated toluene vapor to power the turbine/generator. The boiler can also be operated from a fossil fuel-fired heater to insure continuity of operation during extended cloudy periods. Turbine condenser coolant is pumped to the low-temperature storage tank and becomes the energy source for heating and air-conditioning components of the system.

The overall project consists of five phases (Figure 3) with the work reported in this document being part of Phases IV and V. The project, which began in 1972 with research and exploratory analysis, has progressed to the hardware stage in which the Solar Total Energy System Test Facility is being built to evaluate solar energy subsystems and to provide energy for the 1100 m<sup>2</sup> Solar Project Building.

Phases I, II, and III, which emphasized preliminary studies and designs are complete. Phase IV-A began in July 1974 and lasted through April 1976. It consisted of the design, fabrication, installation, and checkout of the first 200 m<sup>2</sup> collector field quadrant, a high-temperature stratified storage tank, a 32-kW turbine/generator and Therminol-to-toluene heat exchanger, an instrumentation and control subsystem, a cooling tower, the turbine and control building, and all necessary pumps and fluid loops to interconnect these subsystems.

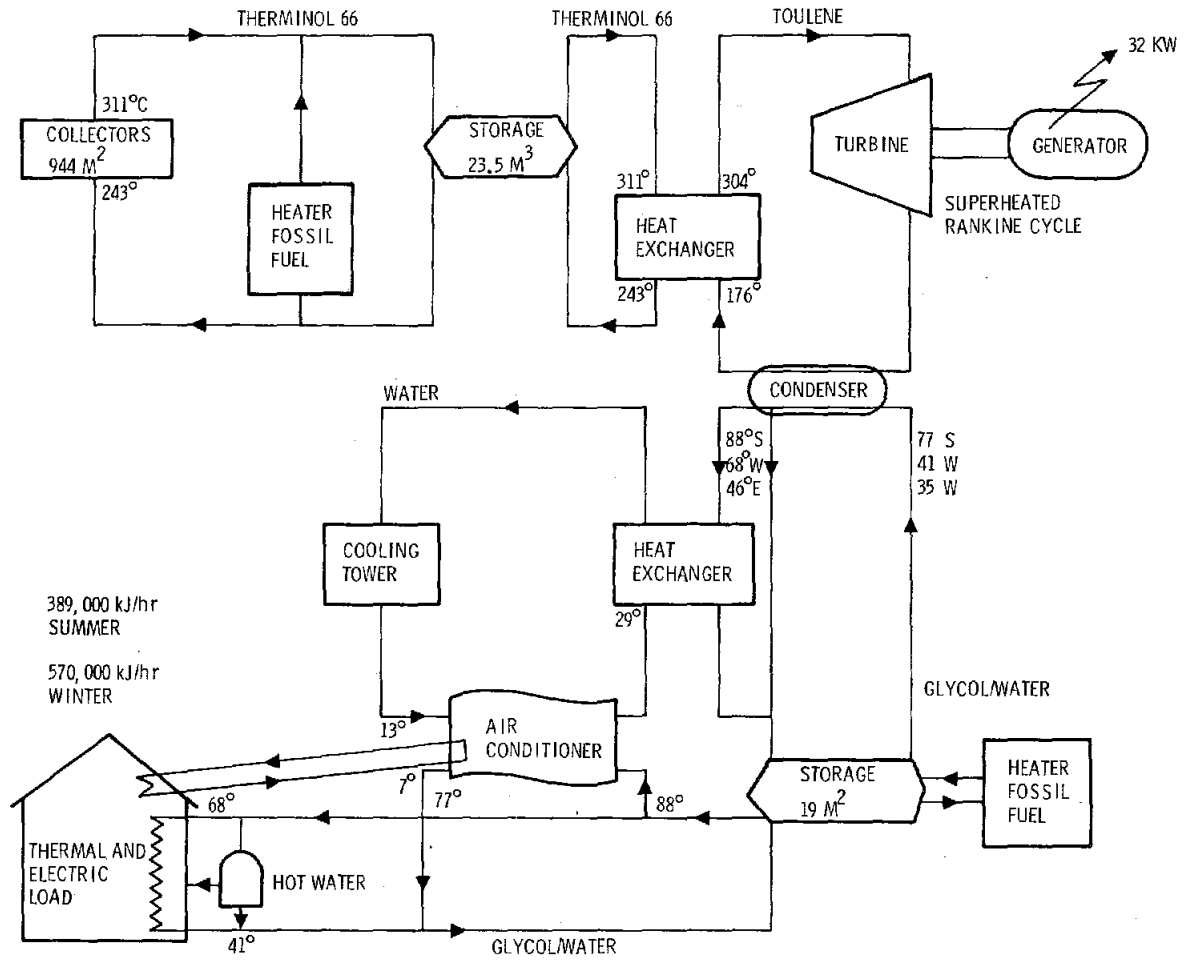


Figure 1. Cascaded Solar Total Energy System Schematic

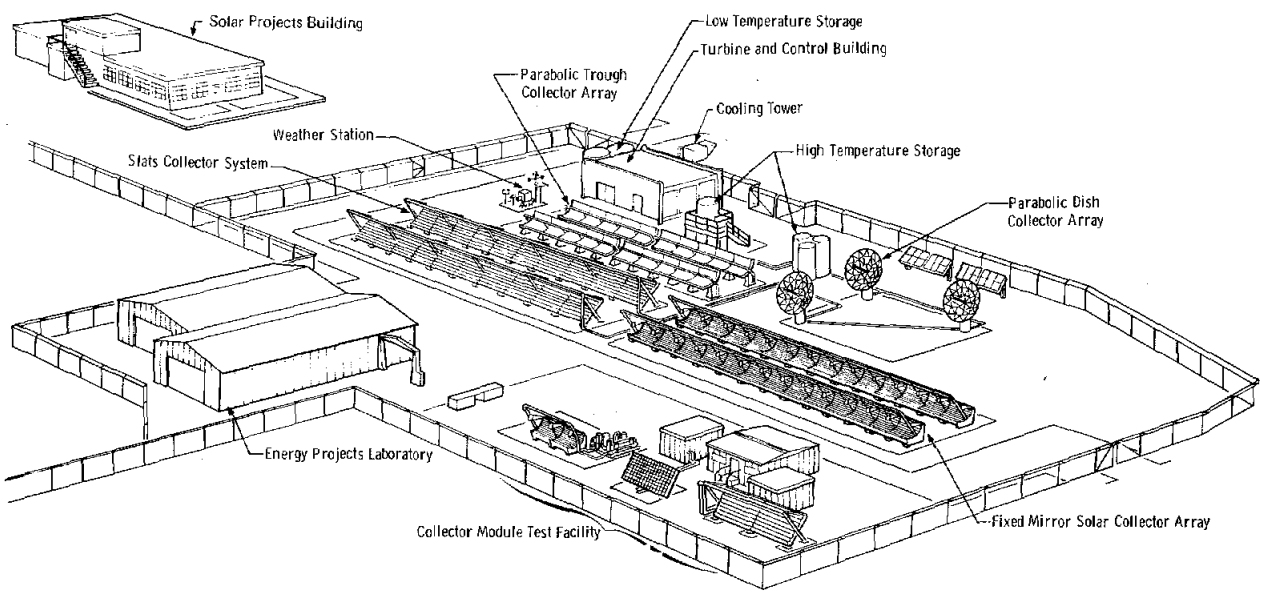
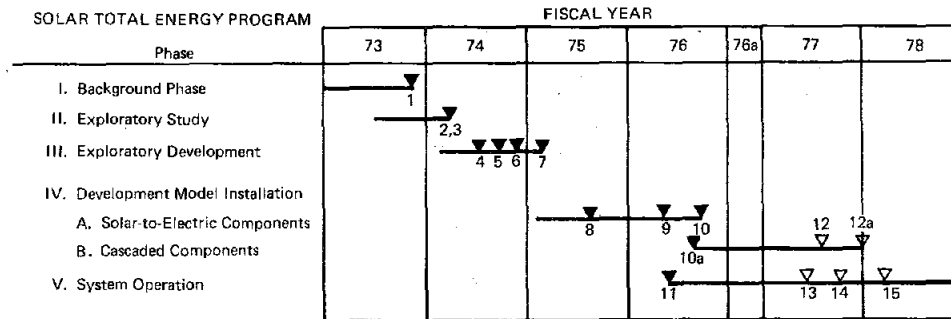


Figure 2. Projected Solar Total Energy Test Facility



Milestones:

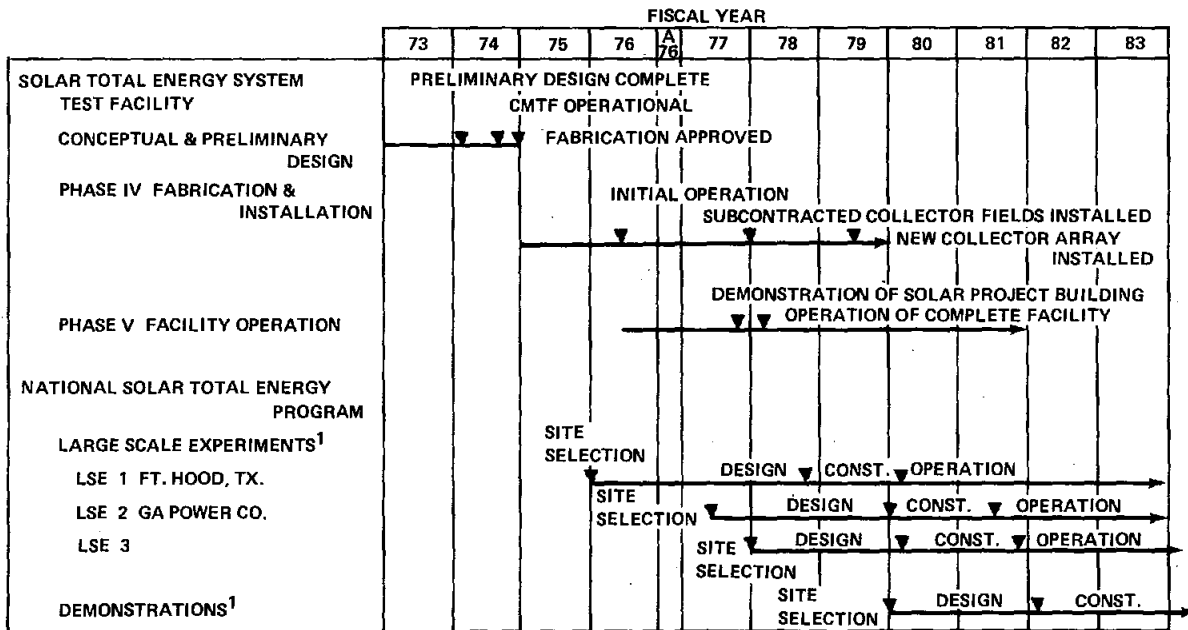
- |                                                                                     |             |
|-------------------------------------------------------------------------------------|-------------|
| 1. Completion of Phase I                                                            | ▼ Completed |
| 2. Preliminary system design complete                                               |             |
| 3. Economic evaluation complete                                                     | ▽ Scheduled |
| 4. Collector evaluation facility complete                                           |             |
| 5. System analysis program (SOLSYS) operational                                     |             |
| 6. Baseline system design complete                                                  |             |
| 7. Phase IV-A proposal submitted                                                    |             |
| 8. Phase IV-A design freeze                                                         |             |
| 9. Partial collector field, storage, and turbine-generator test bed complete        |             |
| 10. Phase IV-A complete, system 100 percent operational                             |             |
| 10a. Subcontracts for collector field subsystems placed                             |             |
| 11. Initial operation of partial Solar Total Energy System Test Facility            |             |
| 12. Low-temperature components of Solar Total Energy System Test Facility installed |             |
| 12a. Subcontracted collector field subsystems completed                             |             |
| 13. System analysis program (SOLSYS) refined and revalidated                        |             |
| 14. Demonstration of Solar Project Building                                         |             |
| 15. Operation of complete Solar Total Energy System Test Facility                   |             |

Figure 3. Solar Total Energy Test Facility Schedule and Milestones

Phase IV-B began in February 1976 and will conclude late in 1977. During Phase IV-B the Solar Total Energy System Test Facility is being expanded to start full operation.

The current capability of collecting  $2 \times 10^6$  kJ per day is being quadrupled to a capacity of about  $8 \times 10^6$  kJ/day. The collector area is being increased from 200 to 825 m<sup>2</sup> (2160 to 8900 ft<sup>2</sup>). High temperature thermal storage capacity will be increased from about 30 minutes to 4 hours. In addition, a subsystem for low-temperature thermal energy storage, a LiBr absorption chiller, heating equipment, plus all necessary additional sensors and controls are being added to the Facility.

Phase V, overlapping Phase IV-A and running concurrently with Phase IV-B, started January 1976. It consists of operating the facility in accordance with a detailed test plan to provide performance data on all subsystems and to accumulate operating and maintenance experience which can provide a basis for the design of large-scale experimental plants and future solar energy systems. During this phase, the electric power, heating, and cooling for the Solar Project Building will also be demonstrated. Figure 4 illustrates how the key system test facility milestones relate to the schedule of some of the early Large-Scale Experiments and Demonstrations within the national Solar Total Energy Program.



<sup>1</sup>There will be several LSE's and Demonstrations. Schedule is for earliest systems.

Figure 4. Solar Total Energy Program Milestones

A Component and Subsystem Development project has been initiated in FY77 as a separate project from the Solar Total Energy Test Facility. Many of the tasks in this project are ongoing efforts which were pursued in previous years in support of the development of the test facility. With the test facility nearing completion, those activities which were sufficiently broad in applicability have been modified in scope so that they support ERDA's National Solar Total Energy, Distributed Collector Development, and Solar Thermal Power Research and Development programs. The major tasks within the Component and Subsystem Development project are: Materials and Process Development, Advanced Collector Development, Distributed Collector R&D, Collector Characterization Techniques Development, and Prime Mover and Storage Development. Figure 5 shows the near-term activities and milestones for the Component and Subsystem Development Project.

TASKS	FY 77						
	MARCH	APRIL	MAY	JUNE	JULY	AUG	SEPT
PROGRAM MANAGEMENT			189 FORM PREPARED ▽	DETAIL FY 78 PROJECTED PLAN ▽			
MATERIAL & PROCESS DEVEL.		RAYTHEON REFLECTOR HAIL QUALIFICATION ▽	ENVIRONMENTAL ASSESSMENT OF REFLECTOR STRUCT. SUMMARY ▽		BLACK CHROME DEVEL. AUTHORIZATION ▽	BLACK CHROME RFP ▽	
ADV. COLLECTOR DEVEL.		INITIAL COLLECTOR DESIGN ▽				DESIGN REVIEW ▽	
DISTRIBUTED COLLECTOR R&D	ORDER COLLECTOR MODULES ▽	ORDER GE & ITEK RECEIVERS ▽	NOVEL COLLECTOR RFP ▽		START COLLECTOR TESTING @ CMTF ▽	ORDER NOVEL COLLECTORS ▽	
COLLECTOR CHARACTERIZATION TECHNIQUES DEVEL.	INITIAL LAB LASER OPERATION ▽				INITIAL LASER OPERATION IN COLLECTOR FIELD ▽		PREL. LASER INSPECTION DATA FROM COLL. FIELD. ▽
PRIME MOVER & STORAGE DEVEL.		LERC PRIM MOVER PLAN REVIEW ▽					

Figure 5. Distributed Collector Systems Component and Subsystem Development Project Near Term Milestones

## SECTION II. OVERVIEW OF ACTIVITIES

### Highlights

The following milestones and significant activities highlight the reporting period:

- Contracts have been placed for three collector field subsystems to be installed in late 1977. Contractors are General Atomic, Raytheon, and Sheldahl (see Task 4).
- Collector field preliminary designs were completed in September 1976. Design freeze took place in February 1977 (see Task 4).
- The remodeling of the Solar Project Building in preparation for its use as a solar total energy load was completed (see Task 7).
- Design of a multiple tank, sensible heat, high-temperature storage system with 3 1/2-hour capacity has been completed and a contract placed for its fabrication and installation (see Task 5).
- A proposed collector evaluation technique is being developed jointly with ERDA/HQ. Inputs from Sandia Livermore and Aerospace Corp. have been coordinated and several development contractors have been asked to participate (see Task 3).
- The charter member of the "resident engineer" project, Robert C. Clarke, has returned to Sun Gas Co. in Dallas, Texas, and is participating in their solar Research and Development effort. Inquiries concerning the resident engineer project are invited (see Task 1).
- An overall test plan for the System Test Facility has been published (see Task 2).
- Interface agreements have been completed with each collector field contractor, and site preparation is underway (see Task 2).

- Expansion of the Collector Module Test Facility (CMTF) has been initiated. Three test stands will be installed and will include capability for testing with high temperature oil (315°C), high temperature water (330°C), and low temperature water (135°C) (see Task 8).
- The high temperature water loop built by Barber-Nichols has been installed at the CMTF and pressure tested (see Task 8).
- A simulated Raytheon receiver was tested for about 150 hours. The test was primarily a high temperature materials compatibility test (see Task 8).
- A series of tests on an Acurex parabolic trough water heating collector was conducted in December 1976 (see Task 8).
- The Solar Total Energy Symposium and the Solar Thermal Power Semi-annual Program Review were held in Albuquerque during the last week in January 1977.
- The Sheldahl SLATS pressurized water collector has been pressure tested and delivered to Sandia and is being prepared for testing at the CMTF. This 37 m<sup>2</sup> (400 ft<sup>2</sup>) module which features a two-pipe plavor receiver will be elevated at outlet temperatures up to 320°C (609°F) (see Task 8).
- The following significant collector field tests were conducted during the reporting period: baseline efficiency tests, optimum focal position, thermal loss determination, all-day baseline performance tests at equinoxes and winter solstice, morning and noon startup, analog and digital tracking system evaluations, and buffer tank and mixing tank control strategy evaluations (see Task 3).
- The design of the in-situ laser ray trace reflector measuring device has been completed and fabrication initiated. A daylight operating capability has been incorporated by changes to the detector scanning electronics (see Task 3).
- High temperature storage testing included thermocline stability tests, and vacuum jacket tests (see Task 5).
- Turbine/generator subsystem testing included solar to fuel switchover, off-design boiler pressure tests, and off-design boiler temperature tests (see Task 6).

- Installation of all low-temperature fluid loop components including low-temperature storage tanks and auxiliary heater have been completed (see Task 7).
- Cold water flow to Solar Project Building has been achieved (see Task 7).
- The parabolic trough solar thermal/photovoltaic solar energy display which had been a bicentennial exhibit at the Washington, DC, Mall was returned to Albuquerque and placed on display at the Albuquerque Museum (see Task 1).
- Collector development contracts have been placed with Del Manufacturing, FMC Corporation, and McDonnell Douglas (see Task 3).
- Receiver development contracts are being negotiated with two companies for a "line cavity" receiver (see Task 3).
- Fixed price contracts for early test collector modules have been placed with Hexcel, Scientific Atlanta, Solar Kinetic Inc., and Soltrax. All these contracts were for four months or better delivery of existing designs (see Task 3).
- An RFP for development of innovative high-temperature concentrating collectors is being prepared following a Sources Sought advertisement in the Wall Street Journal and the Commerce Business Daily (see Task 3).
- A series of temperature and vacuum tests on the Sandia second generation, O-ring sealed, receiver tube has been conducted (see Task 3).
- A total of 1015 visitors to the STETF were hosted during the reporting period (see Task 1).
- Publications and presentations during this reporting period include the following:

## Publications and Presentations

### Publications

S. Thunborg, T. D. Harrison, SAND77-0112, Semiannual Review, ERDA Thermal Power Systems, Distributed Collectors and Research and Development, January 1977, Sandia Laboratories, Albuquerque, NM.

T. D. Harrison, et. al., SAND76-0425, "Solar Collector Module Test Facility, Instrumentation Fluid Loop Number One," January 1977.

T. D. Harrison, SAND76-0662, "Solar Total Energy System Test Facility Project Report, April 1976-September 1976," April 1977, Sandia Laboratories.

R. B. Pettit, "Characterization of the Reflected Beam Profile of Solar Mirror Materials," Solar Engineering Magazine (accepted).

R. B. Pettit and B. L. Butler, SAND77-0111, "Mirror Materials and Selective Coatings," January 1977.

D. M. Mattox, "Optical Materials for Solar Energy Applications," to be published in Optics News, Summer 1976.

D. M. Mattox, "Chemical Aspects of Solar Energy Utilization," to be published in J. Solid State Chemistry, September 1977.

D. M. Mattox, "Applications of Thin Films to Solar Energy Utilization," J. Vac. Sci. Tech. 13, 127 (1976).

### Presentations

T. D. Harrison, "Solar Collector Module Test Facility," Semi-Annual Review, ERDA Thermal Power System, Dispersed Power Systems, Distributed Collectors and Research and Development, January 26-27, 1977, Albuquerque, NM.

S. Thunborg, "Solar Total Energy System Test Facility," Semi-Annual Review, ERDA Thermal Power Systems, Dispersed Power Systems, Distributed Collectors and Research and Development, January 26-27, 1977, Albuquerque, NM.

R. L. Champion, "Component and Subsystem Development Projects," ERDA Solar Thermal Projects Semi-Annual Review, Albuquerque, NM, January 26-27, 1977.

R. B. Pettit and B. L. Butler, "Solar Total Energy Materials Support," ERDA Solar Thermal Projects Semi-Annual Review, January 26-27, 1977, Albuquerque, NM.

J. A. Leonard, "Solar Total Energy System Test Facility and Component/Subsystem Development," Solar Thermal Program Review, January 27, 1977, Albuquerque, NM.

J. A. Leonard, "The Broad Scope of Solar Energy Development," New Mexico State University Adult Education Service, Carlsbad, NM, November 29, 1976.

J. P. Abbin, SAND76-0363, "Rankine Cycle Energy Conversion System Design Considerations for Low and Intermediate Temperature Sensible Heat Sources," October 1976.

D. M. Mattox, "Chemical Aspects of Solar Energy Utilization," presented to the Pacific Conference on Chemistry and Spectroscopy of the Am. Chemical Society, Phoenix, AZ, November 7-10, 1976.

### SECTION III. PROGRAM DESCRIPTION AND STATUS

#### Task 1. Program Management

The Sandia Solar Total Energy Test Facility Project has been organized into a work breakdown structure of tasks and subtasks. This complete structure is shown in the Table of Contents for this section. The detailed status of each program task is described in the subsections which follow.

Figure 6 illustrates the schedule of key activities and major milestones by tasks for the Project during the reporting period and for the remainder of FY77. The Operational Phase of the Project is exemplified by Tasks 2, 3, 5, 6, and 7 in which the primary activities have to do with testing and evaluating the major subsystems of the STESTF. The completion of the fabrication and installation phase is shown in Task 4 in which the collector field is being completed under three different development contracts, Task 5 in which new high temperature storage tanks are being added in order to bring the storage capacity up to the design level of 3.5 hours, and Task 7 in which the low temperature thermal components of the facility are being installed, instrumented and connected to the Solar Projects Building which will serve as an example total energy load for the system. The activities at the CMTF were concentrated on upgrading the facility by adding two additional fluid loops and refurbishing the existing fluid loop. The two new fluid loops were installed to provide a capability for low temperature water and high temperature, high pressure water (332°C and 18.3 MPa). In addition to the facility upgrading, performance tests of three different collector prototypes and a control valve were conducted.

Technology transfer proceeded at a brisk pace during the last six months of FY76. In addition to the publications and presentations listed in the preceding section, an ever-increasing number of visitors were hosted and technical exchanges conducted. During the six-month period, a total of 1015 visitors in 161 groups were given briefings and shown through the Solar Total Energy Test Facility by members of the technical staff and the Community Relations staff. This total contrasts with 620 people in the previous reporting period. In most cases these visitors and groups were also escorted through the Vertical Axis Wind Turbine Facility and through the 5MW Solar Thermal Test Facility. The total included 162 foreign visitors from 17 nations, including Mexico, Canada, Bolivia, Germany, England, Italy, France, Switzerland, Spain, Netherlands, Greece, Israel, Iran, India, Japan, Australia, and West Africa.

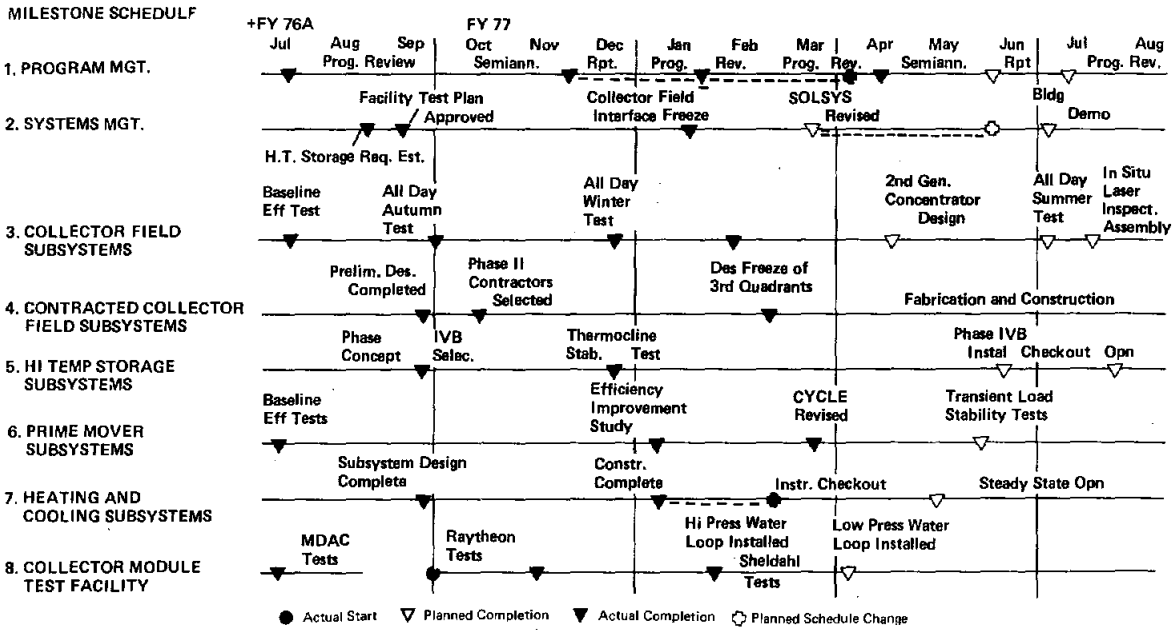


Figure 6. Project Milestones Through FY77

The parabolic trough solar thermal/photovoltaic solar energy display (Figure 7) which had been a Bicentennial exhibit at the Washington, D. C. Mall was returned to New Mexico and put on display at a two-month energy exhibit at the Albuquerque Museum. It has now been returned to Sandia and is being prepared for exhibition at ERDA's Atomic Museum at Kirtland Air Force Base, Albuquerque.

The pilot "resident engineer" project has been completed satisfactorily. Robert C. Clarke, who was with Sandia on temporary assignment from October 1976 to January 1977, has returned to his parent firm, the Sun Gas Company, to form the nucleus of a moderate-sized planning and internal R&D effort in solar energy. Arrangements are being made for the next resident engineer who will start in May 1977. The resident engineer project is a technology transfer technique in which engineers on leave of absence from private companies may reside at Sandia for three to six months and participate in solar or geo-energy projects. Inquiries from interested firms are invited.

Figure 8 illustrates complete program staffing. The technical contributions of these individuals to the Project as well as their written inputs contained in this semiannual status report are gratefully acknowledged.

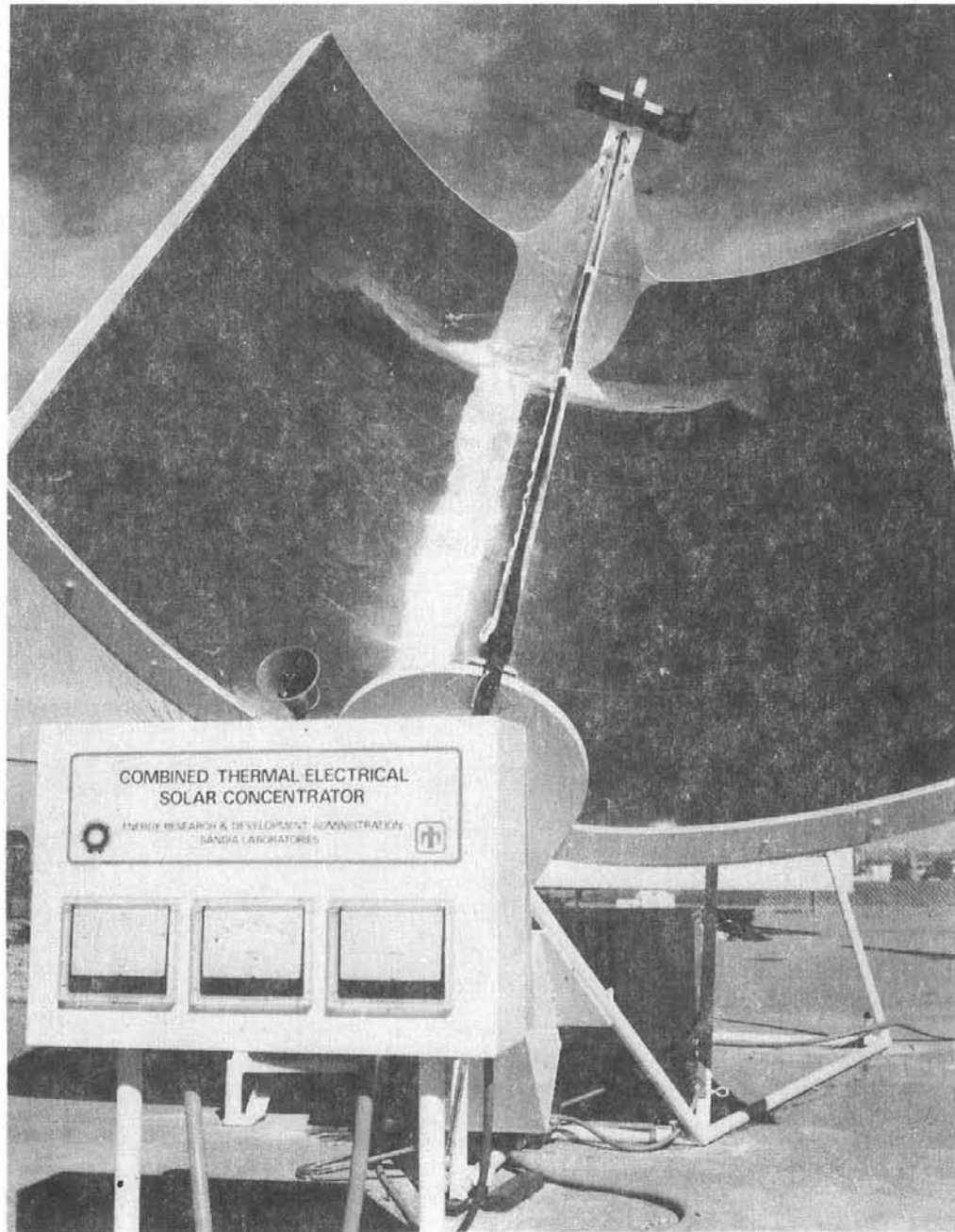


Figure 7. Parabolic Trough Solar Thermal/Photovoltaic Bicentennial Display

Advanced Energy Project Department  
G. E. Brandvold

Solar Total Energy Projects Division

Program Support

J. A. Leonard

System Engineers

R. L. Champion  
T. D. Harrison  
B. J. Petterson  
S. Thunborg  
L. E. Torkelson  
G. W. Treadwell

Technicians

T. J. Bauman  
C. W. Matthews  
G. L. McCoach

EG&G

K. D. McAllister  
H. W. Craig  
G. T. Morin

System Analysis

M. W. Edenburn

Thermal Analysis

C. E. Hickox  
A. C. Ratzel

Data Processing

L. C. Bennett  
W. W. Shurtleff

Turbine Generator

J. P. Abbin  
J. B. Moore

Structural Analysis and Design

J. T. Finger  
P. P. Stirbis

Plant Engineer

C. N. Lowe  
E. E. Rush  
I. N. Humble  
M. H. Wempe  
M. V. Nielsen

Thermal Storage

M. R. Baer  
G. J. Jones  
S. B. Martin  
A. Ortega  
R. A. Randall  
A. W. Reed

Contracted Collector Sub-  
systems

W. H. McCulloch  
R. P. Stromberg

Safety, Fire Prevention,  
Health Physics

J. H. Kesinger  
W. E. Stocum

High Pressure Piping

C. E. Albright  
B. C. Brown  
C. A. Knovorsky  
R. E. Moll  
G. S. Wallace

Theoretical Analysis

F. Biggs  
J. F. Banas

Materials Development

Reflector Structures  
B. L. Butler  
C. B. Frost  
T. R. Guess  
H. R. Sheppard

Reflector Materials

T. M. Meyer  
G. D. Miller  
R. B. Pettit

Receiver Materials

E. K. Beauchamp  
R. S. Berg  
D. M. Mattox  
R. R. Sowell

Testing and Evaluation

J. C. Bushnell  
D. W. Miller  
L. G. Rainhart  
F. Salazar  
W. G. Self  
D. W. Tipping  
D. L. Zamora

Aerodynamics

J. A. Stark  
R. E. Tate

Tracking and Fluid Switching  
Logic

J. W. Hole  
S. M. Kohler  
B. B. Conklin  
E. O. Scussel

Figure 8. Project Staffing

## Task 2. Systems Management

Systems engineering was concentrated on monitoring A & E design for the new high temperature storage subsystem and placing construction contracts.

Due to limited funding, a decision has been made to postpone installation of the Raytheon parabolic dish collector field until FY78. During FY77 one dish will be procured for evaluation at the Collector Module Test Facility.

EG&G personnel have initiated routine test operations with the Solar Total Energy System Test Facility and a series of Letter Test Memos have been issued.

### 2.1 Systems Engineering

A construction contract has been awarded for installation of the high temperature storage and associated fluid transfer system for the three new, contracted collector subsystems. Figure 2 shows the specific area assigned for the high temperature storage and the collector field.

The interface between the high temperature storage system and the three new fields has been established as a bulkhead at the boundary of each contractor's area containing all the mechanical and electrical interface components. Each bulkhead will contain the following:

- Therminol 66 supply and return pipe (76 litre per minute (20 gpm))
- 100 kilopascal gage (15 psig) N<sub>2</sub> line from high temperature storage tank
- Compressed air 684 kilopascal gage (100 psig)
- Control terminal cabinet for control wiring
- Thermocouple terminal cabinet for thermocouple
- Electrical power disconnect switch
- Domestic water
- Valve control air
- Sewer drain

The collector field contractors will have responsibility for installing all items within their designated area, for interconnection to the interface bulkhead and for design and installation of all tracking and performance monitoring systems in the control room.

Efforts have been initiated to design a logic system to control the nine control valves on the three new high temperature storage tanks. These valves determine which tank shall be the supply tank and which shall be the return tank. The logic system monitors incoming fluid temperature, the temperature in each tank, and the amount of fluid in each tank. With these inputs there are over 1000 decisions that must be controlled by the logic system. The logic system will also monitor the total amount of fluid in the system and sound alarms in case of fluid loss.

An access control plan has been determined for the solar test area containing the Solar Total Energy System Test Facility and the Collector Module Test Facility.

A construction contract has been awarded for installation of the necessary equipment. After construction is completed, access will be limited to those with the required three-digit code necessary to dial open the gates. Due to the large number of visitors to the site, over 400 in March, plans are being made for a self-guided tour path through the area for those visitors not requiring a highly technical tour. Initial access for this tour will require appropriate approval.

Consideration has been given to the down-range eye hazard for the new collector field; particularly the General Atomic moving receiver type collector which always has a focal point and cannot be defocused. Initial calculations indicate the most critical time is during early morning or late evening at equinox when the low sun angle can result in more than one sun up to 50 ft. longitudinally down range. For this reason the collector sites have been selected to allow at least 50 ft. to the site parameter fences. All contractors are presently analyzing, in detail, the specific down range hazard for their collectors.

In December a decision was made to do all collector tracking through the computer instead of with the photocell analog system. Testing with the analog tracking indicated it tracked well for short periods of time; but if not continually adjusted, allowed a deviation of more than the required 0.1° accuracy during the day. A program has been initiated to further develop the analog system. Implementation of the computer tracking system required detailed programming solutions to the following problem before all day tracking accuracy was obtained:

- Non-level E/W collectors (0° 45' slope)
- Parallax - collectors located at earth's surface and not at center.
- Refraction - bending of sun's rays at early morning and late evening.

## 2.2 Systems Analysis

A decision has been made to postpone installation of the Raytheon collector field until FY78 due primarily to a lack of funds in FY77, and also to allow more development and testing time for the concept. Instead of a collector field, one Raytheon parabolic dish will be procured for evaluation at the Collector Module Test Facility.

The decision not to fund a full Raytheon collector field in FY77 further aggravates the problem of insufficient collector area to generate 32-kW for 11 hours/day. As discussed in previous reports, the required collector area has increased (primarily due to a 20% lower than planned turbine/generator efficiency from using a turbine/generator system not specifically designed for the application) from  $744 \text{ m}^2$  ( $8000 \text{ ft}^2$ ) to  $944 \text{ m}^2$  ( $10,100 \text{ ft}^2$ ). The Raytheon decision means that in FY77 only 2/3 of the required collector area will be installed.

## 2.3 Test Management

A detailed test plan for the Phase IVA (solar to electric) components has been written and is in the process of publication. This plan discusses the objective, test procedure, and data to be obtained for each test. As each individual test is conducted, it will be described in a Letter Test Report. Letter Test Reports on a given subject will then be compiled into a formal Results Report. Following is a basic outline of all testing planned.

### 1. COLLECTOR SUBSYSTEM TESTS

#### 1.1 Performance

- 1.1.1 Automatic Defocus
- 1.1.2 Reflector/Structure Evaluation (Aperture Test)
- 1.1.3 Focal Position
- 1.1.4 Baseline Efficiency, Instantaneous
- 1.1.5 Baseline Efficiency, Daily
- 1.1.6 Receiver Tube Loss Rate
- 1.1.7 Analog Tracker Evaluation
- 1.1.8 Computer/Encoder Tracker Evaluation
- 1.1.9 Laser Evaluation of Reflector/Structure

#### 1.2 Environmental

- 1.2.1 Dirt Effects
- 1.2.2 Aging Effects
- 1.2.3 Structure Twist
- 1.2.4 Long-Term Distortion of Structure

#### 1.3 Control

- 1.3.1 Mixing Control
  - 1.3.1.1 Morning Startup
  - 1.3.1.2 Noon Startup

- 1.3.2 Buffer Control
  - 1.3.2.1 Morning Startup
  - 1.3.2.2 Noon Startup
- 1.3.3 Effects of Two Parallel Rows of Collectors on Control
- 1.4 Miscellaneous
  - 1.4.1 Field Pipe Heat Loss
  - 1.4.2 Overnight Field Heat Loss
  - 1.4.3 Daily Pump Power Versus Energy Collected
- 2. STORAGE SUBSYSTEM
  - 2.1 Thermocline Stability
    - 2.1.1 Static Stability
    - 2.1.2 Dynamic Stability
    - 2.1.3 Long-Term Stability
    - 2.1.4 Sensitivity to Out-of-Tolerance Fluids
    - 2.1.5 Liquid Level Versus Temperature
  - 2.2 Thermal Losses and Mass Effects
    - 2.2.1 Insulation Thermal Evaluation
  - 2.3 Control
    - 2.3.1 Automatic Cooler Mode Operation
    - 2.3.2 Automatic Heater On/Off Operation
  - 2.4 Miscellaneous
    - 2.4.1 Maximum Withdrawal Rate From Storage
- 3. HEATER BOILER AND ORC SUBSYSTEM
  - 3.1 Performance
    - 3.1.1 Baseline ORC Performance
    - 3.1.2 Transient ORC Performance - Heater Boiler Mode
    - 3.1.3 Transient ORC Performance - Storage Boiler Mode
    - 3.1.4 Maximum ORC Output
    - 3.1.5 Out-of-Tolerance Temperature Effects
  - 3.2 Control
    - 3.2.1 Heater Control Evaluation
    - 3.2.2 ORC Control Evaluation
    - 3.2.3 Automatic Switching
  - 3.3 Miscellaneous
    - 3.3.1 Boiler Piping Steady-State Losses
    - 3.3.2 Boiler Thermal Mass
    - 3.3.3 Pumping Losses
- 4. CONDENSER AND COOLING-WATER FLUID HANDLING SUBSYSTEM
  - 4.1 Maximum Heat Removal

## System Operation and Test

Following is a compilation of the 10 Letter Test Memos issued during this reporting period.

<u>Title</u>	<u>Test Plan No.</u>	<u>Comments</u>
Analog Tracker Evaluation	1. 1. 7	Discusses problems with long-term analog tracking of collectors.
Storage to Fossil Fuel Switchover	3. 1. 3	Discusses effect on turbine of storage to fossil fuel switchover.
Early AM Startup	1. 3. 1. 1	Excessively long collector startup. Shows need for improved control procedure.
Noon Startup	1. 3. 1. 2	Excessively long noon collector startup. Shows need for improved procedures.
Early AM Startup	1. 3. 1. 1	New procedures shorten collector startup time but more improvement needed.
High Temperature Storage Thermocline	2. 1. 1	Determine thermocline stability poor even though little fluid mixing occurs.
Off Design Turbine Inlet Pressure	3. 1. 5	Determines weak dependency of efficiency on inlet pressure.
High Temperature Storage Tank Investigation		Testing conducted to determine leak in fluid inlet diffuser in tank.
Shaft Encoder Consistency Test	1. 1. 8	Determine accuracy and repeatability of encoder positioning of collectors.
Morning Startup	2. 1. 6	Shows new procedures further shorten collector startup time.

In order to maximize operating time on the collector field system, a policy was initiated in February to operate the collectors as long as possible every day even if the collected energy was not utilized. Following are the results of this program.

<u>Month</u>	<u>Sunshine Hours During Work Hours</u>	<u>Operating Time</u>	<u>Percent of Time Operating During Work Hours</u>
Feb.	87.25	80.75	92%
March	133.00	121.00	92%

Downtime was usually utilized to repair, clean, or change collectors.

Our Standards Laboratory recalibrated the solar instruments by using an active cavity radiometer. Our pyrhelimeter has shown negligible calibration shift from the factory calibration after about two years of use. This pyrhelimeter has also been compared with US Weather Service and other laboratory standards. In all calibrations and intercomparisons this instrument has given consistent performance.

Our portable station for recording solar radiation and weather information has been running during most of this reporting period. We have been checking the data from time to time to establish the reliability of the equipment.

### Task 3. Collector Subsystems

This task is directed at the development and evaluation of solar collectors and related components. The primary concern is for the operation and evaluation of the collector field of 200 m<sup>2</sup> of parabolic trough collectors installed as the first quadrant of the Solar Total Energy System Test Facility (STESTF). This effort is discussed in Task 3.1.

The remaining three quadrants of the planned collector field to be installed in the STESTF are covered in Task 4.

Of longer range concern is the development, fabrication, testing and evaluation of collectors, components and materials in a continuing effort to provide mature collector concepts for future total energy applications. This effort falls under the Solar Total Energy Program Plan (Ref. SAND76-0167) and includes a variety of projects, both internal and external.

The major internal effort has been in the area of materials development. This work is described in Task 3.2 and includes reflector materials, concentrator structures and fabrication processes, and receiver tubes. The laser inspection systems and the investigation of cleaning problems are also covered.

Development contracts have been placed with several companies for design, fabrication, testing and evaluation of a variety of collector concepts and collector components. The objective of this Component and Subsystem Development effort is to provide a selection of collectors suitable for use in later generation collector fields such as the Large Scale Experiments (LSE's) or Demonstration projects. This work is also discussed in Task 3.2.

### 3.1 Operation and Testing

Description -- The  $200 \text{ m}^2$  collector field of parabolic troughs installed as the first quadrant of the STESTF has been functional since February 1976. The field consists of four continuous troughs 18.3 m (60 ft) long aligned on an east-west axis in two rows as shown in Figure 9. Center to center spacing between rows is 7.6 m (25 ft). Each of the troughs consists of five  $2.7 \times 3.7 \text{ m}$  (9 x 12 ft) trough units mechanically connected to form a single trough. The parabolic units have a  $92^\circ$  rim angle and a 0.658 m (25.9 in.) focal distance.

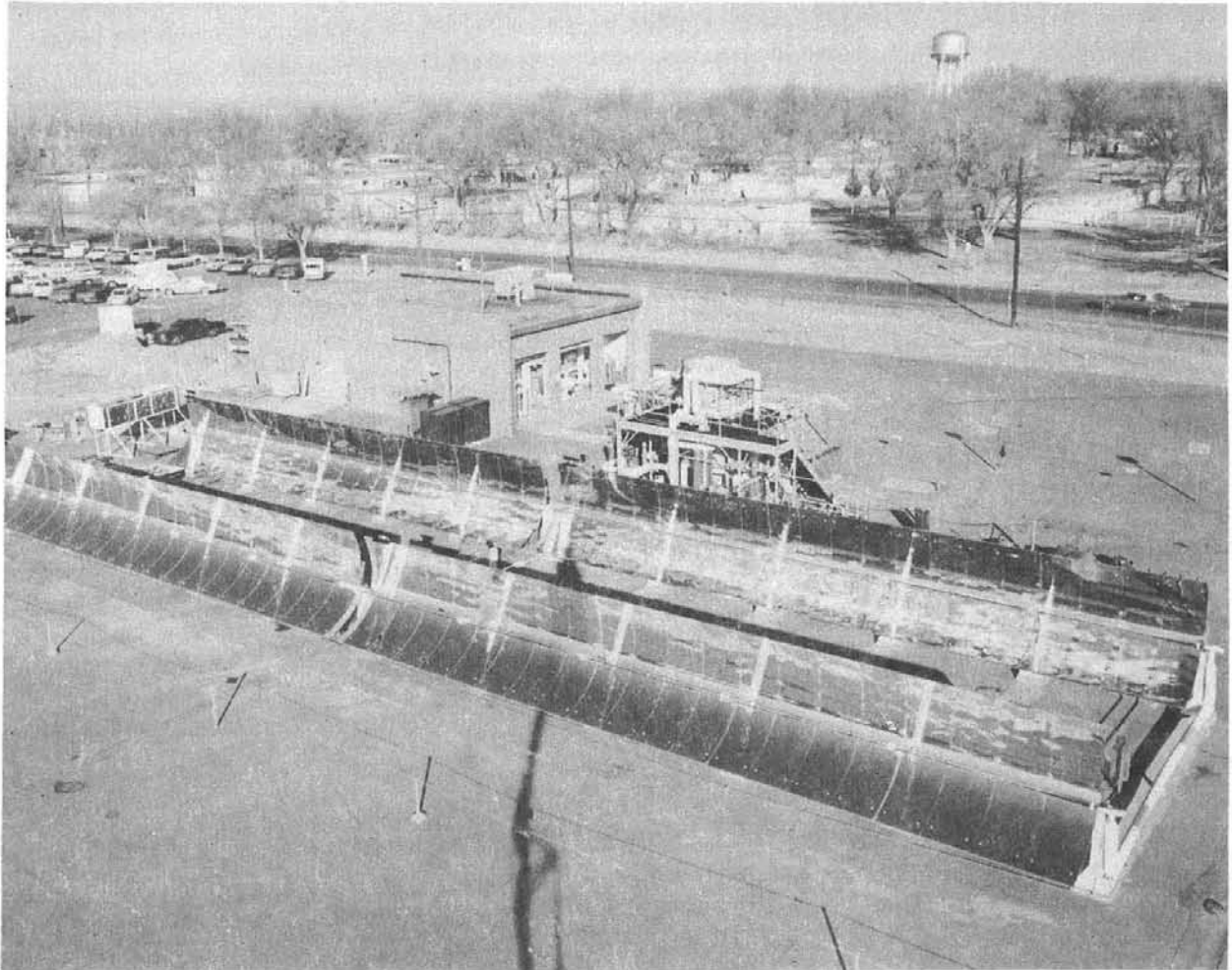


Figure 9. Solar Total Energy Test Facility with Sandia Collectors

Operation and testing of the collector field during the past six months has been conducted at every opportunity within the limits of weather, modifications, malfunctions, and maintenance. Data were collected for all day operation, during days near the fall and spring equinoxes and the winter solstice.

Five reflector panels were replaced from the 24 new panels received from Sheldahl. The five units replaced were those which were still functional but slightly damaged in the April wind-storm or those which had suffered subsequent deterioration. A large number of small cuts in the 1 mil Teflon film were caused by the impact of broken glass from the receiver tube envelopes. During the months of exposure following the damage, the adhesive bonding the aluminized Teflon to the substrate has been eroded, probably by moisture from natural precipitation as well as washing operations. The aluminized coating in the delaminated area surrounding each cut has virtually disappeared and each spot has slowly and consistently increased in size.

Patches of 3M's aluminized acrylic film with an adhesive backing were placed over several of the cuts in an attempt to stop the deterioration. The patches appear to have worked well on the small spots but the deterioration and spot growth has continued under some of the large spots and have outgrown the patch. The 3M 5400 acrylic film which was placed on the added mechanical clamp strips for the reflector panels has survived six months of exposure very well with little or no peeling and no detectable deterioration from the raw edges.

Several reflector panels were removed from the collectors in mid-October 1976 after nine months exposure. Specular reflectance measurements on these panels indicated that the reflectance had decreased slightly and also changed slope slightly so that the reflectance was more sensitive to aperture width than it was previously. Earlier reflectance measurements indicated that the reflectance value was virtually constant with apertures of 12 to 15 milliradians. Measurements of several cleaned samples from one panel indicated that the reflectance was still slightly increasing at 15 milliradians and ranged from .79 to .75. Additional samples of other panels will be measured for comparison.

Receiver Tubes -- Modifications were made to the original receiver tube design in an effort to eliminate some of the problems encountered in operation. The changes included several minor manufacturing changes in addition to:

- Increasing the vacuum pumping port to 1/4 in.
- Locating all thermocouple feed throughs in the end flange, rather than in the glass envelope.
- Using a rotatable flange to simplify field installation.

Fifteen of these modified design tubes were fabricated by Bendix Kansas City and by Sandia shops. Delivery for installation is scheduled for April. These units will be used as spares as well as installation of a sufficient number to run a series of tests to determine the actual efficiency differences due to a good vacuum in the receiver envelope annulus.

Tracker Systems -- The analog tracking system with its photocell/shadow board sensor encountered problems in providing accurate control of the collector troughs.

The problems included difficulty in obtaining accurate alignment of the sensor with the trough focal plane; cloud effects which reflect light unevenly on the sensor cells; different light reflective characteristics of surrounding buildings, pavement, etc.; reflections from aluminum roofs with low sun angles in winter; and reflections from the opposite side of the trough from where the sensor is mounted. Most of the enumerated problems produce bias in the sensing cells and cause offset from the proper position. Cloud sensor circuitry was devised to limit erroneous defocusing travel but it could not be set at diffuse light levels to accommodate the wide variety of existing conditions. These conditions prevented establishing a consistent, accurate tracking capability.

Analysis and tests were conducted to investigate solutions to these problems. Additional shielding was also installed on the sensor mounts to improve performance.

The accurate alignment of the plane of the tracker sensor with the focal plane of the collector trough is critical in two of the three mutually perpendicular axes. Errors in alignment of the two axes within the focal plane (one axis is parallel to the trough vertex, the other is perpendicular to it) will produce respectively, a constant offset of the trough throughout the day or a varying offset as the day passes.

The analog tracker consistency and accuracy was such that decisions were made to: (1) use the computer command control tracking system for all testing of the collector field and (2) initiate a development effort into tracker sensors and tracking control systems.

Tracker Development -- After preliminary discussions with the components development organization of Sandia Laboratories, assignment of personnel was made in early February 1977 to begin a development project on tracking systems, including sensors, for solar collectors. This project is not aimed at immediate application to the existing parabolic troughs; but is intended to be a thorough look at the entire tracking system--sensors, logic, controls, etc., with approximately one year effort to first unit implementation.

The initial work has included analysis of existing tracker systems, definition of requirements and formulation of basic design concepts. The primary thrust to date is to use microprocessors as building blocks to form a digital controller for the tracking motor. A secondary conclusion is that the sensor should sense that which it is intended to control rather than sense the position of the sun and depend on alignment of the sensor and the focal plane. To this end, the project will investigate installation of sensors on or near the receiver tube so that the maximum input to it is sensed and control is based thereon.

Miscellaneous -- The four 18.3 m troughs have been equipped with limit switches which interrupt power to the drive motor. Override switches have been provided to allow movement of the troughs off the limit switches. There were indications that use of the override switches had resulted at some time in driving the wrong direction (further into the limit switch rather than away from it). For this reason the alignment of the receiver tubes and the receiver tube support brackets needed checking. The receiver tube support bracket is the first item to contact an immovable portion of the pylon and may have been slightly shifted in using the limit switch override.

To avoid human error, the limit switch override circuitry has been modified so that it can drive only in the proper direction--away from the limit switch.

Slit Aperture Inspection -- To check the receiver tube alignment the slit aperture device was used to inspect each of the twenty 2.7 x 3.7 m troughs in the field. This device is described in the previous report. Although this is not a sophisticated tool, it does provide relatively good information regarding receiver tube position and reflector accuracy.

The inspection indicated that the receiver tubes were properly located at the design focal distance from the vertex of the parabola. Two of the troughs required slight realignment of the tubes in the rim-to-rim plane.

The inspections indicated, as have previous ones, that the outer portions of these reflector panels do not adhere to the plywood trough. A strip approximately 30 cm (12 in.) wide adjacent to each trough rim reflects up to 40% of its light over the top of the receiver tube. This error would represent as much as 9% of the total reflected energy which does not strike the receiver tube.

The cause of the reflector inaccuracy is primarily the difficulty of clamping the reflector panel to the trough structure near the outer rims where the radius of curvature becomes quite large. This inaccuracy also helps to explain some of the lower than expected operating efficiencies of the system.

Most of the twenty receiver tubes in the collectors have been installed for about thirteen months. The last five tubes of the series loop, those units nearest the high temperature outlet, have apparently suffered degradation of the black chrome coatings. These coatings have changed color and have become mottled. These tubes are scheduled for replacement with the fifteen spares of the new design. One or more of these old units will be postmortemed to establish the characteristics of the coatings and attempt to determine the cause.

Operational Testing -- A broad series of operational tests were conducted on the collector subsystem during the six months reporting period which spanned from near the autumnal equinox through winter solstice and the vernal equinox. Testing appropriate to these seasonal variations was scheduled, and in most cases, executed. The tests included baseline efficiency tests, optimum

focal position tests, thermal loss tests, baseline all-day performance tests at both equinoxes and winter solstice, tracking systems evaluations, and an extensive series of tests to evaluate the interdependent effects of fluid levels in the buffer tank, fluid control strategy and start up times. Most of these tests have been documented in Letter Test Reports forwarded to ERDA Headquarters (Refs. 1 through 7). Data from the tests are being used in a continual evaluation of collector subsystem performance as time passes.

The planned testing program is defined in a document which has been completed and is in publication channels, titled SAND77-0690, Solar Total Energy System Test Facility Operational Phase Test Plan. This document is the culmination of the testing and test program planning of a couple of years. The letter test reports mentioned above reference specific tests defined in the Test Plan.

A policy of maximum collector operation during normal working hours was initiated during this reporting period. The reason for the policy was to provide maximum data collection under all conditions and to exercise the system for maximum real time usage to determine wear rates, maintenance requirements, typical daily energy collection, etc. Subsequent to establishing this policy, the collectors were operated as much as weather and maintenance requirements permitted. The collector field and subsystem was operated 92% of the possible time in both February and March.

Baseline Efficiency Tests -- Two types of baseline efficiency tests are defined: an instantaneous efficiency in which the total heat energy collected is determined as a percentage of the total direct insolation intercepted by the reflectors, and a daily baseline efficiency in which the collector efficiency is determined throughout a full day of operation.

The instantaneous baseline efficiency takes into consideration solar intensity, dirt on collectors, vacuum in the receiver tube envelopes, wind, ambient temperature, flow rate, input temperature,  $\Delta T$ , etc. The system is operated until stable conditions are achieved and data taken. A spread of data points can be achieved in the course of a full day of operation, but multiple days are required for non-controllable variables such as wind and ambient temperature. Data points for instantaneous efficiencies are achieved virtually each time the collectors are operated. Correlation of the data is an ongoing task.

The daily baseline efficiency tests are planned for all equinox and solstice periods (along with some interim occasions) so that full day performance can be determined to compare with design predictions. Constant conditions are maintained on those parameters which can be controlled (input temperature, flow rate, etc.) so that effects of various non-controllable climatic conditions can be determined. Over long periods, the effects of changes in the collectors (reflectance, absorptance, etc.) can be seen. Data are compared with previous tests and conditions.

The daily baseline efficiency tests for the autumnal equinox was not conducted because the active sensing tracker system could not provide accurate all day tracking. Although scheduled for late September or early October, the tests could not be conducted until November when the computer command control tracker system was fully functional.

The winter solstice all day baseline efficiency test was conducted on December 21, but the storage tank outlet temperature was significantly lower than the design operating temperature of 243°C (470°F).

The vernal equinox all day baseline efficiency test was conducted on March 22. Maximum collector efficiencies ranged from 44.5% for the 18.3 m NE trough to 40.5% for the NW trough which is the final trough in the loop with the highest operating temperatures. None of the receiver tubes had a vacuum in the annulus. Peak solar input near noon was  $1000 \text{ w/m}^2$ . The five receiver tubes in the NW trough have been observed to have black chrome coatings which have changed in color from a dark rich black to lighter hues, mostly an amber brown with some dark purplish casts and a one-half-meter length with a greenish tinge. These five units are scheduled to be replaced with new tubes and the coatings postmortemed.

#### Optimum Focal Position

Another series of tests which are run at intervals are the optimum focal position tests which produce a plot of collector performance vs. offset angle from the focal plane. While tracking with the minicomputer program, the collectors are offset from the specified program by intervals of  $0.2^\circ$  so as to obtain a plot of collector performance vs. offset angle. This test is run to verify the tracking program and to aid in assessing the accuracy of receiver tube position. Improved software was available for use after October.

The optimum focal position tests are run each time adjustments are made to a trough to assure that the trough will be operated subsequently at peak performance.

#### Thermal Loss Test

The thermal loss test is devised to determine the heat losses of the fluid loop from storage tank outlet, through the collectors to the storage tank inlet. The collectors are defocused as far as possible to limit the solar input to the receiver tube to one sun. Therminol-66 fluid is brought to the desired temperature in the storage tank and then pumped through the collector loop to simulate the temperature of normal collector operation. Flow rate and temperature drop are used to calculate heat losses. Thermocouple instrumentation is used to establish losses for each of the 18.3 m collectors and for the various segments of interconnecting plumbing. The temperature of the storage tank fluid was reduced incrementally so that a spread of data could be obtained for various operating temperatures. With this data, correlation can be made between theoretical analyses and actual losses and operating efficiencies.

Preliminary thermal loss tests were run in October, January, and March; the data produced were scattered and uncertain. Additional tests are scheduled in conjunction with thermal mass tests.

A series of tests of the receiver tube loss rate were conducted in June, July, October, and January, and are documented in Ref. 7, dated March 14, 1977. The data are plotted to show thermal losses vs. wind velocity, flow rate and temperature. Scatter of data prevents clear conclusions.

#### Early Morning Start Up Tests

A series of start up tests have been conducted for the purpose of determining the time required for the collector field to collect enough energy to heat both the fluid loop and its fluid and to deliver 310°C (590°F) fluid to the storage tank. This start up time--the period between initial focusing of the collectors and delivery of 310°C fluid to the tank -- is dependent on several factors, including solar intensity, overnight ambient temperature, thermal mass of the fluid loop (plumbing, insulation, fluid in plumbing and in blending tank), and collector aperture interception for time of day. The initial series of tests are discussed in Refs. 2, 3, 4 and 6 which present the data and results of tests in September, November, December, January and March. Additional tests are planned.

Start up tests were run beginning at sunrise and at noon; sunrise represented regular day-to-day operation while noon represented cloudy conditions with clearing during the day. Start up times (the time period from initial focus to deposit of 310°C fluid in storage) varied significantly in these tests. Once tracking problems in early morning hours were solved, useful data were obtained. Start up times were reduced to approximately one hour, thirteen minutes for early morning start up in January and fifty-five minutes for noon start up in November.

Two control modes have been utilized in operating the blending tank and fluid loop, the mixing mode and the buffer mode. Both modes are described in SAND76-0078, Solar Total Energy Program Semiannual Report, April 1975 - September 1975. The mixing mode, used in all operations to date, circulates fluid from a full blending tank, through the collector field and back to the blending tank until fluid temperatures of 310°C are achieved. The full blending tank represents a major contribution to the thermal mass of the fluid loop. Tests were also run with only minimum fluid in the blending tank, resulting in important reduction in start up time. Better insulation of the blending tank offers additional reduction potential.

Operation of the fluid loop in the buffer mode has not been achieved. Attempts were made but were not successful. Appropriate parts have been ordered for retrofit so that buffer mode operation and start up tests may be conducted.

Reference 5 describes a series of comparison measurements made to determine the accuracy and consistency of the shaft encoder/minicomputer tracking system. This system operates by reading the shaft encoder position, comparing it with the computed solar position and driving the trough until the two agree. Indications had been noted that the system was slightly inconsistent.

An inclinometer with an accuracy of 1/2 minute of arc was attached to the framework of the troughs so that the shaft encoder and inclinometer readings could be compared as the trough was rotated throughout its 170° of travel. This test was repeated for several cycles for each of the four 18.3 m troughs.

Tabulation and plotting of data indicated maximum errors of 20, 72, 114 and 196 minutes of arc for the four troughs, i. e., 0.3 to 3+ degrees of arc error. Close inspection of the shaft encoder mountings and connections revealed that the two shafts were poorly aligned and the trough shafts extended too far into the couplings. After careful realignment and rework, the inclinometer and shaft encoder measurements were repeated.

The second set of measurements revealed that the deviation between the inclinometer readings and those of the shaft encoder never exceeded 0°20' of arc and averaged less than 0°10'. Acceptable consistency was also demonstrated by taking data for several cycles.

This test provided confidence in the minicomputer/shaft encoder command tracking system to provide accurate, consistent tracking throughout the day.

#### Cleaning of Collectors

The accumulation of dirt on the reflector surfaces of a collector and on the glass envelope of the receiver tube cause degradation of performance. This decrease in collector efficiency has been demonstrated by measurement of poor collector performance as well as by specular reflectance measurements. Reflector material samples have been measured clean, subjected to both normal outdoor environment and accelerated aging chambers and measured again before and after cleaning. These measurements indicate that total hemispherical reflectance values are virtually not changed; the dirt merely scatters the light rather than absorbing it. The specular reflectance measurements of dirty reflectors clearly demonstrate that specular reflectance can be reduced by as much as 20 percentage points, from the mid-eighties (~.83) to the mid-fifties (0.56) with very dirty reflectors. Slightly dirty reflectors may reduce the specular reflectance by only a few percent. The worst case measurements were made after a severe wind storm which would have necessitated cleaning immediately afterward. Routine cleaning, perhaps every two weeks, should limit the performance degradation to a few (6 to 8%). Certain storms with wind, rain and blowing dust will require immediate cleaning. Other gentle rain conditions will do the cleaning naturally if the reflector is in a position to allow it.

It should be noted that the glass envelopes on the receiver tubes have acquired dirt films and have also required cleaning. Those clear glass surfaces may make their dirt accumulation more visible than the reflector materials, but the receiver tubes seem to require a manual wiping and drying after washing to get them visibly clean.

A variety of cleaning materials and methods have been used on the collector troughs; these include: spray rinse with water; manual mopping (with minimum pressure and soft mops to limit scratching of the soft Teflon) with warm water and detergent; spraying of several other types of cleaning agents, and several types of sprays. All cleaning operations culminated in a final rinse with deionized water to prevent spotting. Surfactant additives were discussed with cleaning companies to allow maximum draining of the final rinse.

The cleaning effort must involve industry in the near future to develop techniques and agents to clean collector components quickly, easily and cheaply. Because of the variety of collector configurations, it appears that spray-on and rinse off techniques must be developed. Increased efforts on cleaning are planned. The effects of cleaning agents on all other parts of the system must be considered along with their environmental impact.

#### References for Task 3.1

1. Analog Tracker Evaluation Test Plan 1.1.7 dated November 2, 1976.
2. Collector Subsystem Control Test Plan 1.3.1.1, Early Morning Start Up Tests on September 29-30, 1976, dated November 15, 1976.
3. Collector Subsystem, Mixing Control, Test Plan, No. 1.3.1.2, Noon Start Up Test, November 2, 1976, dated November 24, 1976.
4. Collector Subsystem, Mixing Control Test Plan, No. 1.3.1.1, Early Morning Start Up Tests on November 3, 1976, dated November 24, 1976.
5. Collector Subsystem Test, Test Plan No. 1.1.8, Shaft Encoder Consistency Test Conducted November 5-December 3, 1976, date January 31, 1977.
6. Collector Subsystem Tests, Control Test Plan, No. 2.3.1.1 Morning Start Up, January 10 and 11, 1977, dated March 14, 1977.
7. Collector Subsystem Tests, Performance Test Plan, No. 2.1.6, Receiver Tube Loss Rate, dated March 14, 1977.

### 3.2 Component and Subsystem Development

Funding for the Component and Subsystem Development Project has been provided by the Special Applications Branch of ERDA's Division of Solar Energy for development projects with contractors with solar experience and promising collector or component designs. This effort is in support of the National Solar Total Energy Program as defined in SAND76-0167. Some of the contracts were placed as follow-on to the evaluation of proposals for the three STESTF field quadrants. Additional Requests for Proposal (RFP's) have been sent out and other contracts placed as a result. These various projects are discussed in the following paragraphs.

Immediate Procurement Collector Testing -- In an effort to survey the near-term availability of developed collectors, a Request for Proposal was issued to a list of companies known to have collectors under development. The RFP required proposals for furnishing a collector module capable of supplying 240° to 315°C (462° to 600°F) output temperatures within a period of four months. The collector modules are to be fabricated and tested per an approved test plan on Sandia's CMTF to establish performance characteristics. Responses were evaluated and contracts have been placed with four companies. They are Hexcel; Scientific Atlanta, Inc.; Solar Kinetics, Inc.; and Soltrax, Inc. Each contractor will furnish a test director and appropriate support personnel for a period of approximately one month of testing.

Sandia personnel will operate the test facility in accordance with a coordinated test plan for determining the performance characteristics of the test modules which range from 14.9 to 21.9 m<sup>2</sup> (160 to 236 ft<sup>2</sup>) of aperture. Contractors will write a final report with all test data available for unlimited distribution.

Hexcel will fabricate a parabolic trough of aluminum honeycomb structure 2.4 x 6.1 m (8 x 20 ft) with a 60° rim angle. The unit is to be tested in both N-S and E-W horizontal axis alignment. Reflector material is a second-surface aluminized acrylic film.

The collector to be furnished by Scientific Atlanta, Inc., is a Fixed Faceted Mirror Concentrator (FFMC) in which the reflector portion is fixed while only the receiver tube moves to follow daily and seasonal sun position. The mirror facets are narrow, second-surface silvered mirror strips mounted on an aluminum framework. Both the mirrors and the receiver tube are located along the circumference of an imaginary cylinder. The unit will be tested in an E-W orientation.

Sagged glass parabolic troughs with 0.57 m (1.9 ft) rim-to-rim dimension are to be provided by Soltrax, Inc. An array of these collectors with 21.9 m<sup>2</sup> (236 ft<sup>2</sup>) will be tested in a N-S orientation. The ~120° rim angle troughs rotate about fixed receiver tubes.

Solar Kinetics, Inc. has designed a 90° rim angle parabolic trough of cast aluminum with an aluminized acrylic film reflector. The module will be approximately 18 m<sup>2</sup> of aperture with a 1.06 m width. Receiver tubes of several sizes with glass envelopes with and without vacuum have been proposed.

#### Collector Development Projects

Collector development projects are in progress at Del Manufacturing Co., Monterey Park, CA, and at FMC Corp., Santa Clara, CA. The Del collector is a relatively small parabolic trough collector with a fixed receiver tube with a glass envelope, about which the trough rotates. Trough rim angle is approximately 105° with two silvered sagged glass sections, each of which extends from near the vertex to a rim. The trough is .61 m (2 ft) wide and constructed of a simple steel framework designed for economical production. The sagged glass provides its own structural support to form the parabolic curve. Multiple glass pieces are fitted end to end in a steel framework to form the required length of trough. The array of troughs can be oriented either N-S or E-W. These collector development contracts require analysis, design, fabrication, pressure testing for safety purposes, testing of the collector module on Sandia's test loop, evaluation of data and a final report. The reports will be available for distribution.

FMC Corp. is developing a concentrating collector in which the receiver tube is fixed at the centerline of a cylindrical section on which is mounted a fresnel belt reflector which moves to follow the sun. The fresnel belt contains individual mirror facets attached to a flexible belt which is driven around the circumference of the 90° cylindrical section. The belt offers potential for low cost with large production rates. The initial test module will establish the performance characteristics of the concept.

#### Receiver Tube Development

A 37 m<sup>2</sup> (400 ft<sup>2</sup>) collector module of the Sheldahl SLATS concept has been installed at the Collector Module Test Facility at Sandia with a 12.2 m (40 ft) long receiver tube. Testing on Test Loop No. 3 with high pressure water as the working fluid is scheduled to begin in mid-April 1977.

Two additional receiver tube configurations are planned for testing on this collector module. Final negotiations are in progress on contracts for 12.2 m receiver tubes from two companies - General Electric and Itek. Testing of these receiver tube designs on the same collector will offer opportunity to compare performance of these different concepts for narrow angles of acceptance. The reflector width of this collector subtends an angle of approximately 60° as viewed from the focus; this configuration corresponds to a rim angle of 30° for a parabolic trough.

## Sandia Receiver Tube Development

Development of the Phase IV-B receiver design has continued at Sandia. Studies have been completed on heat losses with various levels of vacuum and their effects on overall efficiency of the receiver assembly. For the purposes of experimental verification, the Phase IV-B receiver design, shown in Figure 10, was utilized; it included an O-ring seal to provide a vacuum between the glass envelope and coated receiver tube. The obvious advantages of this design over the bellows and glass-to-metal seal design are that (1) the system is less expensive and (2) replacement of a broken glass envelope does not necessitate replacing the entire receiver assembly.

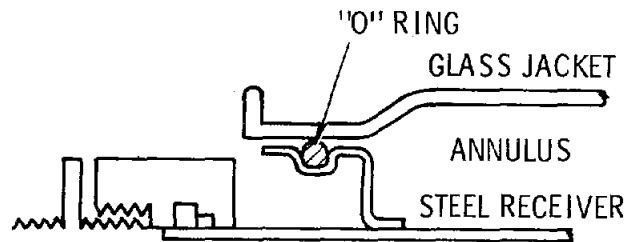


Figure 10. Sandia Phase IV-B Receiver Design

The experimental work attempted to provide data on expected vacuum loss rates due to O-ring permeation and to investigate the vacuum level requirements necessary to substantially limit conduction heat loss. Convective heat losses through the receiver assembly annulus had previously been limited through sizing of the annular space so that the Rayleigh number was maintained near 1000. Radiative heat losses were primarily fixed by the selective coating properties of the receiver tube.

An eight-foot experimental receiver assembly was heated internally with a Chomalox <sup>®</sup> resistive heater element. Power input was monitored by controlling the input current and voltage drop across the resistance heater. Receiver assembly temperatures were monitored with twenty-five chromel-alumel thermocouples. Annulus vacuums were principally monitored with a Wallace and Tiernan Pressure gauge and with a Pirani Gauge (thermocouple gauge). Vacuums were maintained using a single stage vacuum pump.

Analytical modeling involved writing energy balances for the receiver tube and glass surfaces that could be used to (1) predict the resultant receiver assembly temperatures for known heat inputs or (2) predict the receiver assembly heat loss for a fixed receiver tube temperature. The analysis assumed steady state conditions and utilized correlations for the effects of pressure, wind, geometry and temperature on the heat transfer terms.

Figure 11 presents comparative results of the analytical and experimental work undertaken to reduce receiver heat loss. Theoretical calculations are shown as solid lines with experimental data plotted with triangular points. The curves of this figure indicate that the heat loss is relatively independent of the annulus vacuum until pressures below 1000 microns Hg are reached.

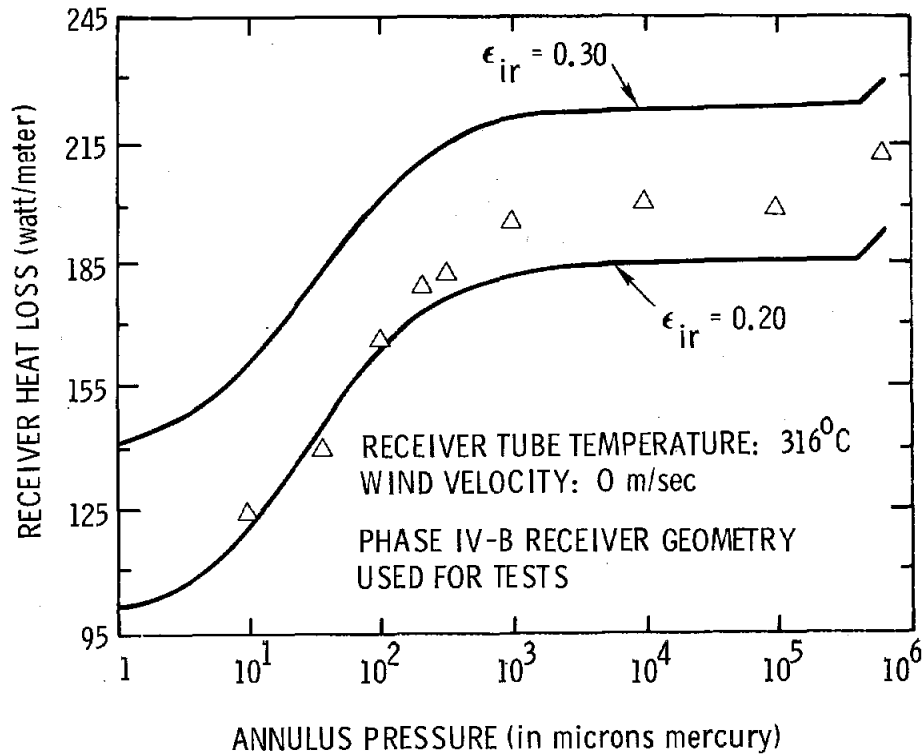


Figure 11. Effects of Pressure on Receiver Tube Heat Loss

Reduction of thermal losses by 4 to 6% of the absorbed incident solar energy may be achieved by reducing the annular pressure below 10 microns Hg; these percentages correspond to heat loss reductions of 70 to 100 watts/meter of receiver tube length. Further analytical modeling which considers the effect of wind on receiver heat loss indicates that heat loss reductions may be even more substantial ( $\geq 110$  W/m), if the annulus pressure is such that the heat loss is solely radiation energy transfer.

Other studies of reducing heat losses have considered: (1) use of gases other than air in the annulus to limit conduction losses and (2) use of partial vacuums ( $\geq 1000$  microns Hg) for oversized annular spaces. Savings associated with each technique appear comparable, with savings of 15 to 50 W/m of receiver tube length possible. Such savings may amount to as much as 2% of the absorbed incident solar energy. Experimental verification of these projected savings are planned in the future months.

Vacuum loss tests were conducted using commercially available silicone O-rings. Problem areas which were addressed included investigating O-ring temperature limitations and O-ring permeability. Receiver tube temperatures were maintained near 316° C (600° F) to simulate receiver operating conditions, resulting in O-ring flange temperatures over 121° C (250° F). Following two months of vacuum integrity and heat loss testing, no thermal degradation of the O-rings could be detected. This was expected since the silicone O-ring material does not decompose until temperatures above 232° C (450° F) are obtained. Vacuum integrity tests were not nearly so successful, as losses ranging between 20 and 40 microns Hg/hr were measured. Silicone permeability properties were obtained from the manufacturer, and vacuum loss calculations indicate that such losses are to be expected for the operating conditions and volume of gas considered. Further vacuum loss testing is currently being undertaken using a less permeable O-ring of Viton. The improved properties of this O-ring material should reduce the vacuum loss by over an order of magnitude to about 1 to 4 microns Hg/hr. Vacuum loss tests are planned to verify these loss rates. Even such vacuum loss reductions, however, will necessitate intermittent vacuum pumping to maintain vacuum levels below 10 microns Hg.

RFP for New Concepts -- New and innovative collector concepts must be encouraged so that collector technology can benefit from simplification, improved operational efficiency and reduced cost. To this end, a Request for Proposal (RFP) has been drafted and promulgated to over seventy companies and universities which indicated interest and capability in the solar collector area.

An advertisement was placed in the Wall Street Journal and in Commerce Business Daily in January requesting firms interested in participating in solar collector development projects on a contract basis to send appropriate information regarding their experience and capabilities to Sandia. More than one hundred responses were received from interested firms, individuals and universities.

These responses were assessed and a list of respondents compiled for receiving the RFP. Also included on the mailing list were several companies presently engaged in project work and known to have extensive background and capabilities.

The RFP requested proposals for a component development project for the design, fabrication and testing of novel prototype solar collectors which will operate with outlet temperatures greater than 230° C (446° F). The primary objective of the project is to stimulate new and innovative collector designs suitable for use in large fields of distributed collectors.

The project is planned for two phases, as follows, with funding only available for Phase I.

Phase I

1. Economic and performance analyses
2. Preliminary design
3. Reports and drawings

## Phase II

1. Detailed design
2. Performance test planning
3. Collector fabrication and procurement
4. Collector testing
5. Phase II reports and drawings

The RFP's are to be mailed in mid-April with responses due in June 1977. Evaluation of the responding proposals will be accomplished within four to six weeks. Placement of several Phase I contracts is planned with a performance period of six months.

Solar Collector Proposal Evaluation Technique -- The result of a meeting with representatives of ERDA/HQ on November 18, 1976, at Sandia Laboratories in Albuquerque was a directive to compile a technique for solar collector proposal evaluation which would include a feature comparison chart. On December 9, 1976, a second meeting was held to evaluate the ideas compiled as a result of the first meeting. At the second meeting a solar collector/receiver proposal evaluation package was outlined. After it was written up and reviewed, the package was circulated to seven groups in industry currently under solar collector/receiver development contracts. They were asked to respond by completing and returning the questionnaire portion of the package. Most of the groups responded to and provided their comments on the package. This led to a revised version which should prove more useful.

Concentrator Structures Development -- As described in previous reports, many types of parabolas have been fabricated from a pair of precision .6 x 1.2 m (2 x 4 ft) parabolic molds. Each contractor has tried to optimize his fabrication technique to yield the highest optical quality parabolas of the materials with which he was most skilled. Some of the constructions used for these small parabolas are shown in Figure 12. The resistance of these structures to flexure produced by wind and structural loading is of primary importance when designing a mirror support. Also the transverse or out-of-plane properties are important when attachment designs are being developed. The flexure resistance of a sandwich structure is defined as its effective modulus,  $E \cdot I$ , which combines both geometric and material properties together. If one knows  $E \cdot I$ , the behavior of a sandwich panel can be determined from Equation 3.1,

$$E \cdot I = \frac{P L^3}{\delta 48} \quad (3.1)$$

where  $P$  is the load applied at the center of span  $L$  and  $\delta$  is the center deflection of the sandwich panel. Effective modulus and transverse property data from some 5.01 cm (2 in.) thick composite structures are given in Table I. Because many of the reflector structure designs are self-loading, the weights of each material in 5.01 cm (2 in.) thick sections is included. The spans and support structures can be obtained from these data, if concentrator design and wind loading criteria are established.

TABLE I

## Mechanical Properties of Mirror Support Structures

Skin*	Description		3-Point Bend Test		Transverse Compressive Strength Pa (psi)	Transverse Tensile Strength Pa (psi)	Weight Kg/m <sup>2</sup>
	Core (5.01 cm Thick)	Core Orientation	Effective Modulus (EI) N. m <sup>2</sup> (lb. in. <sup>2</sup> )	Maximum Skin Stress ( $\sigma$ ) Pa (kpsi)			
Micarta	Corrugated Paper	Across Corrugations	6887.5 (2.4 x 10 <sup>6</sup> )	139.9 x 10 <sup>6</sup> (20.3)	.434 x 10 <sup>6</sup> (63)	.51 x 10 <sup>6</sup> (74)	9.58
Micarta	Corrugated Fiberglass	Across Corrugations	7174.5 (2.5 x 10 <sup>6</sup> )	141.3 x 10 <sup>6</sup> (20.5)	.8 x 10 <sup>6</sup> (117)	.4 x 10 <sup>6</sup> (58)	5.78
Melamine	Corrugated Paper	Across Corrugations	2869.8 (1.0 x 10 <sup>6</sup> )	83.4 x 10 <sup>6</sup> (12.1)	.38 x 10 <sup>6</sup> (56)	.42 x 10 <sup>6</sup> (62)	11.93
Melamine	Corrugated Fiberglass	Across Corrugations	3730.7 (1.3 x 10 <sup>6</sup> )	65.5 x 10 <sup>6</sup> (9.5)	.65 x 10 <sup>6</sup> (95)	.24 x 10 <sup>6</sup> (36)	8.38
Fiberglass	Corrugated Paper	Across Corrugations	3156.8 (1.1 x 10 <sup>6</sup> )	----	.38 x 10 <sup>6</sup> (56)	.72 x 10 <sup>6</sup> (105)	---
		With Corrugations	4304.7 (1.5 x 10 <sup>6</sup> )	----			
Fiberglass	Corrugated Fiberglass	Across Corrugations	3730.7 (1.3 x 10 <sup>6</sup> )	----	1.05 x 10 <sup>6</sup> (153)	.47 x 10 <sup>6</sup> (69)	10.85
		With Corrugations	4304.7 (1.5 x 10 <sup>6</sup> )	----			
Fiberglass	Sinewave Core	Across Corrugations	487.8 (.17 x 10 <sup>6</sup> )	----	----	----	5.03
		With Corrugations	1980.2 (.69 x 10 <sup>6</sup> )	----	----	----	

\* Micarta® - Westinghouse trade name for high pressure laminate of resin and paper similar to Formica®, made by the Formica Division of CYANAMID Corp.

Melamine - A resin-paper laminate primarily used for kitchen counter tops.

Fiberglass - 30 volume percent fiberglass mat in a polyester matrix.

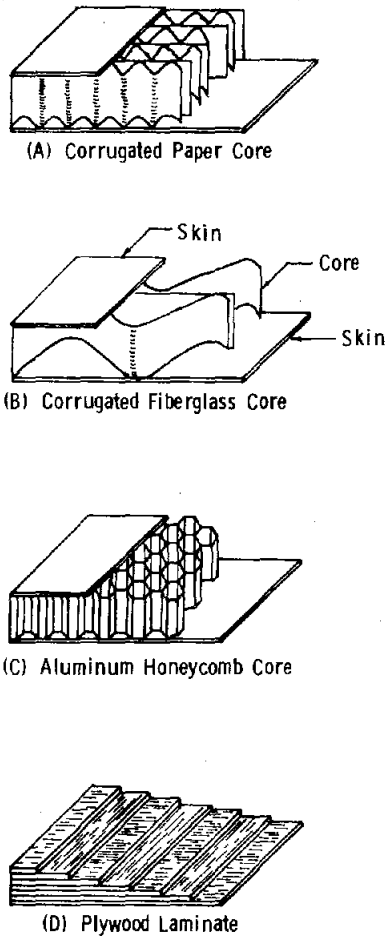


Figure 12. Sandwich Structures

Reinspection of environmentally tortured test parabolas using the laser ray-trace has been completed. The resulting changes in focal length,  $F$ , and surface slope error are given in Table II. Only two of the parabolas that started environmental exposure in this group of 16 were degraded so as to be unmeasurable. These units had melamine and Micarta<sup>R</sup> skins on paper cores. The moisture and thermal cycling deteriorated the skin-core bond, which resulted in the complete separation of skin and core. It should be noted that no special precautions were taken to insure the survival of any units. Waterproof coatings were not applied to the paper cores or skins. Thus paper structures should not be ruled out before the effects of moisture proofing have been evaluated.

Each temperature/humidity cycle is 8 hours long and cycles between  $-29^{\circ}$  and  $54^{\circ}\text{C}$  ( $-20^{\circ}$  and  $130^{\circ}\text{F}$ ), spending 2 hours at each extreme and 2 hours in transition from one extreme to the other. The chamber relative humidity is controlled between 50 and 85%. As the temperature goes below freezing, frost is formed on the test troughs. Initially it was feared that this cycle was too severe and would destroy a large fraction of the test parabolas; obviously it was not. This type of cycle simulates about one year of freeze-thaw environment in one month. Even though other degradation mechanisms such as polymer degradation, fungus growth or rotting, etc. are not accelerated by this test, freeze-thaw was judged as the major threat to long-term reflector structure stability.



The data in Table II indicate that a number of constructions will provide environmentally stable reflector structures. Even under room conditions, small changes did occur, indicating that in many cases the severe environmental cycling had less effect than room storage.

Ice ball impact testing (hail simulation) using a range of balls from 12.7 to 38 mm diameter has given some insight into how sandwich structures behave under impact. Plastic deformation and crushing of the core materials appears to govern the size of the dent. Composite indenter hardness measurements are being made using indentors with from 12.7 to 38 mm diameters. The sandwich structure hardness and work of indentation may give numbers which will quantify the structures' resistance to hail impact damage.

#### New Materials

The specular reflectance properties of several silver plated brass samples obtained from International Silver Co. were measured. These materials offer high solar averaged hemispherical reflectance values ( $\geq 90\%$ ) and potential for low cost ( $\$1.50/\text{ft}^2$ ), although they will require a transparent protective coating over the silver. A potential area of concern in using these materials in a focusing collector system is the large amount ( $\sim 10\%$ ) of reflected radiation that is diffusely scattered from the residual polishing marks in the brass substrate, resulting in a decrease in the specularly reflected beam. Also of interest is the width of the specularly reflected beam from these materials.

The samples received included mechanically buffed and silver plated 90-10 brass (90% Cu, 10% Zn), 80-20 brass and 70-30 brass. The reflectance of silver-plated 430 stainless, 301 stainless and a (70% Cu, 22% Zn, 8% Ni) material could not be measured because the samples were too stiff to be mounted on our optically flat vacuum chuck.

The specular reflectance properties of the brass samples were determined at 500 nm for collection apertures from 1 mrad to 12.8 mrad for an angle of incidence of  $20^\circ$  from normal. The reflectance properties are assumed to be isotropic since a polishing direction was not evident from a visual inspection of the samples. The reflectance data are presented in Figure 13 together with the hemispherical reflectance,  $\rho(2\pi)$ , at 500 nm as measured with a Beckman DK-2 Spectroreflectometer. The hemispherical reflectance represents the reflectance value for an angular aperture of  $\pi$  radians (i. e., over a hemisphere). For comparison, the specular reflectance properties of an optically flat mirror would be represented by a horizontal line in Figure 13.

Ignoring the absolute value of  $\rho(2\pi)$  for each material, since this is known to decrease rapidly upon exposure to the atmosphere, the most straightforward analysis of the specular reflectance curves involves curve fitting the data to a normal distribution of the form

$$R(\Delta\theta) \propto R_o e^{-\frac{\Delta\pi^2}{2\sigma^2}}$$

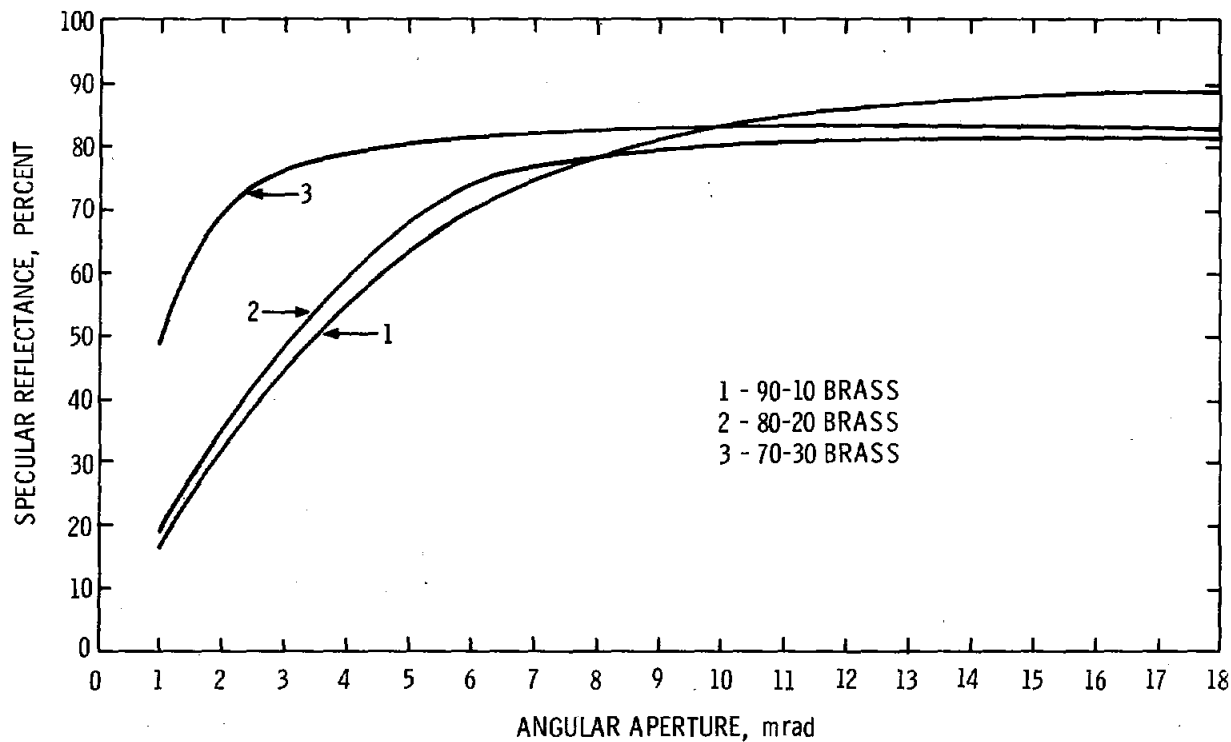


Figure 13. Specular Reflectance of Silver-Plated Brass Samples at 500 nm

where  $\sigma$  is the standard deviation of the distribution (i. e., width),  $\Delta\theta$  measures the angles with respect to the specular direction and  $R_o$  would be a measure of the intensity of the specularly reflected beam.<sup>1</sup> Then the difference between  $\rho(2\pi)$  and  $R_o$  could be considered as a reflectance loss for each candidate material, at least for a focusing solar collector system. From the data, the values in Table III were determined.

TABLE III

Specular Reflectance Properties at 500 nm

Material	$\rho(2\pi)$	$R_o$	% Loss	$\sigma(\text{mirror})$
90-10	0.90	0.86	4	2.5 mrad
80-20	0.88	0.80	9	1.7 mrad
70-30	0.91	0.81	11	0.7 mrad

<sup>1</sup>"Specular Reflectance Properties of Mirror Materials," by R. B. Pettit, presented at the Joint Conference American and Canadian Solar Energy Societies, Vol. 6, p. 331, August 15-20, 1976.

For comparison, note that the standard deviation which characterizes the sun is  $\sigma(\text{sun}) \sim 2.5$  mrad (even though the full width of the sun is 10 mrad).

The results show that as the reflected beam width decreases ( $\sigma$  becomes smaller), the percent reflectance loss increases. However, the results for the 80-20 brass are comparable to the results which have been measured for some laminated plastic mirrors, and, therefore, are in the right ballpark for consideration.

Two special aluminum reflectors from Aluminum Company of America (ALCOA) were also measured. Special material S460667 represents their highest quality reflector sheet and has a hemispherical solar reflectance of 0.92. The second material (S460666) is the same as the first material but with an experimental anodizing treatment. The solar averaged specular reflectance properties are shown in Figure 14 together with the properties of Alzak Type I specular reflectance sheet. Note that both of the experimental materials have a higher specular reflectance value than Alzak although the hemispherical solar reflectance of S460666 is less than that of Alzak (see Table IV). Because the specular reflectance values at a large angular aperture ( $\sim 18$  mrad) are below the hemispherical reflectance values, a large amount of the reflected radiation is diffusely scattered, probably from the residual polishing marks in the substrates.

An indication of the fraction of the reflected beam that is diffusely scattered is given in Table IV, together with the approximate width of specularly reflected beam. Note that both special samples have less diffuse reflectance as compared to Alzak, while the specular beam widths are almost identical.

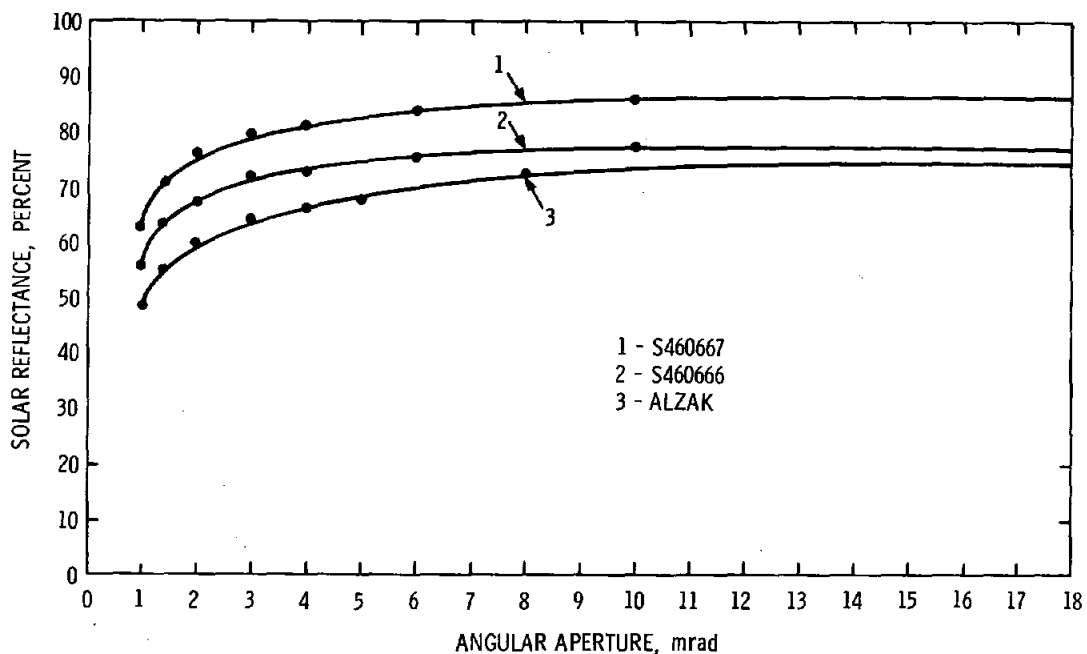


Figure 14. Solar Reflectance Properties of Special Aluminum and Alzak Reflectors

TABLE IV

Reflectance Properties of Special Alcoa Aluminum Reflectors and Alzak

<u>Material</u>	<u>Hemispherical Solar Reflectance</u>	<u>Diffuse Reflectance</u>	<u>Specular Beam Width</u>
S460667	0.92	6%	1.0 mrad
S460666	0.82	7%	1.0 mrad
Alzak	0.85	17%	1.0 mrad

## Cleaning Procedures Applied to Al-FEP Reflector

The specular reflectance properties of both dirty and clean aluminized FEP teflon mirror material have been obtained. Weathered mirror materials obtained from the Solar Total Energy Test Facility were subjected to one of four different field cleaning procedures:

1. High pressure water cleaning, deionized water rinse and air dry (Mirror R54, sheet #16).
2. Hot soapy water cleaning, cloth wipe, deionized water rinse and wipe dry (Mirror R56, sheet #19).
3. Jet-X with cream-cote detergent cleaning, deionized water rinse and air dry (Mirror R58, sheet #18).
4. C-120 (a commercial cleaner from McGean Chemical Co.) sprayed in a mist with the sample mounted at 45° to the horizontal, tap water rinse, deionized water rinse and air dry (Mirror R60, sheet #14).

Specular reflectance properties at 500 nm were obtained for each mirror in the as-received (dirty) condition, after the field cleaning listed above, and then after an ultrasonic cleaning for 2 minutes in the C-120 solution. It was hoped that the ultrasonic cleaning would represent the "best" cleaning possible. The specular reflectance properties of these mirrors in the as-received condition and after the field cleaning procedures, together with the properties of unexposed material are shown in Figure 15. The specular reflectance values at an angular aperture of 10 mrad are listed in Table V.

TABLE V

Specular Reflectance Values at 10 mrad for the Al-FEP Mirrors

<u>Sample</u>	<u>As-Received</u>	<u>After Field Cleaning</u>	<u>After Field and Ultrasonic Cleaning</u>
R54	0.57	0.72	0.76
R56	0.58	0.70	0.73
R58	0.54	0.75	0.75
R60	0.60	0.75	0.78

Note the following:

(1) The additional improvement in the specular reflectance at 10 mrad for the ultrasonic cleaning compared to the field cleaning averaged about 3% (the maximum was 4% while the minimum was 0%). Note that the specular reflectance of the sample that was wiped also increased ~3% after the ultrasonic cleaning. Thus to within a few percent, all the field cleaning techniques listed above are equivalent.

(2) After the ultrasonic cleaning, the specular reflectance at 15 mrad for mirrors R54, R56, and R60 is only 1 - 3% below the value for the unexposed material. This difference can be easily accounted for as manufacturing, material and/or sample mounting variations. However, mirror R56 has a residual reflectance loss at 15 mrad of over 7%. Optical microscope pictures of the outer teflon surface show a large number of small scratches which are not present in the other mirror samples. The scratches are all in the same direction as opposed to being random. Because this is the only material that was wiped during the field cleaning procedure, it appears as if the scratches, and thus the reflectance loss, are a result of the wiping. Therefore, wiping of these materials is not advised.

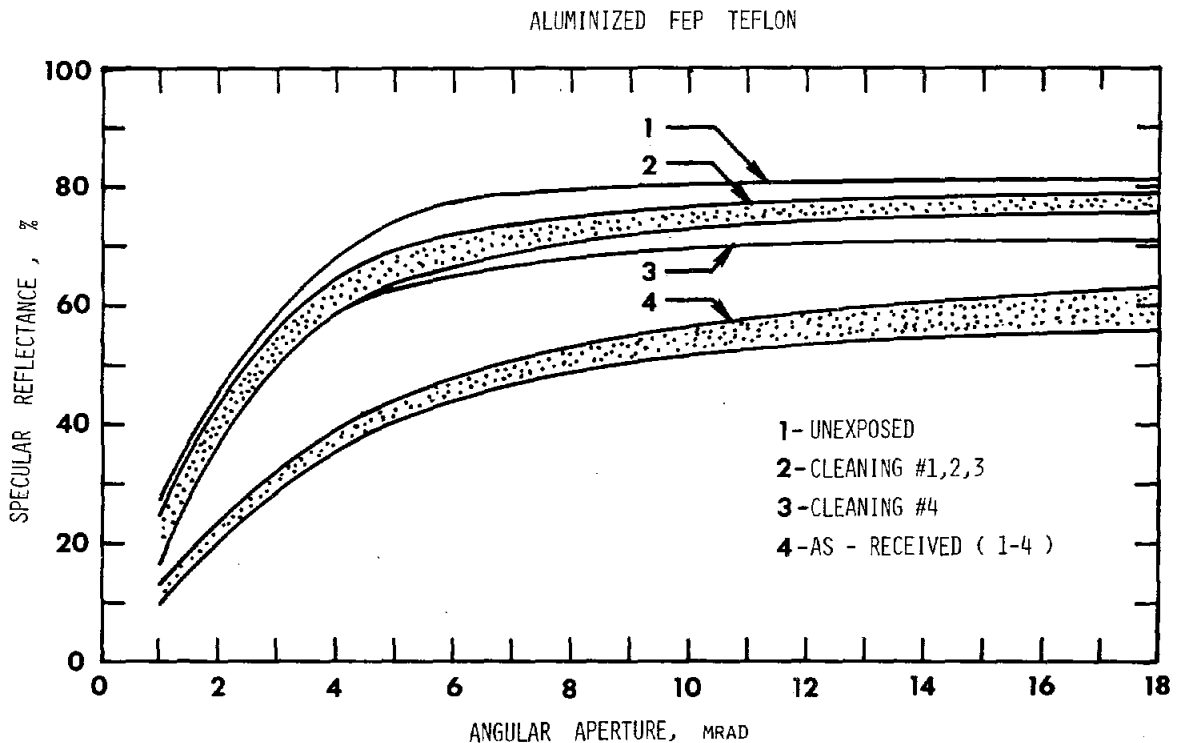


Figure 15. Specular Reflectance Properties of Aluminized FEP Reflectors

It is interesting to note that this set of weathered Al-FEP mirrors do not show the large residual reflectance loss reported in the previous semiannual report (SAND76-0662). In that report reflector sheet #20 showed a residual reflectance loss of ~9% after careful cleaning. Optical microscope pictures of the exposed teflon surface show what appear to be small nicks or cuts. There do not appear to be any scratches in the teflon even though sheet #20 was "lightly" wiped during the final cleaning. The origin of these nicks is unknown at the present time.

#### Reflectance Properties of 3M Scotchcal 5400 After 50, 67 and 84 Months Outdoor Exposure

Weathered samples of 3M's 5400 Brand "Scotchcal" film bonded to aluminum panels were obtained from B. Johnson, Manager, Product Development, Decorative Products Division at 3M. All panels had been mounted at a 45° angle, facing south at a location in the Miami, Florida, area for exposure times of 50 months (sample LI-4-2), 67 months (sample LR-2) and 84 months (sample 10-4). Also obtained were unexposed controls for each exposure sample.

Each sample consists of two 10-cm by 7-cm 5400 films bonded to a painted aluminum panel approximately 28-cm by 7-cm wide. The two films overlap at the center of the panel so that film-to-film bonding can be studied. In addition, a short razor slit was made in one film on each panel before the outdoor exposure. There is no visible edge protection on any of the panels. The adhesive used to bond the films to the panels is the same adhesive used today. In addition, each film exhibits the characteristic orange-peel texture that has been eliminated in 3M's new 5400 film designated FEK-163.

The hemispherical reflectance from 250 nm to 2500 nm was measured with a Beckman DK-2 Spectroreflectometer, while the specular reflectance was measured at 400, 500, 700 and 900 nm using a bi-directional reflectometer as previously described.<sup>1</sup> For the latter measurements, the panels were mounted on an optically flat vacuum chuck.

#### Hemispherical Reflectance

The solar averaged hemispherical reflectance values of all panels, exposed and unexposed, were identical (within experimental error) at 0.85 and also equal to currently manufactured material. Thus, the solar averaged hemispherical reflectance of this product has not changed after 7 years outdoor exposure. In addition, these results indicate that the hemispherical reflectance of this product as manufactured over the past 10 years has been constant. The one exception to these results is one of the two films mounted on the 84 month sample. This film appears to have a milky or fogged appearance to the unaided eye; this will be commented on later.

The wavelength in the ultraviolet where the reflectance decreases to less than one-half the solar averaged reflectance occurs at ~360 nm for the unexposed samples, while for all the exposed samples, the cutoff occurs at ~250 nm (Figure 16). The reason for this change is unknown at the present time. Because this occurs at such a low wavelength, it has very little effect on the solar average reflectance.

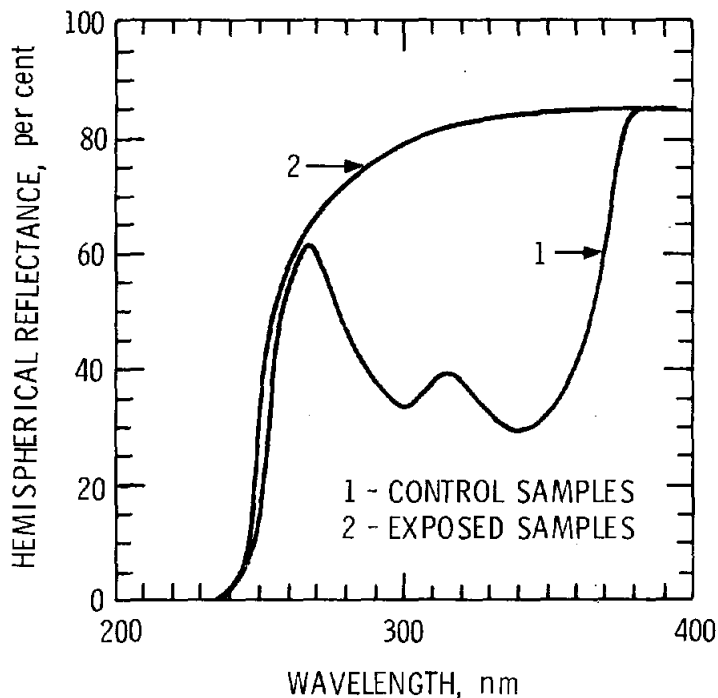


Figure 16. Hemispherical Reflectance of 3M Scotchcal 5400

#### Specular Reflectance

The outdoor exposure samples do not represent an ideal sample for detailed specular reflectance measurements, because the samples were prepared by 3M mainly to study the overall performance of the 5400 film in an outdoor environment, such as: delamination, undercutting from the exposed film edges or the razor cuts, visual loss or change in the reflectance, etc. From this standpoint, the samples have held up very well. Delamination, either from the panel, at the film-to-film overlap region or near the razor cut, is not evident in any of the exposed samples. In addition, there appears to be no undercutting or other change in the aluminum film, in agreement with the hemispherical reflectance measurements.

However, there are numerous scratches in the exposed acrylic surface. Because most of these scratches are along the length of the panel, they probably result from adverse handling and/or mechanical cleaning of the surface and not as a result of the environmental exposure. The scratches definitely will reduce the specular reflectance, although it is difficult to estimate by how much. As evident from the hemispherical reflectance, the scratches do not absorb radiation, they only scatter the reflected radiation.

The specular reflectance properties of the controls showed as much variation as previously measured unexposed material. However, all materials have the same specular reflectance values to within 2% at an angular aperture of 10 mrad. Thus an appropriate angular aperture for the comparison of specular reflectance values of the controls with the exposed samples is at ~10 mrad.

In addition, because of the variations in the reflectance properties of the controls, the presence of the surface scratches and the variability of the mounting procedure, it was felt that curve fitting the resulting specular reflectance profiles with normal distributions would not be profitable (see Figure 17). Therefore, listed in Table VI are the specular reflectance values at 10 mrad angular aperture as a function of the exposure time and wavelength.

TABLE VI  
Specular Reflectance at 10 mrad Angular Aperture

Sample	400 nm		500 nm		700 nm		900 nm	
	R	Decrease	R	Decrease	R	Decrease	R	Decrease
0 mo	.84	0%	.83	0%	.81	0%	.82	0%
50 mo	.74	12%	.77	7%	.77	5%	.79	4%
67 mo	.73	13%	.65	22%	.69	14%	.77	6%
84 mo	.61	27%	.66	20%	.70	13%	.69	16%

Note the following points:

(1) The percent loss increases as the outdoor exposure time increases, with the loss for the 67 mo and 84 mo sample being quite similar. Thus the specular reflectance has decreased only 15-20% after 7 years exposure. If the samples had been subjected to more careful handling, the loss after this time would have been less.

(2) Generally, the percent loss decreases as the wavelength increases, as expected. However, the trend is not uniform for all the samples.

(3) As previously mentioned, one film on the 84 month sample had a milky appearance, while the other film did not show any fogging (the specular reflectance properties of the better film are listed in Table I). The fogging reduced the specular reflectance ~20% below the values for the unfogged film. Optical micrographs showed that the fogging was due to a fine pattern on the acrylic surface. The pattern appears to be composed of ~0.4 micron diameter particles with a density of  $\sim 10^8/\text{cm}^2$ . This means that the particles cover ~20% of the acrylic surface. Because the particles are small, it is difficult to determine from the optical micrographs whether they are contaminants on the acrylic or defects in the acrylic.

(4) There were very few defects at the acrylic-aluminum interface in the control or exposed panels, except for the 50 month sample. There were some defects for this panel but their density is less than  $5 \times 10^5/\text{cm}^2$  and the fractional area covered is less than 1%. However, the defects appeared similar to the defects found in the FEK-163 mirror after temperature and humidity cycling in the environmental chamber.<sup>2</sup>

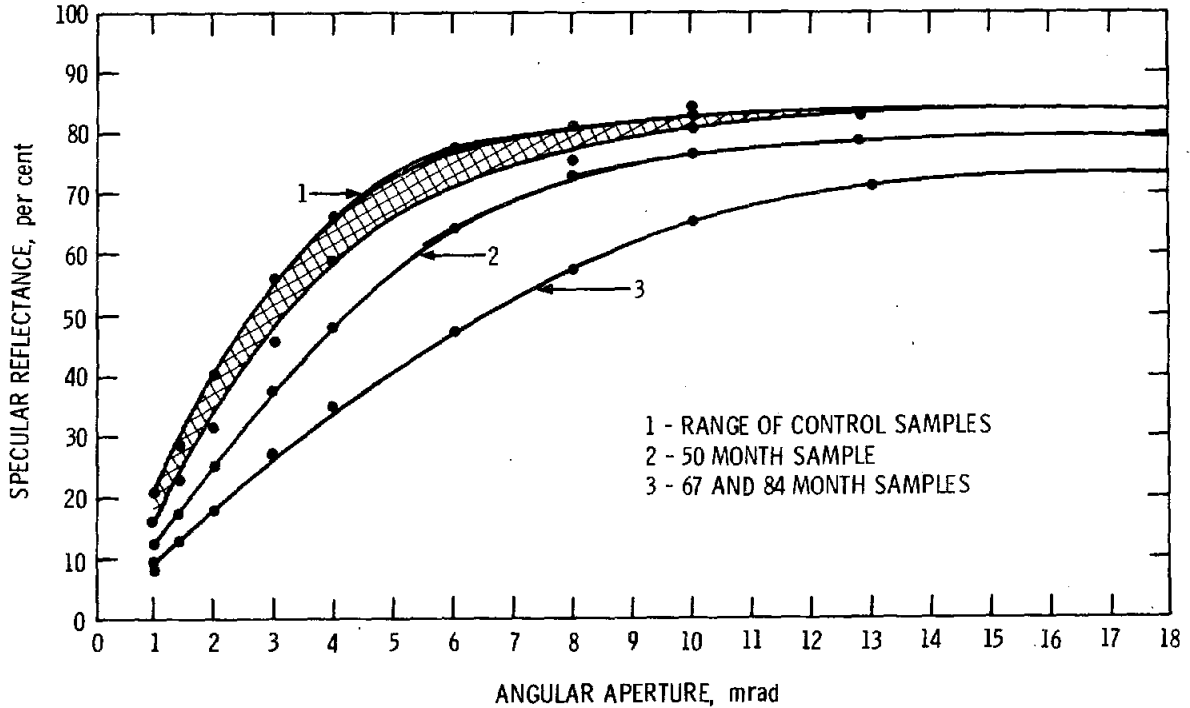


Figure 17. Specular Reflectance Properties of 3M Scotchcal 5400 at 500 nm

In-Situ Collector Characterization -- The in-situ laser ray trace inspection apparatus was described in previous semiannual reports (SAND76-0205, SAND76-0662). Responsibility for development of this inspection system has been consolidated within one group for completion and implementation. Figure 18 is a photograph of the in-situ tester positioned in front of a small section of a solar parabolic trough reflector.

The control and data collecting microprocessor is also visible in the photograph. A laser beam is directed onto the mirror by the scanning mechanism and the returning reflection strikes the long detector bar.

The detector bar assembly contains a linear array of 360 photodiodes spaced 2.54 mm on centers. This detector system was selected as a result of the work reported in the last semiannual report. The detector scanning electronics is being rebuilt so that high ambient light levels do not saturate the output and to allow scanning of a subarray of the entire detector array for more efficient data collection.

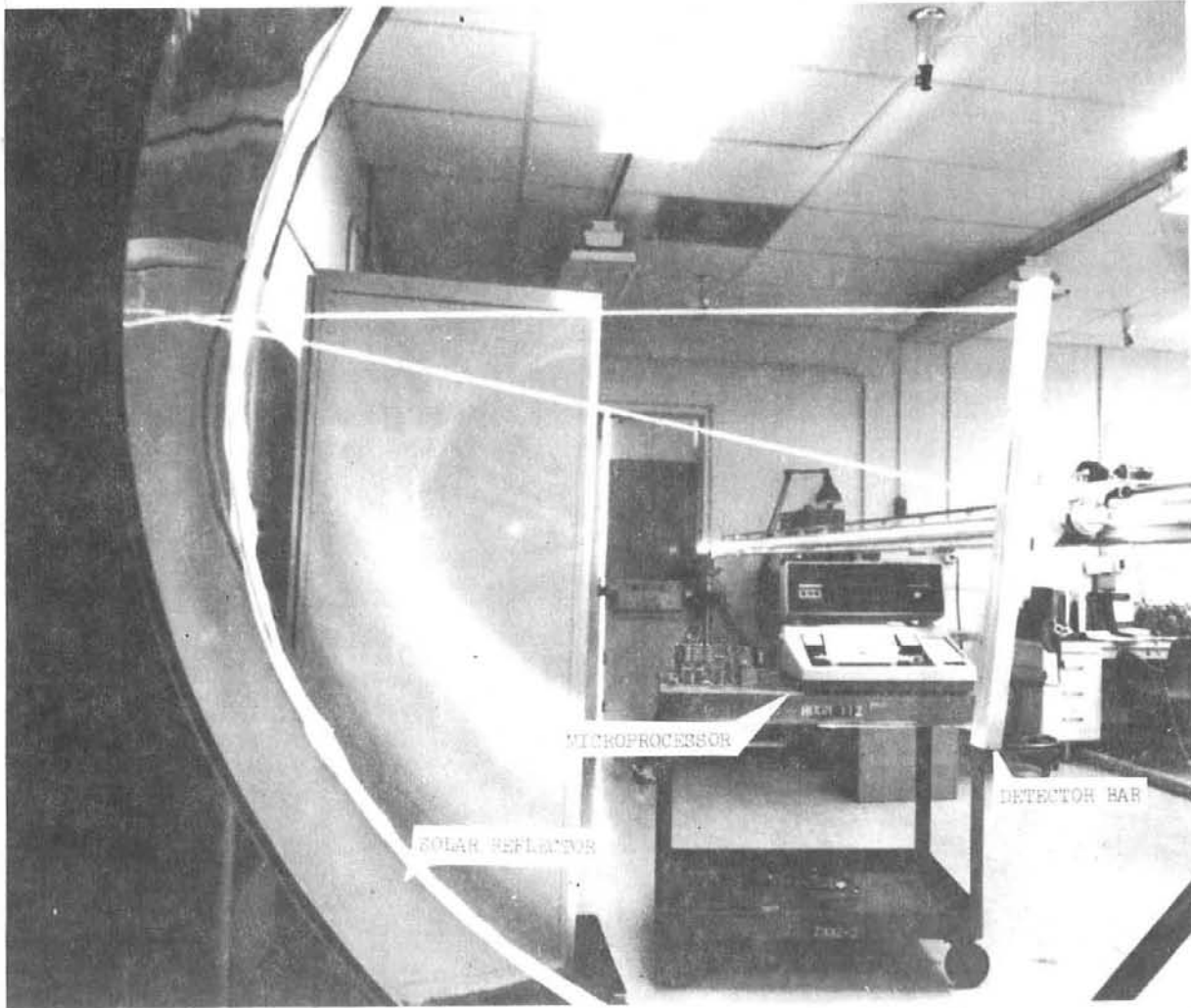


Figure 18. In-Situ Laser Ray Trace Tester

A fast A/D converter will be used to measure the detector outputs instead of the previous threshold detector. In this way, variable dark current and sensitivity of individual detector diodes can be compensated. Methods for measuring the deviations of the scanning system in the vertical and horizontal planes and angular variations due to twisting of the support beam are being implemented in the error analysis study.

Necessary electronics and interfacing hardware to move the beam truck and scan the parabolic troughs is presently under design. All necessary position encoders have been selected and ordered from data obtained from an error analysis study. This study is continuing to better define needs and future problems. The long delivery time on magnetic torque motors to power the vertical scanning has forced the use of the presently installed synchronous motor drive even though some error introducing vibrations may occur. Thermal distortion effects are also being evaluated on the existing hardware.

Parallel efforts in electronic design, software development, systems analysis and mechanical design are underway to decrease the completion time of the in-situ tester. Component delivery schedules along with necessary shop time are presently problems that are being closely monitored.

References, Task 3.2

1. R. B. Pettit, "Specular Reflectance Properties of Mirror Materials," Joint Solar Energy Society Meeting, August 15-20, 1976, Winnipeg, Canada.
2. Memo, R. S. Berg to Distribution, dated March 7, 1977, subject: "Degradation Mechanism in FEK-163 Mirror Surfaces of Sample SL58."

Task 4. Collector Subsystems Contracted

General Atomic, Raytheon and Sheldahl have been awarded contracts for the design, construction, installation and preliminary operation of a variety of solar collector field subsystems. Figure 2 illustrates where the various collector field subsystems will be located in the Solar Total Energy Test Facility. Installation of the subsystems is scheduled to be complete by the end of September 1977, with the exception of the parabolic dishes. Only one dish will be installed this fiscal year.

Table VII lists the projected characteristics of the Solar Total Energy Systems Test Facility when completed.

TABLE VII  
Projected Characteristics of Solar Total Energy System Test Facility

Collector Concept	Contractor	Area		Output kJ/Day x 10 <sup>-6</sup>		No. of Modules	Size of Modules (m)
		(m <sup>2</sup> )	(ft <sup>2</sup> )	Winter	Summer		
Parabolic Trough	Sandia	200	2160	2.14	2.39	20	2.7 x 3.6
FMSC	General Atomic	260	2800	2.19	2.66	32	2.1 x 3.8
Parabolic Dish	Raytheon	106	1140	2.04	2.73	3	6.7 diam
SLATS	Sheldahl	<u>260</u>	<u>2800</u>	<u>2.26</u>	<u>2.89</u>	14	3 x 6.1
		826	8900	8.63	10.67		

### General Atomic FMSC Collector Field Subsystem

Figure 19 illustrates the General Atomic FMSC (Fixed Mirror Solar Collector). This collector field subsystem will be located in the southeast quadrant of the Solar Total Energy Systems Test Facility. The subsystem will consist of two rows of collectors each 61 m (200 ft) long and the associated plumbing, hardware, and control systems. Each row of collectors will be made up of 16 reflector modules positioned end-to-end and measuring 3.8 m (12.5 ft) long and 2.1 m (7 ft) wide. The receiver consists of 4 continuous sections interconnected at their ends with a piece of flexible tubing. Each section is 15.2 m (50 ft) long and the assembly swings through a circular arc as shown in Figure 20 to keep it positioned at the focal line as the sun changes elevation angle. A discussion of each of the major elements of the subsystem follows.

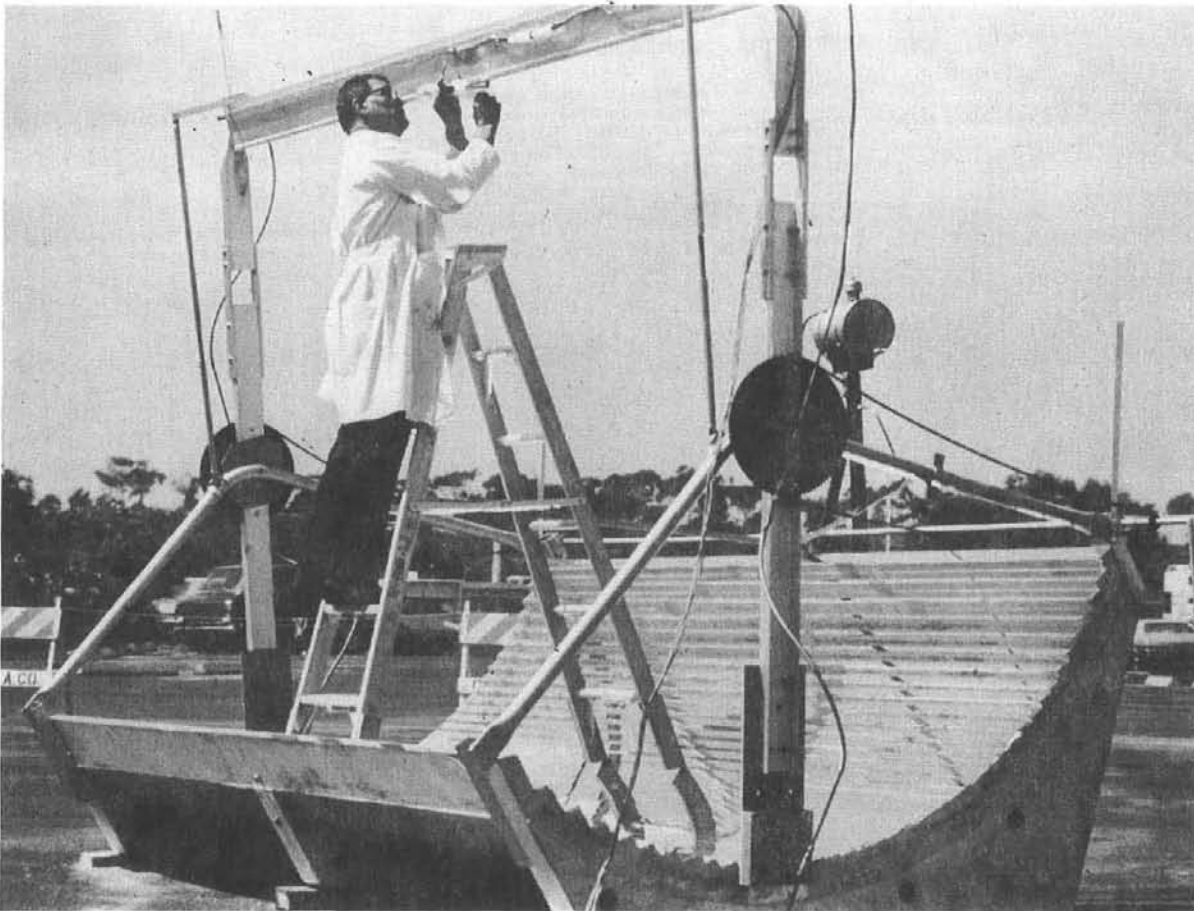
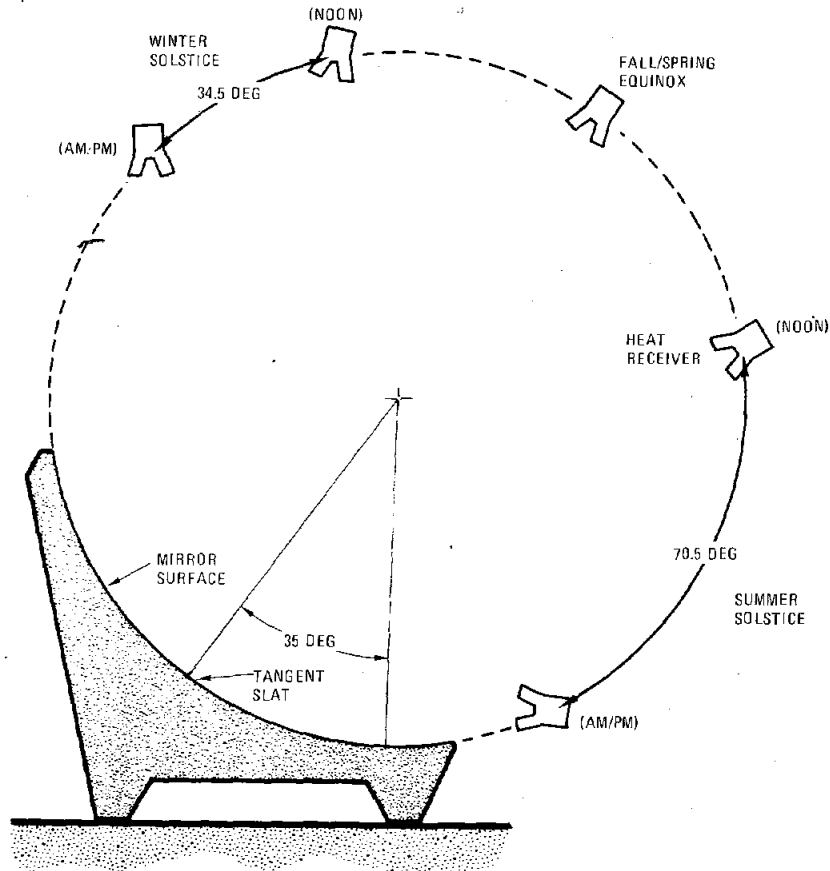


Figure 19. General Atomic Fixed Mirror Solar Collector



NOTE: 1. 90-DEG MIRROR MODULE  
 2. 35-DEG TILT  
 3. TANGENT SLAT 35 DEG FROM VERTICAL  
 4. 35-DEG LATITUDE  
 5. HEAT RECEIVER POINTS TO TANGENT SLAT  
 GA-A14209

Figure 20. Annual Movement of Receiver on General Atomic Collector

Reflector -- The reflector consists of a cast reinforced concrete trough with 5 cm (2 in.) wide flat glass mirror strips bonded to it. Precision forms have been constructed and techniques developed for casting the concrete troughs.

A variety of techniques for attaching the glass mirror strips to the trough have been evaluated. Three concrete samples with mirror strips bonded to them have been subjected to freeze-thaw cycling in Sandia's environmental chamber. To date a satisfactory combination of concrete sealant, adhesive, and mirror coating has not been found.

Tests on transferable adhesive and two-sided tape are being performed as a means of bonding the mirror strips to the concrete. Initial results are very encouraging. Not only does the adhesive give a very tenacious bond, the bond is slightly pliable permitting some differential thermal expansion, and it readily permits accurate positioning of the mirrors. The development of this technique could lead to automating the placement of the glass mirror strips on large systems. Test modules are being prepared for the environmental chamber.

A quantity of 1.5 mm (.060 in.) thick 0317 fusion glass has been purchased from Corning Glass Works for the collectors to be installed at the Solar Total Energy Test Facility. When silvered the result is a mirror with a specular reflectance of .94.

Receiver -- A cross section of the receiver design is shown in Figure 21. The development of a secondary concentrator that will maintain high values of specular reflectivity at relatively high temperatures may be a problem. This will be examined during a one-month test series scheduled to begin in June 1977 at Sandia's Collector Module Test Facility. During this test series a 16.2 m<sup>2</sup> (175 ft<sup>2</sup>) collector module will be operated under a variety of conditions using two different reflector materials--silvered glass and Kinglux.

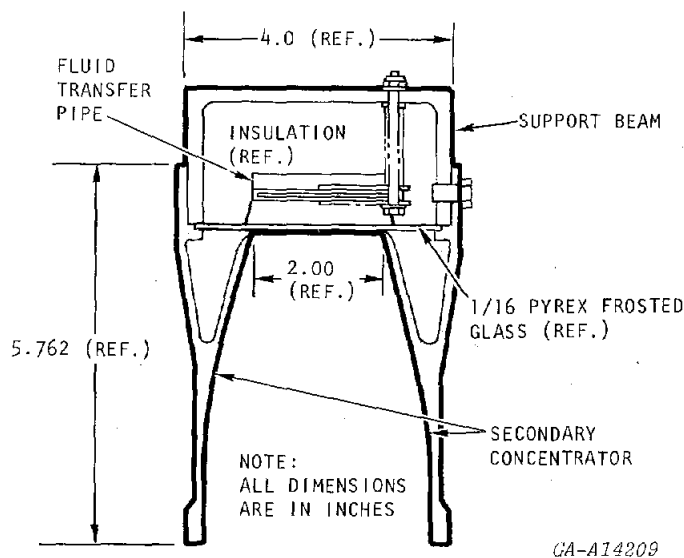


Figure 21. Cross-Section of General Atomic Receiver Design

A receiver tracking and control module has been ordered. This module is designed to control the receiver tracking, prevent over temperature and regulate the fluid outlet temperature. The prototype module will be tested during the test series in June. Figure 22 illustrates the receiver tracking control schematic.

Fluid Loop and Control System -- Figure 23 shows schematically the fluid system model used by General Atomic in the development of their control scheme. The fluid being used is Therminol 66.

A multivariable control scheme was developed in order to meet the startup and temperature control requirements. The scheme uses signals from the diagnostic and performance sensors required to monitor the collector subsystem's performance. A schematic of the multivariable control is shown in Figure 24.

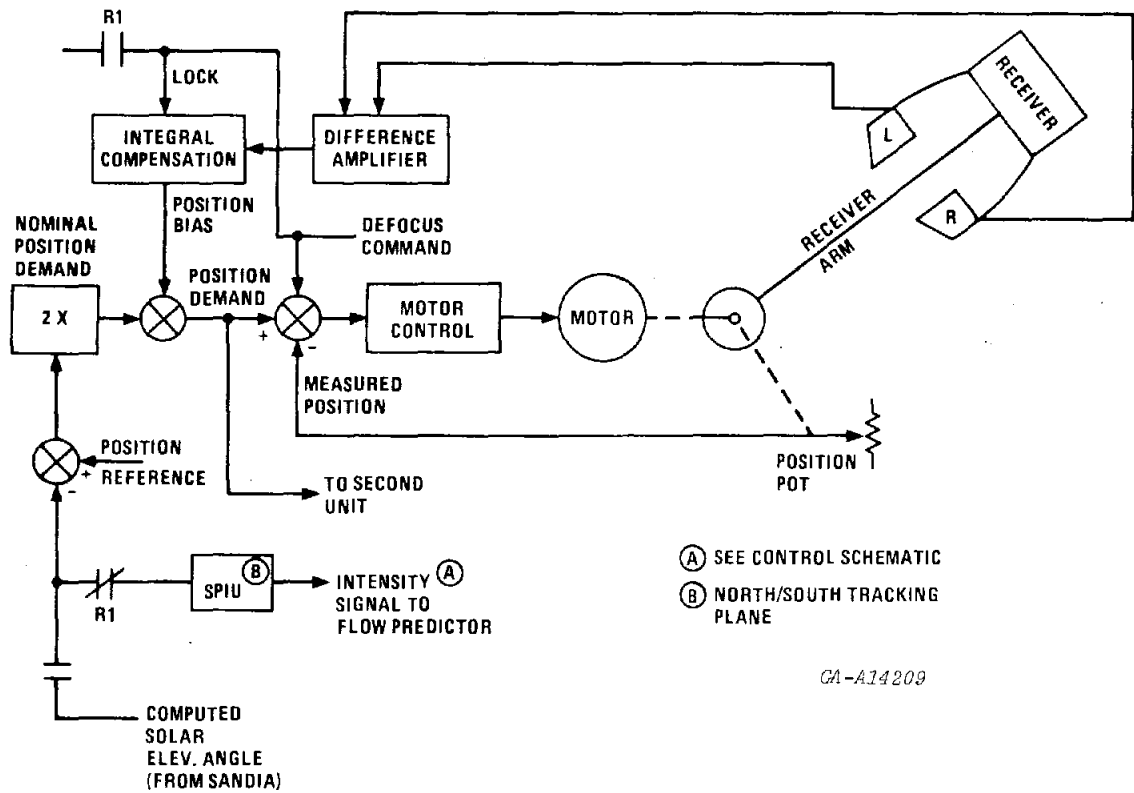


Figure 22. General Atomic Receiver Tracking Control Schematic

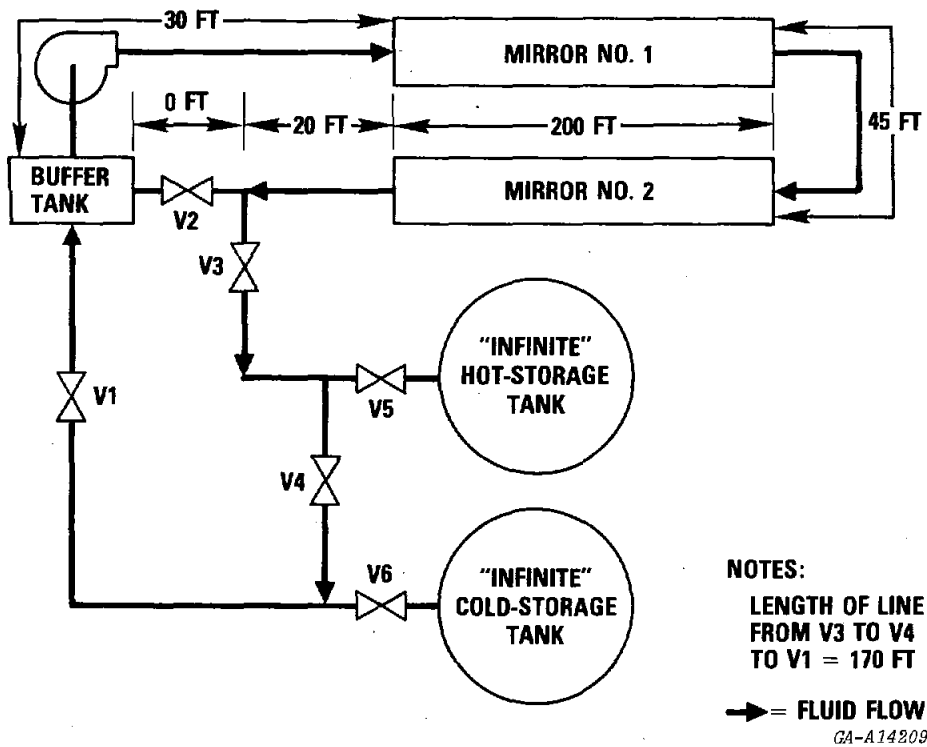


Figure 23. General Atomic Fluid System Model

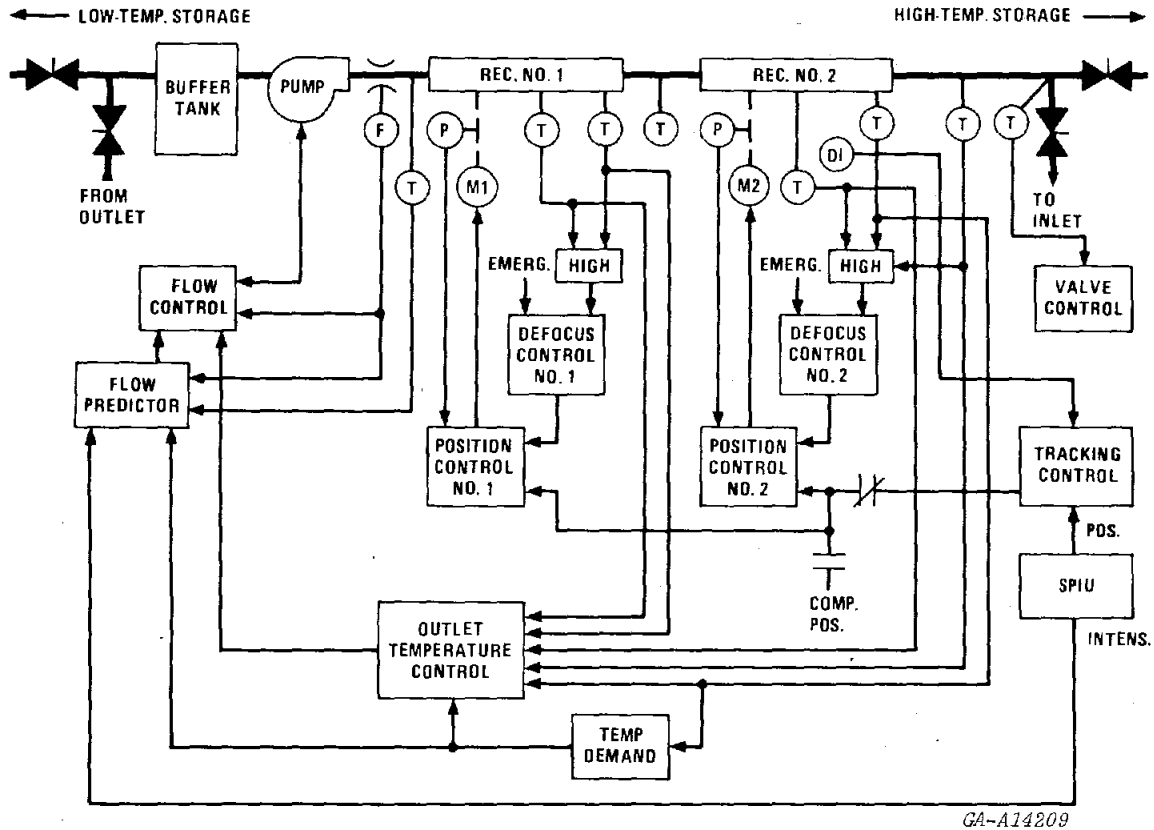


Figure 24. General Atomic Multivariable Control Schematic

The control consists of the following:

1. A temperature-regulating control, via flow adjustment, that uses a low-gain integral control on outlet fluid temperature and various proportional gains controls on receiver pipe temperatures at the midpoint and 10 ft from the outlet of both sections of the collector.
2. Temperature-limiting control, via defocus, which uses a proportional-gain control on the higher of the midpoint and 10-foot-from-outlet receiver pipe temperatures in each section of the collector.
3. A high-gain proportional emergency control, via defocus, on the outlet fluid and receiver pipe temperatures. This is an upper-bound setpoint control that does not act during normal conditions.
4. The standard sun-tracking and position controls previously described.
5. Flow setpoint control based on solar intensity, measured inlet temperature, demand outlet temperature, and an integrated flowrate/inlet-temperature product.

An example of the results of the multivariable control scheme applied to the FMSC system model is shown in Figure 25. In the example the problem of morning startup was examined. The initial conditions of the system were a buffer tank filled with Therminol 66 at 232°C (450°F) and the remainder of the fluid loop purged with nitrogen at ambient temperature. At time zero Therminol 66 was pumped out of the buffer tank, circulated, and recirculated through the system until warmup was complete.

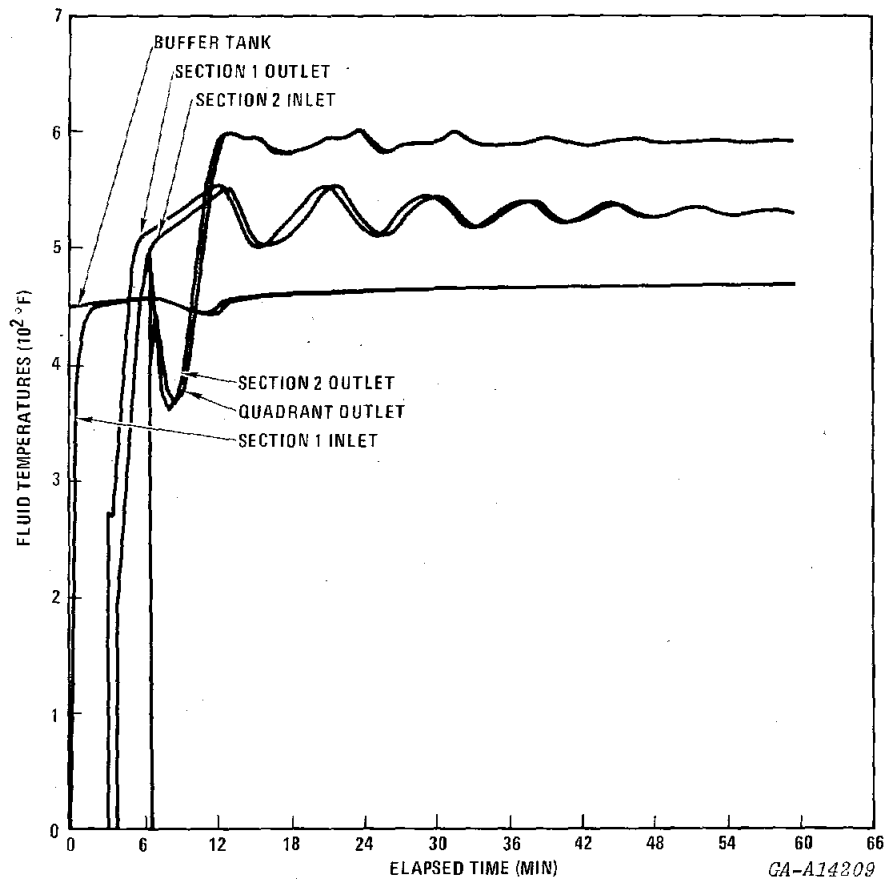


Figure 25. Fluid Temperatures for Purged System with Recirculation and Variable Minimum Flow (60-gal. Buffer Tank)

#### Raytheon Parabolic Dish Collector Field Subsystem

Figure 26 illustrates the Raytheon parabolic dish solar collector. This collector field subsystem will be located in the northeast quadrant of the Solar Total Energy Test Facility. The subsystem will consist of three individual collectors and the associated plumbing, hardware and control systems. Raytheon has a contract to deliver one collector this fiscal year. The other two will be provided when funds become available.

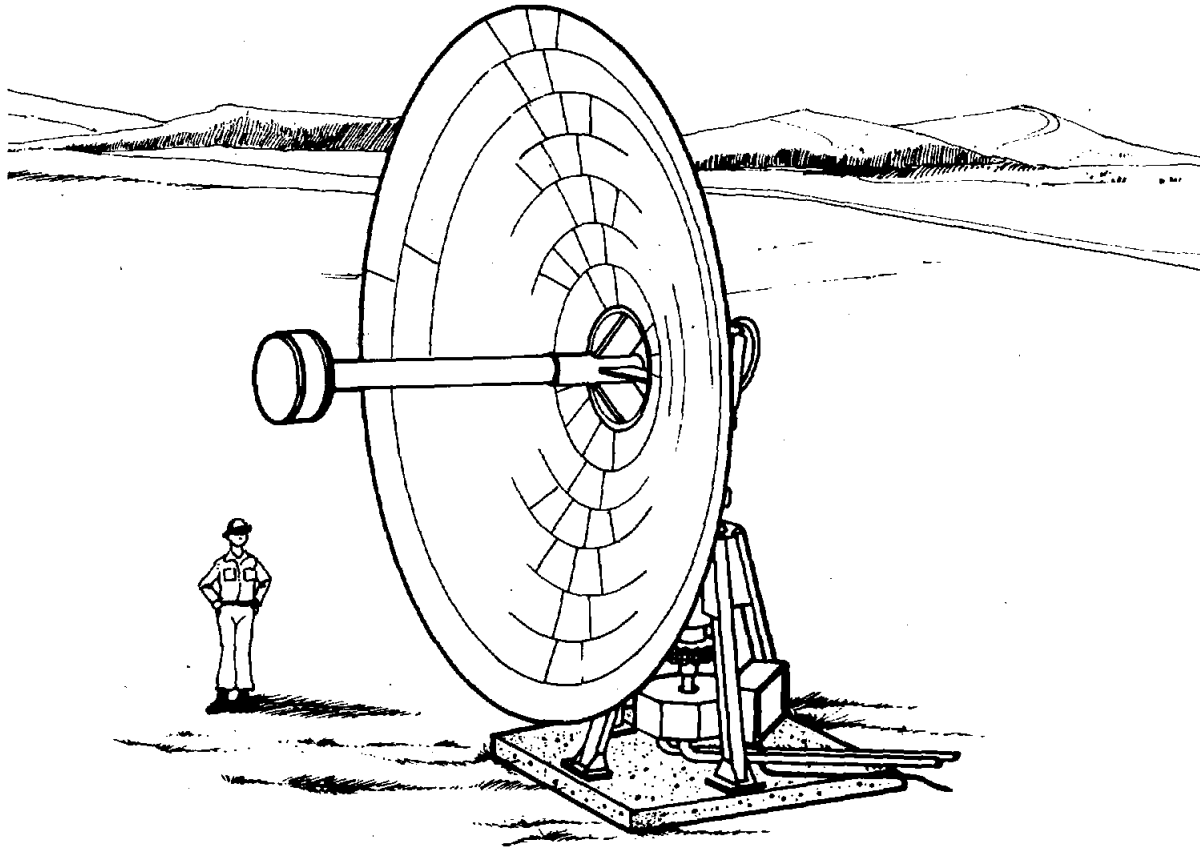


Figure 26. Raytheon Parabolic Dish Collector

The collector consists of a 6.7 m (22 ft) diameter fully tracking parabolic dish, which focuses sunlight into a cavity-type absorber. The absorbed thermal energy is carried away by the heat transfer fluid, Therminol 66.

#### Reflector

The parabolic dish reflector consists of a toric parabola, Figure 27. This is a figure of revolution around the collector center line. The reflecting surface is made up of approximately 200 spherical mirror segments. The segments are 3.2 mm (.125 in.) thick water-white crystal glass, silvered on the back side for a specular reflectance of .93. The segments are fastened to the support points by cap screws with rubber grommets through holes drilled in the glass as shown in Figure 28. The selected mirror mounting configurations have been subjected to simulated wind pressure loads in excess of 90 mph. The data generated was then used to verify the structural analysis previously performed. A dynamic loading test series will also be conducted including vibration and hail impact tests.

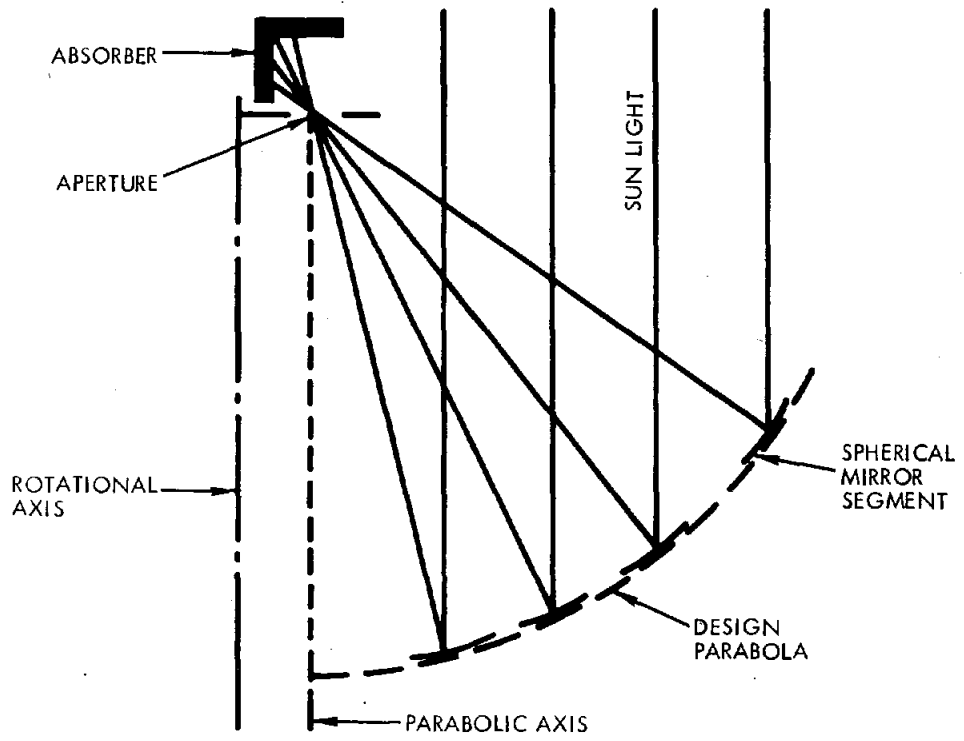


Figure 27. Toric Parabola Collector

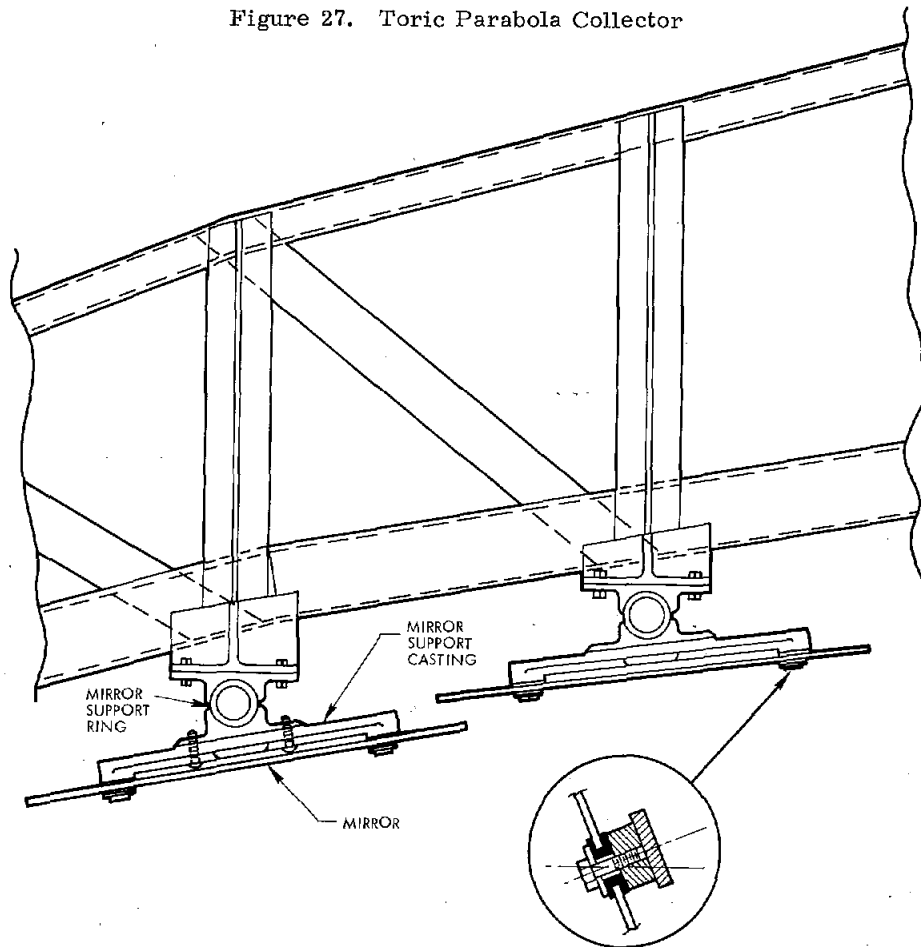


Figure 28. Reflector Mirror Mounting Details

## Receiver

A cross section of the receiver design is shown in Figure 29. The annular cavity has absorbing surfaces made of zirconium/copper. Therminol 66 flows through tubing that has been bonded to the back side of the zirconium copper. The tubing will initially be made of CuNi primarily due to its availability. Ultimately zirconium copper will be used because of its superior heat transfer characteristics. Material compatibility tests are being conducted by Raytheon to evaluate the possibility of chemical reactions between Therminol 66 and the zirconium/copper or copper/nickel at elevated temperatures. The absorbing surfaces will be plated with black chrome using a process developed by Highland Plating Co., Los Angeles, CA.

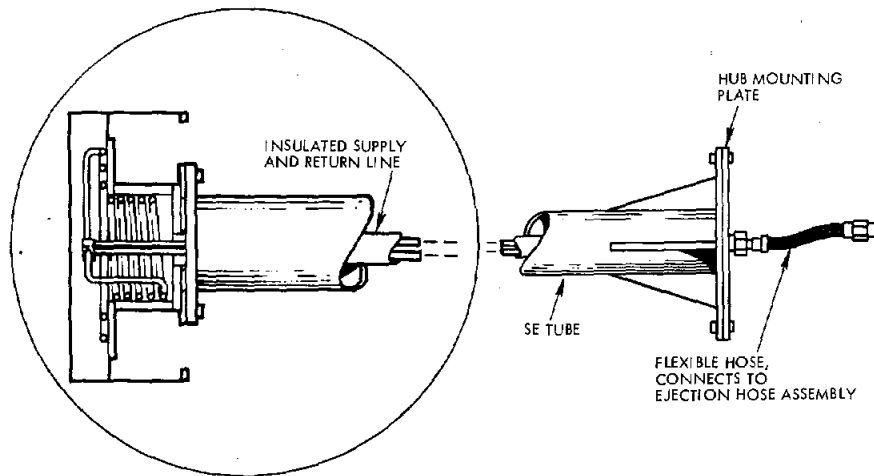


Figure 29. Raytheon Receiver Design

## Fluid Loop and Control System

Under the current contract the emphasis in the control area is on the tracking system for the collector. An open loop system is being developed. The collector to be delivered and tested will be equipped with a pair of shaft encoders to check the accuracy of the open loop system and provide the option of closed loop operation.

## Sheldahl SLATS Collector Field Subsystem

Figure 30 illustrates the Sheldahl SLATS solar collector. This collector field subsystem will be located in the southwest quadrant of the Solar Total Energy Test Facility. The subsystem will consist of two rows each 42.7 m (140 ft) long. Each row contains seven segments 6.1 m (20 ft) long. In each segment there are ten reflectors .3 m (1 ft) wide and 6 m (20 ft) long for a total reflector area of  $260 \text{ m}^2$  ( $2800 \text{ ft}^2$ ). The reflectors are concave arcs with a radius of 6.6 m (21.7 ft). This subsystem differs from the others in that it will use water as a heat transfer fluid. The thermal energy collected is transferred to the Therminol 66 in the remainder of the system via a heat exchanger. This subsystem heats the water to  $332^\circ\text{C}$  ( $630^\circ\text{F}$ ) in order to efficiently heat the Therminol 66 to  $311^\circ\text{C}$  ( $592^\circ\text{F}$ ) at the heat exchanger.

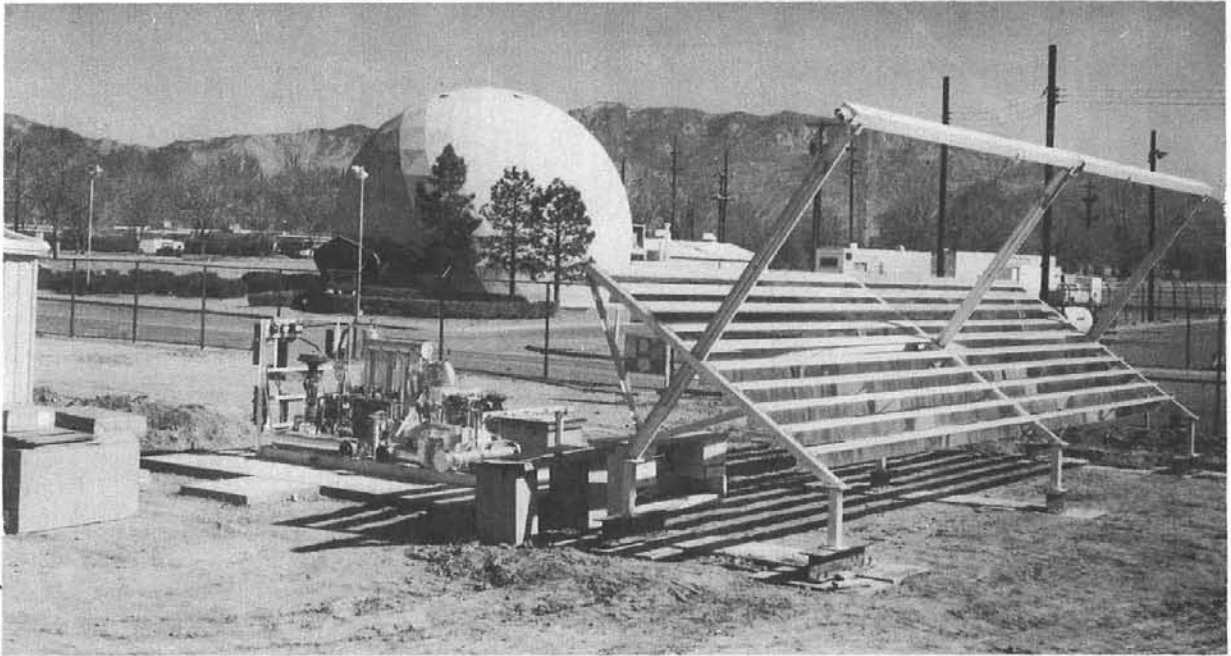


Figure 30. Sheldahl Solar Linear Array Thermal System (SLATS)

A discussion of each of the major elements of the collector field subsystem follows.

#### Heat Transfer Fluid

The heat transfer fluid is water. It costs approximately three orders of magnitude less per unit volume than Therminol 66. It is not flammable, creates no environmental problems in sanitary sewer systems, and has a much higher convective heat transfer coefficient,  $h$ , as determined by the equation.

$$h = \frac{k}{L} \left[ R_e^{0.8} P_R^{0.4} \right]$$

A comparison of water and Therminol 66 at 260°C (500°F) results in  $h_{\text{water}}/h_{\text{T66}} = 19.6$ .

A distinct disadvantage of water is the high saturation pressure associated with temperatures in excess of 260°C (500°F). Figure 31 shows how saturation pressure varies with temperature. By contrast, the vapor pressure of Therminol 66 at 315°C is only 50 kPa (7.5 psi). The heavier pipelines and receiver tubes required to contain the higher pressures associated with water adds to the thermal mass of a subsystem. This resulted in a warmup time of 1.7 hours for the water subsystem compared to 0.5 hour for the Therminol 66 subsystems. The high saturation pressure of water makes a fixed receiver almost mandatory until a reliable, long life, flexible connection can be designed and demonstrated.

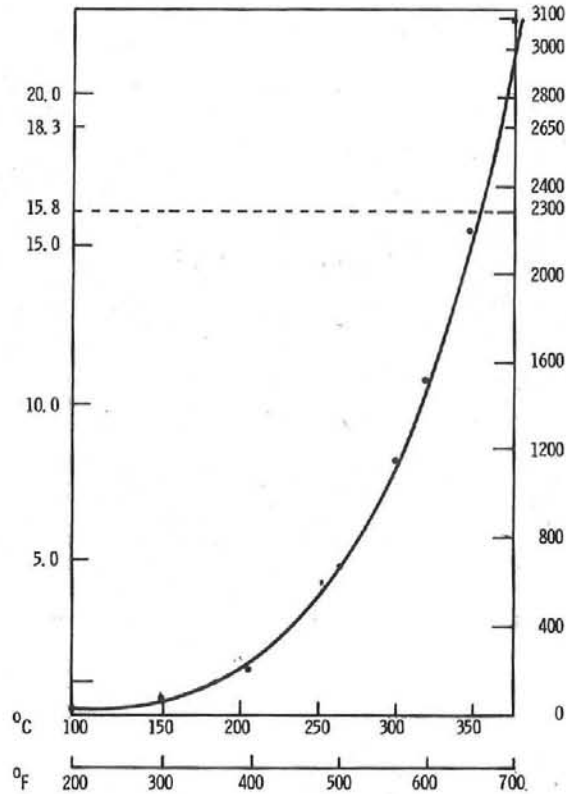


Figure 31. Pressure vs. Saturation Temperatures for Water

#### Receiver

The receiver was designed for a maximum allowable working pressure (MAWP) of 20.7 MPa (3000 psi) at 343°C (650°F). The actual operating conditions will be 19.3 MPa (2800 psi) at 330°C (626°F). At this temperature the saturation pressure of water is 15.8 MPa (2300 psi).

The above conditions violate a rule of thumb that the operating pressure should be 1.5 times the saturation pressure of the water. This is a good rule at lower temperatures, but used at temperatures near 300°C would require unduly heavy equipment. The value of 20.7 MPa for the MAWP was selected on the basis that local temperatures in the receiver might reach 360°C (680°F) for which the saturation pressure is 18.6 MPa (2700 psi).

The receiver for each of the two rows consists of two parallel lengths of schedule 160 carbon steel pipe (ASTM A-106B) with a schedule 40 carbon steel plug inside. The annulus between the ID of the pipe and the OD of the plug is 3.2 mm (.125 in.) wide, Figure 32. Water enters the east end, traverses the 42.7 m length, makes a "U" turn and returns to exit at the east end. Empty, the receiver weighs 13.7 kg/m (9.24 lb/ft). Filling the annulus with water adds .71 kg/m (.39 lb/ft). To heat the entire receiver from an early morning temperature of 20°C (68°F) to an average operating temperature of 308°C (587°F) requires 215,000 kJ.

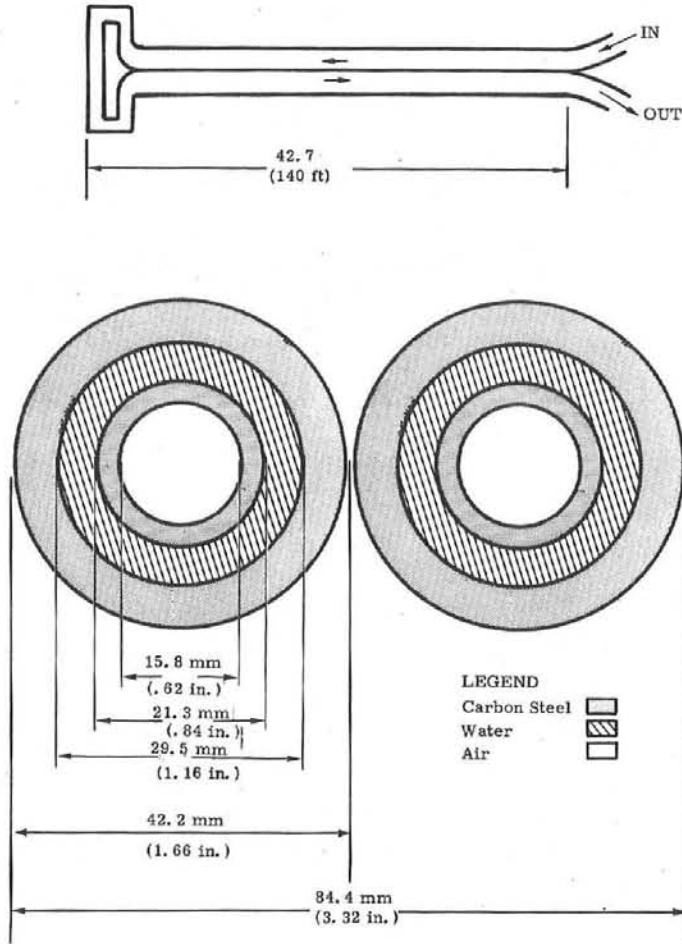


Figure 32. SLATS Receiver, Plan View and Cross Section

It should be noted that the 84.4 mm (3.32 in.) receiver width is the result of predicted dispersion of reflected light and not of any limitation imposed by the heat transfer characteristics of water. Thus, if the focus could be sharpened so that all of the reflected light would fall on one pipe, the receiver weight and the warmup time could be cut by approximately 50%.

Further, if the operating temperature could be reduced from 332°C to 315°C, the temperature used in the other collector subsystems, the operating pressure could be reduced by 2.6 MPa (380 psi) to 16.7 MPa (2420 psi).

The size of the pipe in the receiver is determined by calculating the wall thickness required for a maximum stress of 0.25 x ultimate yield. Added to this thickness is an arbitrary 1.7 mm (.065 in.) for corrosion and an allowance for pipe threads. The pipe with the next larger wall thickness is then selected.

The use of high strength low alloy steels such as 4130 or croloy will reduce the thermal mass of the receiver. Their use was rejected in this application because of increased cost and welding problems.

In summary, the thermal mass of receivers which use water as a heat transfer fluid can be reduced by:

1. Sharpening the focus so as to reduce the required area of the receiver,
2. Lowering the operating temperature, especially when it is in the area of 330°C, and
3. Using high strength, low alloy steels such as 4130 or croloy.

#### Reflector

As the result of poor life characteristics as reported in the previous semiannual report,<sup>\*</sup> Sheldahl decided to abandon the second surface (teflon reflective surface) and to switch to glass. The glass is silvered, formed to shape, and bonded to a stiff retaining surface.

Through Corning Glass Works quantities of 1.5 mm (.060 in.) 0317 fusion glass became available. Measurements at Sandia showed this glass (when silvered) to have a specular reflectance of .94 which is better than most float glass. The glass is first silvered and then cut into rectangles 30.5 x 118.4 mm (12 x 46 5/8 in.). Next the glass is bent to shape over a mandrel using a vacuum. Polyester and a catalyst are sprayed on, then a piece of high density plywood is bonded to the glass and "Z" bar is bonded to the plywood as shown in Figure 33. In the meantime, edges are formed on a piece of 61 mm (2 ft) wide sheet of 28 gauge galvanized steel sheet. The sheet is bent into a semicircle and attached to the "Z" bar with a dimpling tool as shown in Figure 34. Caps are placed over the ends, and the reflector is ready for mounting.

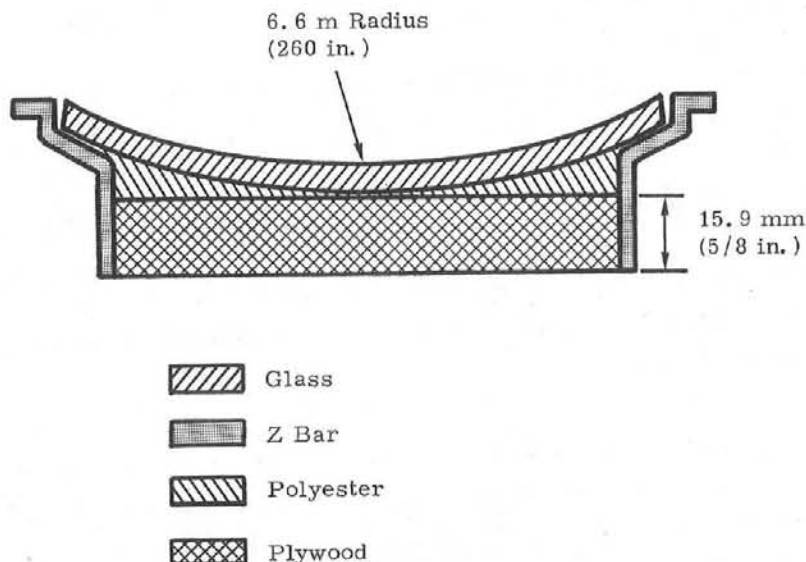


Figure 33. Reflector Bonded to Plywood

<sup>\*</sup> SAND76-0662, pp 33-35.

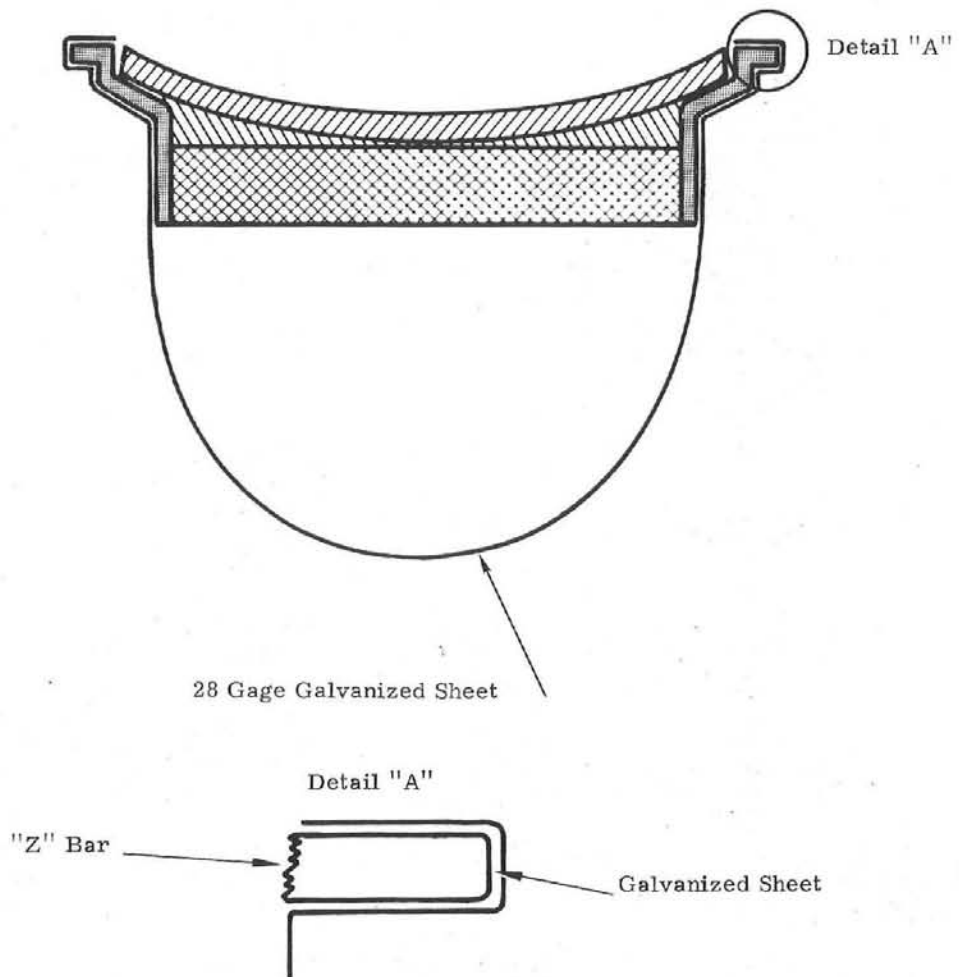


Figure 34. Reflector and Substrate Assembled to Galvanized Sheet Support

The tensile stress in the outer surface of the glass is of some concern since it approaches the practical limit for reliability. Also, the compression stress on the inner surface should make the glass less vulnerable to impact as from hail. Tests will be conducted to determine the vulnerability of the glass to impact.

#### Field Controller

The field controller monitors the demand signal from the system user and the intensity of the sun. A control logic flow chart is shown in Figure 35. If there is a demand and collectable energy, the controller signals the fluid loop to operate. When the heat transfer medium is circulating, a signal is returned to the field controller which permits the module controllers to be enabled. If the outlet temperature from each row is within operational limits and the mode selector switch on the field controller is in the "ON-AUTOMATIC" position, the rows are then enabled (the module controllers will then focus their set of mirrors on the receiver). Failure of any of these conditions causes the "DISABLE" (or protect) signal which the module controllers respond to by rotating the mirrors into the storage position.

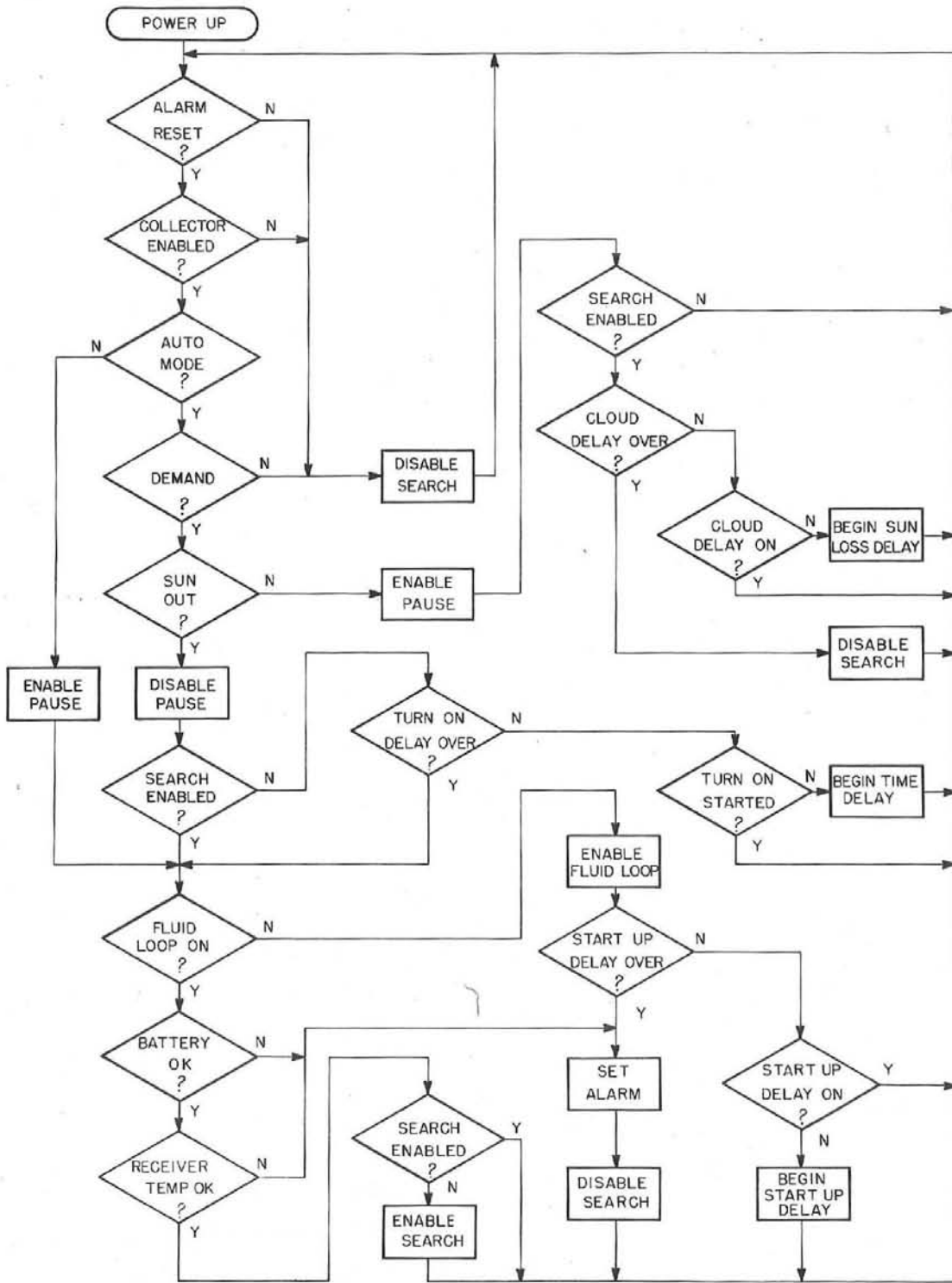


Figure 35. Field Control Logic Flow Chart

Besides the "ENABLE" signal, the field controller generates "PAUSE" and "AUTO" (manual) signals. When the rows are enabled, the "PAUSE" signal causes the mirrors to remain stationary. This is to inhibit tracking errors which can occur when clouds cover the sun. To facilitate focusing and cleaning of the mirror arrays, module controllers have manual direction control switches. When the "AUTO" signal is output from the field controller, these switches are inhibited to provide limited access to the control of the collector.

A key component of the field controller is the sun sensor. It consists of two photocells, each under a protective acrylic hemispherical dome. The domes have light apertures such that one dome transmits light from the region of the sky that the sun moves through when the SLATS can do useful work and the other dome accepts light only from the rest of the sky. A junction box is mounted under the mounting plate and a mounting bracket attached so that the sensor can be mounted on one of the H beams of the collector array or some other appropriate surface.

#### Module Controller

The module controllers operate sections of the SLATS. A module control logic flow chart is shown in Figure 36. Given power and "ENABLE" from the field controller, the module controller finds the target and focuses the sunlight upon it.

Positional feedback is provided by an optical sensor mounted at the receiver. The tracking sensor remains in basically the same configuration as earlier designs though the number, size and placement of apertures may be varied and they may be left unsealed.

The module control circuitry is on one circuit board which mounts in a weatherproof box fastened to the structure near the motor. As with the field controller, inputs and outputs are isolated. Connection to the circuit is made via barrier strips. The battery for the module power supply is also housed in the same enclosure.

The actuator for the module is a permanent magnet DC motor with several stages of gear reduction. Magnetically actuated reed relays are used for limit switches.

#### Fluid Loop

The fluid loop shown in a very simplified schematic in Figure 37 was designed by Barber-Nichols Engineering, Denver, CO. On the water side pressure is maintained in the line by the hydraulic intensifier which adds water when the pressure drops below a preset value. The regulating valve relieves water back into the reservoir when pressure exceeds a preset value. These two features eliminate the need for ullage to accommodate expansion and contraction of the water.

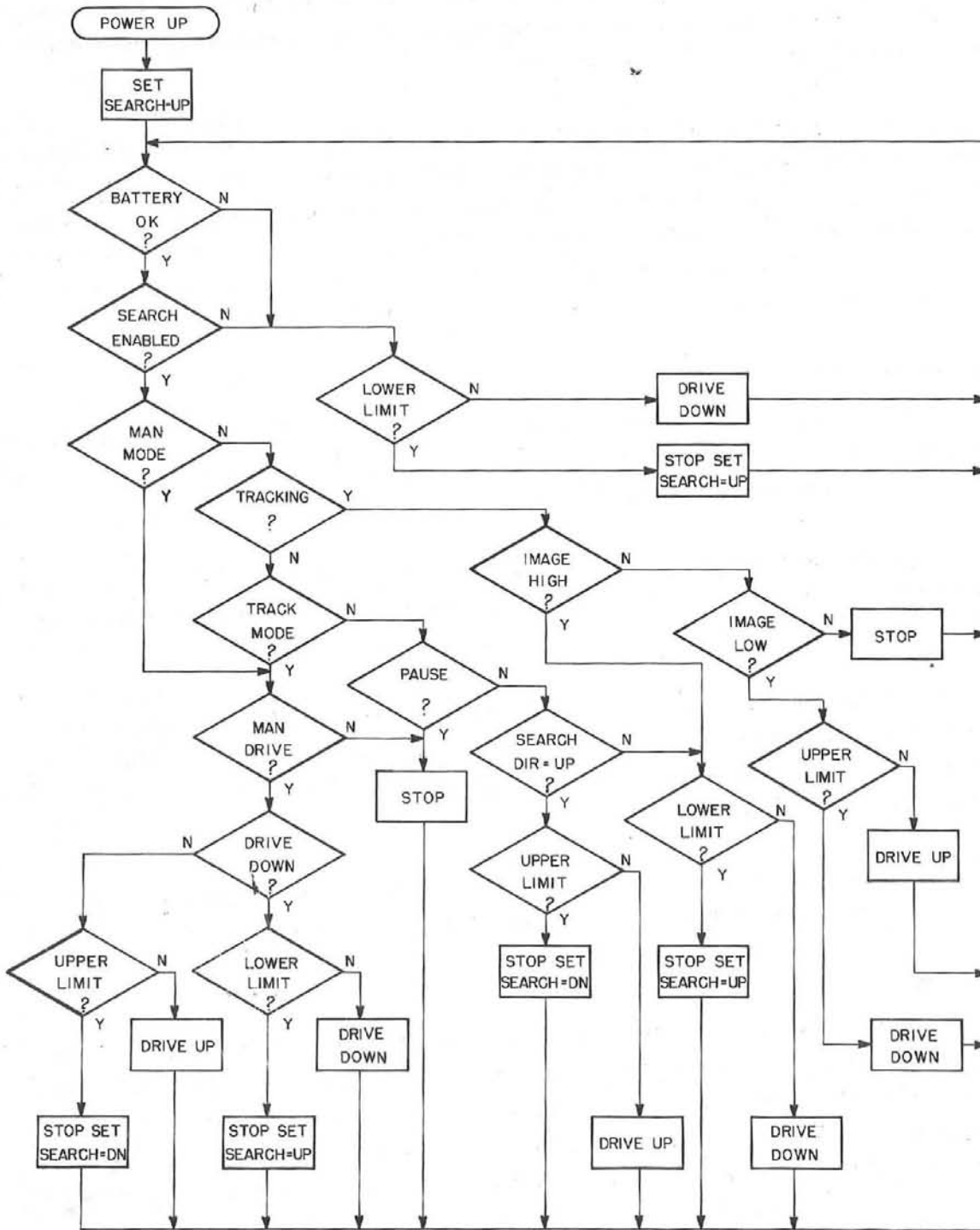


Figure 36. Module Control Logic Flow Chart

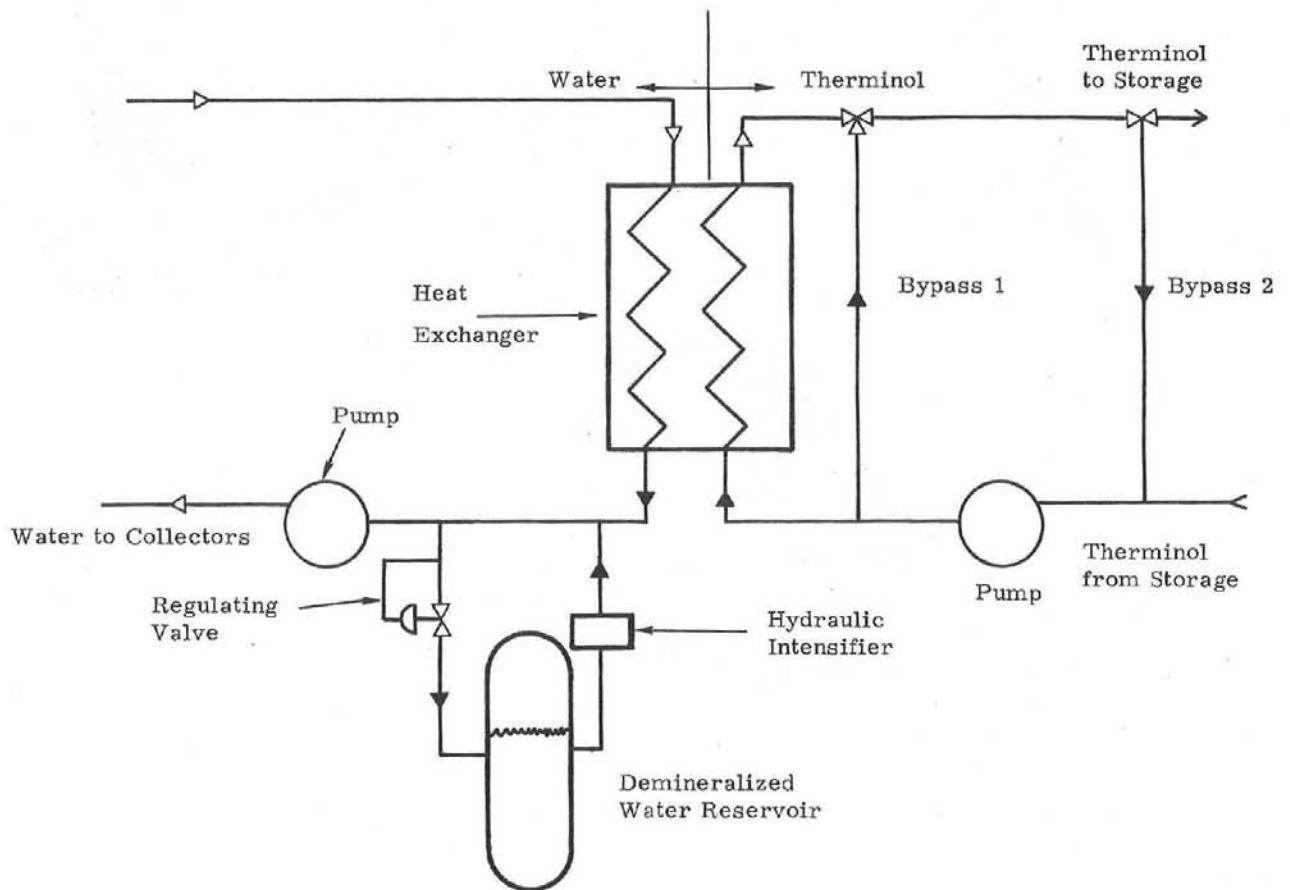


Figure 37. Fluid Loop Schematic

The heat exchanger is a counterflow shell and tube type heat exchanger with water in the tube. Pressure drop through the exchanger at full flow, 132 liters/min (35 gpm) is 69 kPa (10 psi) or less. The heat exchanger was made by Thermal Design International, St. Thomas, Ontario, Canada.

The Therminol pump is a gear type, water-cooled pump also driven by a variable speed motor which is controlled by the temperature of the Therminol coming from the heat exchanger. Fluid which is not hot enough to be sent to storage will be returned to the heat exchanger by by-pass 2.

#### McDonnell Douglas Fresnel Solar Collector Test Model

Figures 38 and 39 illustrate the McDonnell Douglas Fresnel Solar Collector Test Model. The  $16.3 \text{ m}^2$  ( $175 \text{ ft}^2$ ) model represents 1/6 of the full scale commercial unit shown in Figure 37. McDonnell Douglas is under contract to Sandia to provide a model for test and evaluation in mid-July 1977.

The collector is made up of a linear refractor, four receiver tubes and their supporting structural members. The collector is mounted on a two-axis tracking mechanism on a central pivot.

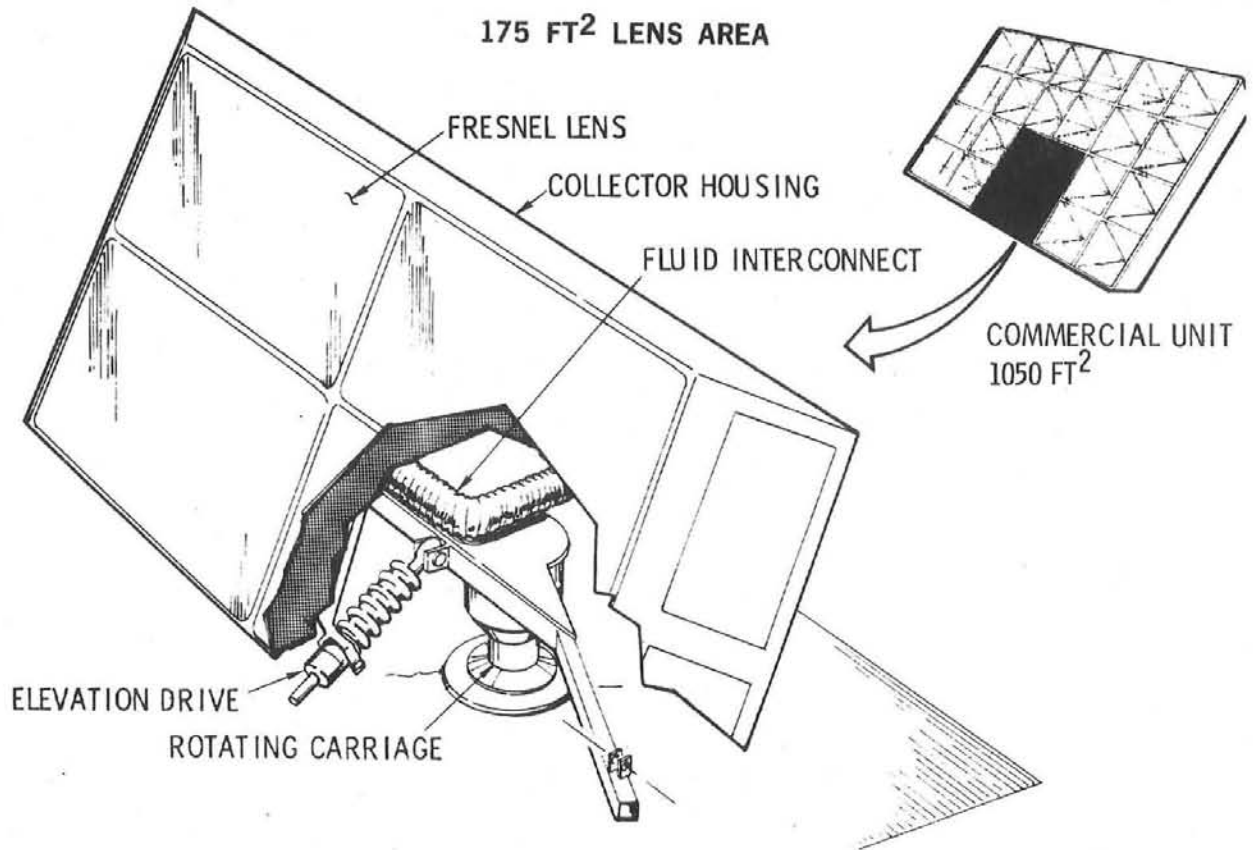


Figure 38. Fresnel Solar Collector Test Model

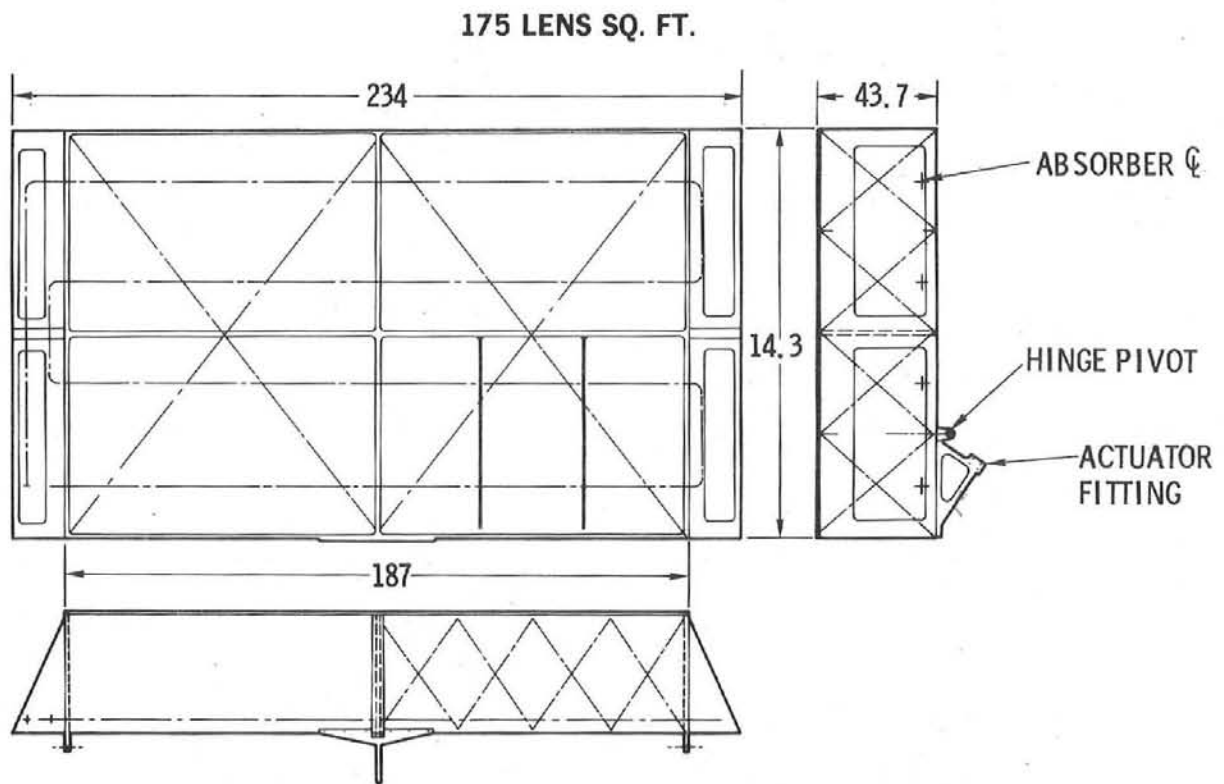


Figure 39. Fresnel Distributed Collector Housing

### Refractor

The refractor consists of an array of flat Fresnel lenses with a .9 m (3 ft) focal length. Each lens was fabricated by trimming and edgebonding individual panels together approximately 18 inches square. The acrylic lens panels were cast on three different electroform tools replicated from a single 18-inch square machined master. The Fresnel lenses were manufactured by Swedlow, Inc.

### Receiver

Each of the four receivers consist of a low carbon steel tube with a black chrome exterior coating surrounded by a glass tube. The glass tube is insulated on the side away from the lenses.

### Tracking System

The tracking controller will monitor the output error signal from a solar sensor until a predetermined error has been accumulated, at which time the drive motors will be actuated to bring the error back near zero. The tracking drive mechanism will consist of an oribidrive unit for the azimuth drive and a Duff Norton linear actuator for the elevation drive.

### Collector Features

Table VIII compares the features of the two McDonnell Douglas designs with those of the other three contractors and Sandia's parabolic trough. The McDonnell Douglas designs are identified as the MDAC First Generation and the MDAC Second Generation. The first generation design was reported in the previous semi-annual report.\* It consisted of a fully-tracking array of smaller individual collectors oriented north-south with their receivers connected in series. The second generation design is the one reported here and, as shown on the chart, represents a significant reduction in cost with an accompanying improvement in performance. The improved performance resulted mainly from earlier acquisition of the sun and less shadowing losses.

---

\* SAND76-0662, p. 41.

TABLE VIII  
Comparison of Collector Features

Feature	General Atomic	MDAC First Generation	MDAC Second Generation	Raytheon	Sandia	Sheldahl
Construction Cost, $\$/m^2$	168	270	190	234	199	194
20-Year Operating Cost, $\$/m^2$	172	258	161	258	199	172
Net Energy (Winter), $\text{kJ}/m^2\text{-day}$	8,425	10,000	10,979	12,500	11,216	8,675
Net Energy (Summer), $\text{kJ}/m^2\text{-day}$	10,200	13,550	16,146	21,605	13,810	11,100
Figure of Merit (Winter) $\$/\text{kJ-day}$	0.040	0.052	0.032	0.039	0.035	0.042
Figure of Merit (Summer) $\$/\text{kJ-day}$	0.033	0.039	0.022	0.023	0.029	0.033
Material Cost, $\$/m^2$	60	167	62	105	70	77
Concentrator Reflectivity/ Transmittance	0.92	0.84	0.84	0.92	0.92	0.92
Concentrator Efficiency, %	67	71	71	87	85	77
Receiver Efficiency, %	75	70	72	93	70	79

## Task 5. High Temperature Storage Subsystem

The major effort in this task was directed to the continued development of the multiple tank, high temperature storage subsystem. The design of the tanks and the insulation was completed and orders were placed for both tanks and insulation.

Studies continued on the existing thermocline high temperature storage subsystem to determine the reasons for the high energy losses. Until the reason for these losses can be determined and corrected, further studies on thermocline stability will not bear fruit.

### 5.1 Development

It was decided to use the minimum number of tanks required to evaluate all combinations of the multitank system, which is three. The required storage for an additional 3-1/2 hrs turbine running time is  $2.48 \times 10^6$  kJ, plus losses, between 250° and 309°C. Our goal was to hold losses for a 24-hour period below 2% of the stored energy, or  $5 \times 10^4$  kJ, but preliminary calculations of insulation thickness indicate that goal is unrealistic. They show that 0.6 m (24 in.) of insulation with a k factor equal to 0.05 W/m°C (0.03 BTU/hr-ft-°F) are required to maintain thermal losses below  $15 \times 10^4$  kJ. To meet our goal of  $5 \times 10^4$  kJ per day maximum losses would require a thickness of between 1 and 2 meters of insulation with properties similar to those of 64 kg/m<sup>3</sup> (4 lb/ft<sup>3</sup>) density Kaowool.

Flow rates from and to storage are shown in Figure 40 for a sunny December 21, the shortest day of the year. In the morning and in the evening insufficient energy is collected to operate the system. During the day there is an excess of collected energy which is stored. For the conditions shown in this figure, there will be a startup time (about 7 a. m.) one tank of hot fluid at 310°C, one tank of cold fluid at 250°C, and one empty tank (Figure 41). The hot fluid will be used and dumped into the empty tank. During the day both tanks of cold fluid will be heated by the collectors. Starting at midafternoon, the system will draw upon and exhaust one hot tank. When the system is shut down in the evening, there will be one tank of hot fluid, one of cold fluid, and one empty tank. Each tank has a capacity of at least half the total liquid to be stored. The total stored liquid in the system will be 23,847 liters (6300 gallons) with each tank having a capacity of 11,923 liters (3150 gallons), plus ullage of roughly 10%, making 12,870 liters (3400 gallons). The three-tank system allows flexibility in the management of the heat storage liquid without the necessity of mixing hot and cold liquid in the same tank, with a lower total required tank capacity than with two tanks.

Each tank will be free standing vertically on three supports. The tanks will be clustered in a triangular pattern to minimize heat loss, and to afford some mutual protection from wind forces. Other arrangements were considered, including nesting or stacking the three tanks, to minimize further heat loss. These approaches are worthy of further consideration, but at this time are not compatible with schedules, since the use of nonstandard shapes, special materials, and special structures would be necessary.

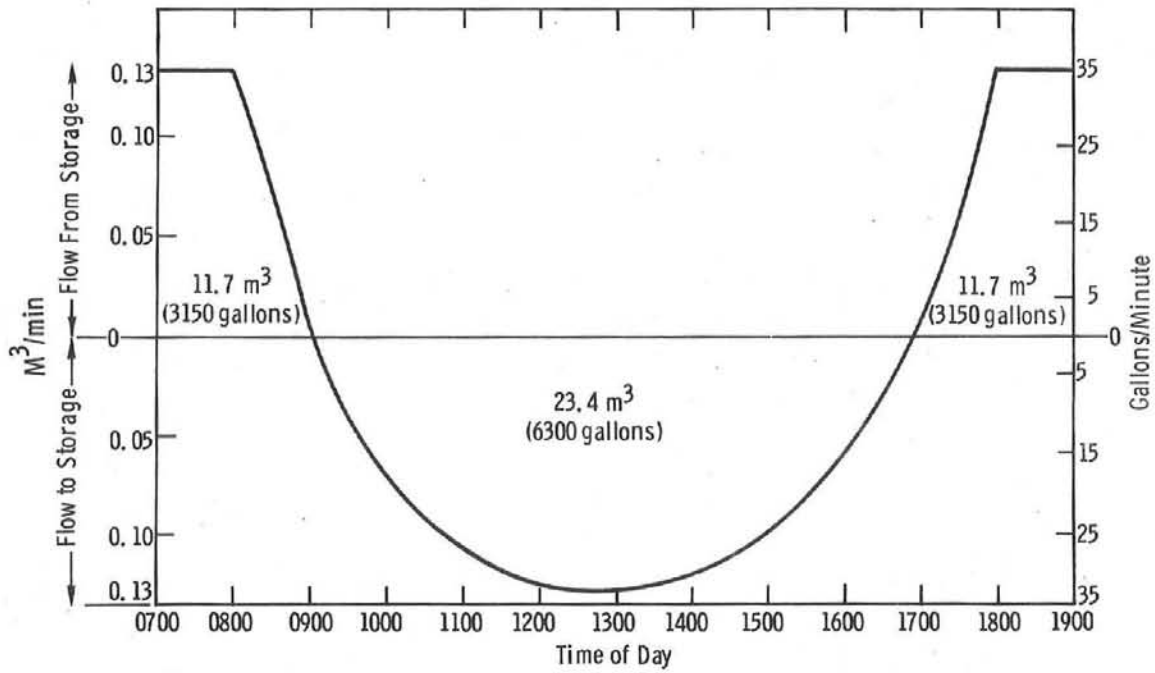


Figure 40. Flow Rates to and from Storage

$$\text{VOLUME OF EACH TANK} = \frac{\text{REQUIRED FLUID VOLUME}}{\text{NUMBER OF TANKS} - \text{ONE}}$$

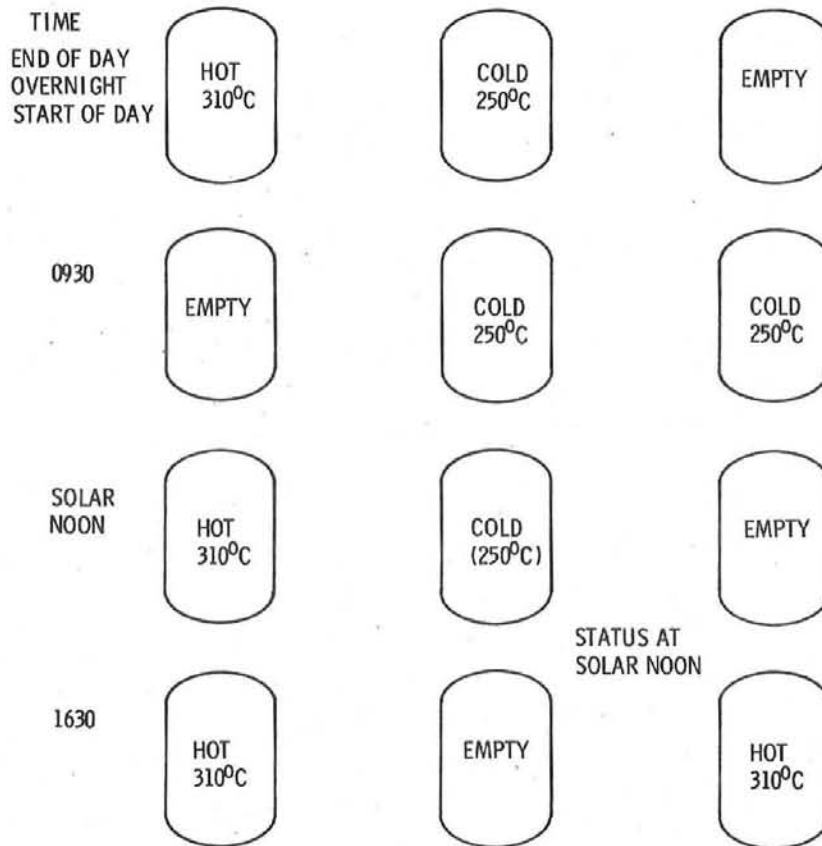


Figure 41. Status of Multiple Tank Storage at Selected Times of Day

To assure that schedules could be met, and for economy reasons, it was decided that the general tank design would be a conventional cylindrical shape with semi-elliptical ends. A program was written for the CDC 6600 which computed heat loss and temperature conditions during 24 hours of operation of the system, given tank dimensions, thermal insulation type and thickness, and ambient temperature and wind conditions. The results of this computer study showed that a tank with approximately equal altitudes and diameter would result in minimum heat loss.

The legs are designed so that the tanks will be able to withstand wind loads of up to 144.8 km/hr (90 mph), and seismic loads typical of seismic Zone 2. At the bottom of each tank a .457 meter (18 in.) diameter well is provided so that all of the liquid in the tank can be used. Three fittings extend from the sides of this well for connection to the heat fluid lines. Ninety degree elbows will be attached to each of these fittings inside the well, to direct the flow of liquid inside the tank. A fourth fitting extends from the bottom of the well for draining of the tank.

The tanks are made of normalized mild steel; and although the internal pressure is low, 110 kPa (~16 psi), they conform to Section 8 of the ASME Pressure Vessel Code, with Charpy V notch tests being required for both plates and welds.

An order was placed in early January 1977 with Lubbock Manufacturing, Inc. for fabrication of the three tanks. Delivery is expected by the end of April 1977.

Each tank will contain instrumentation for sensing internal temperature and liquid level. Temperature will be sensed by a probe extending vertically from the top to the bottom of the tank, near the center, with thermocouples at 1-foot intervals. Thermocouples will also be placed on the skin of the tank. Level sensing will be done by measuring capacitance between the tank wall and a probe oriented vertically near the center. This will provide information on tank liquid level, will be used to sense full and empty conditions, and to sense if liquid is being lost from the system if, for example, a break occurred in a line to a collector. This instrumentation will be mounted in the tank by means of flanged fittings at the top. Flanged fittings are also provided for man access, relief valve mounting, and nitrogen manifold connections. (Nitrogen is used to provide a non-oxidizing atmosphere above the liquid.)

The computer program, as previously mentioned, produced information concerning heat loss from the tanks during the operation cycle, for various insulation types and thicknesses. Using this information, cost studies were made evaluating the total cost of various thicknesses of insulation plus the cost of added solar collector area which would be needed to compensate for the total heat loss. Several types and combinations of insulation were considered in these studies. The results of these studies are summarized in Figure 42. As the figure shows, the most economical material is intermediate service fiberglass. The thickness chosen for the insulation is .533 meters (21 in.). This is slightly thicker than the optimum shown by the chart, but results in only a slightly higher cost. Figure 43 shows heat loss through the insulation as a function of insulation thickness. Each supporting leg for each tank will rest on a pad of load bearing thermal insulation.

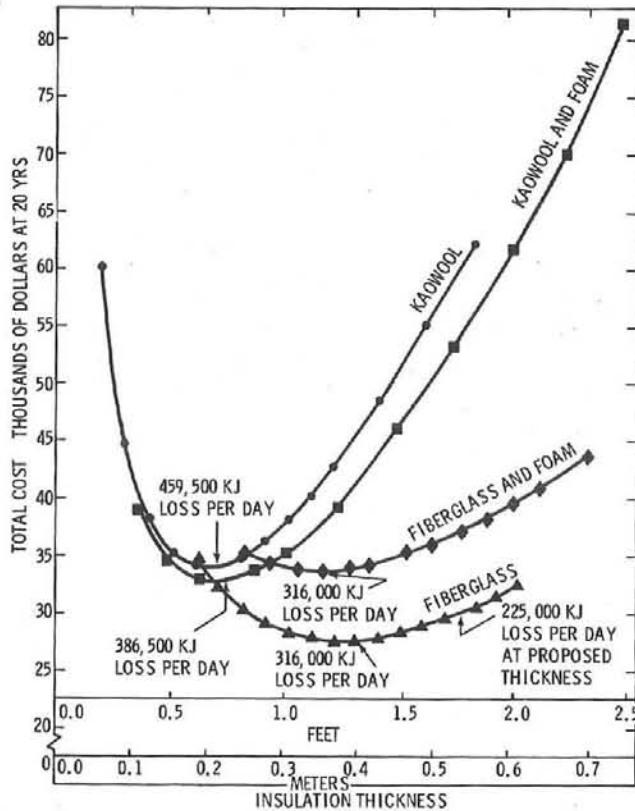


Figure 42. Thermal Storage Tank Insulation Cost Comparison, Winter Day Cycle, Three Tanks

Calculations showed that this method of insulating the supporting legs is more effective and less expensive than attempting to minimize the leg cross-section and specifying a low thermal conductivity steel. The tanks will be located far enough apart that each tank can be thermally insulated individually. Some savings in insulation could be achieved by having some of the insulation cover all three tanks together, but complications involved in installation would offset this saving.

For spill protection (mentioned earlier) sensors from Endress and Hauser capable of constantly monitoring the volume of fluid will be installed in each tank. Using these sensors, a computer will constantly monitor the total quantity of fluid in all three tanks. If this quantity drops by some predetermined amount (our goal is 570 liters (150 gallons) or less) a spill in the field will be indicated and all valves from the tanks will automatically close.

A berm is provided for fire protection or broken tanks. In case of fire a deluge system will automatically go into action flooding the tanks and the berm. The berm is sized to hold the volume of the tanks plus all the water which would enter before the fire department could arrive from a distance of about three blocks.

Costs of the three tanks are estimated as in Figure 44. The total cost is \$91,000 which adds approximately  $\$110/\text{m}^2$  ( $\$10.22/\text{ft}^2$ ) to the cost of the collector field.

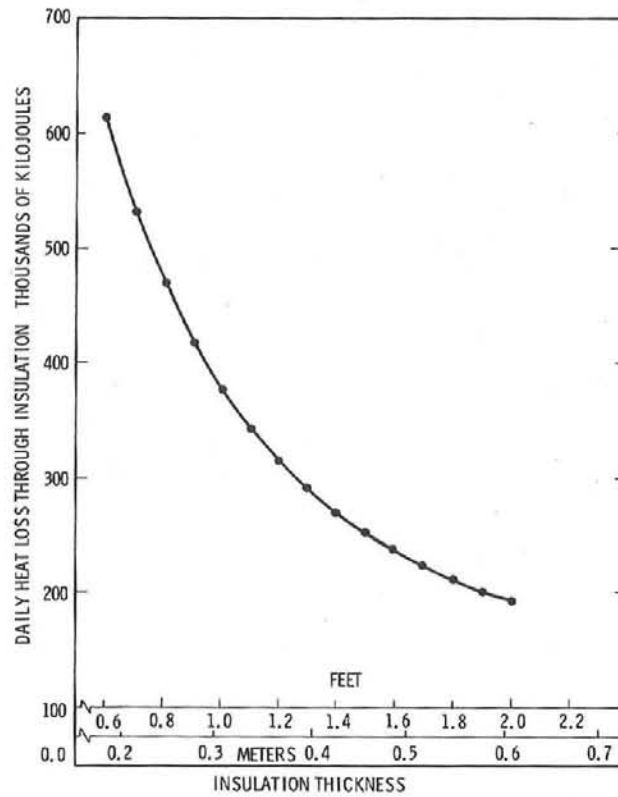


Figure 43. Calculated Heat Loss Through Insulation, Intermediate Service Fiberglass Board, Three Tanks, Leg Loss not Included

	<u>Dollars</u>	<u>Percent of Total</u>	<u>Cumulative Percentage</u>
Therminol 66 Required for Storage	\$38,000	42	42
Three Tanks	25,000	27	69
Insulation	20,000	22	91
Valves	8,000	9	100
	<u>\$91,000</u>		

Figure 44. Estimated Cost of Multiple-Tank, High-Temperature Storage Subsystem

Sandia expanded the studies required to design the multiple tank storage system to include a system 100 times as large. The system would collect .9 MJ/day in the winter and 1.0 MJ/day in the summer. Storage capacity would be  $2.5 \times 10^8$  kJ, which would require  $2300 \text{ m}^3$  ( $6.3 \times 10^5$  gallons) of Therminol. The system would generate 3.2 MW electricity for the same shape load as is shown in Figure 40.

The percentage of collected heat loss per day is shown in Figure 45 as a function of insulation thickness. As tanks become heavier, insulating them from the ground becomes more difficult. Figure 46 shows how losses through the base vary as a function of the thickness of insulation on the walls.

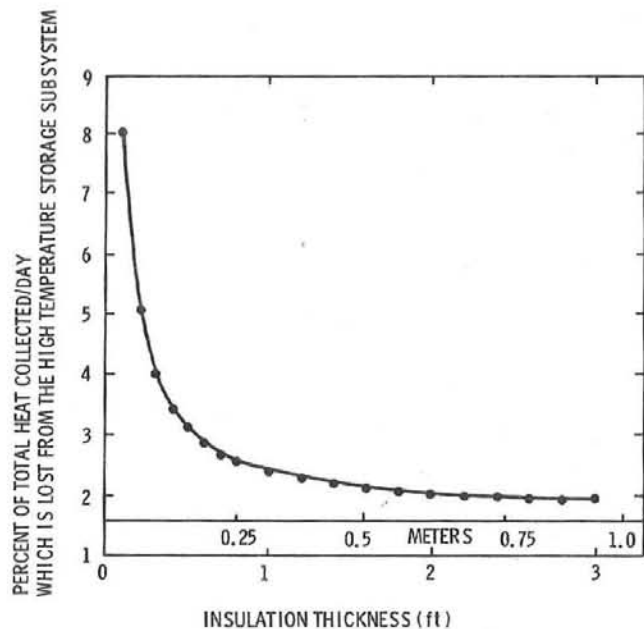


Figure 45. Percentage Heat Loss vs. Insulation Thickness for a Large System

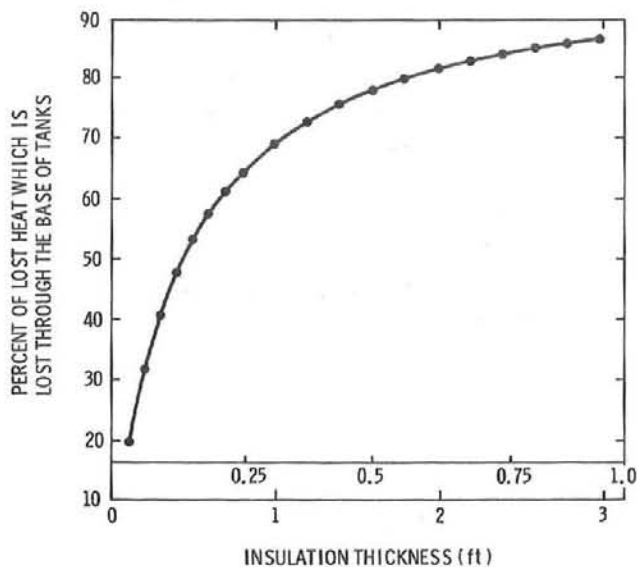


Figure 46. Percentage of Heat Loss Through Tank Bases vs. Insulation Thickness Over Walls and Tops

## 5.2 Operations

Operations were concerned primarily with testing the high temperature thermocline storage subsystem and with preparing the site for the new multiple tank, high temperature storage.

The high temperature thermocline subsystem was designed by Sandia Laboratories, Livermore, to study storage problems either with water at 232°C (450°F) or Therminol at 310°C (590°F). The saturation pressure of water at 232°C is 2.9 MPa (425 psi). As a consequence, the walls of the tank, are 25.4 mm steel (Figure 47).

These thick walls absorb about  $.13 \times 10^6$  kJ when the cold fluid, 243°C (470°F), is replaced with hot fluid, 310°C (590°F). This represents 18% of the theoretical maximum thermal storage capacity of  $.69 \times 10^6$  kJ.

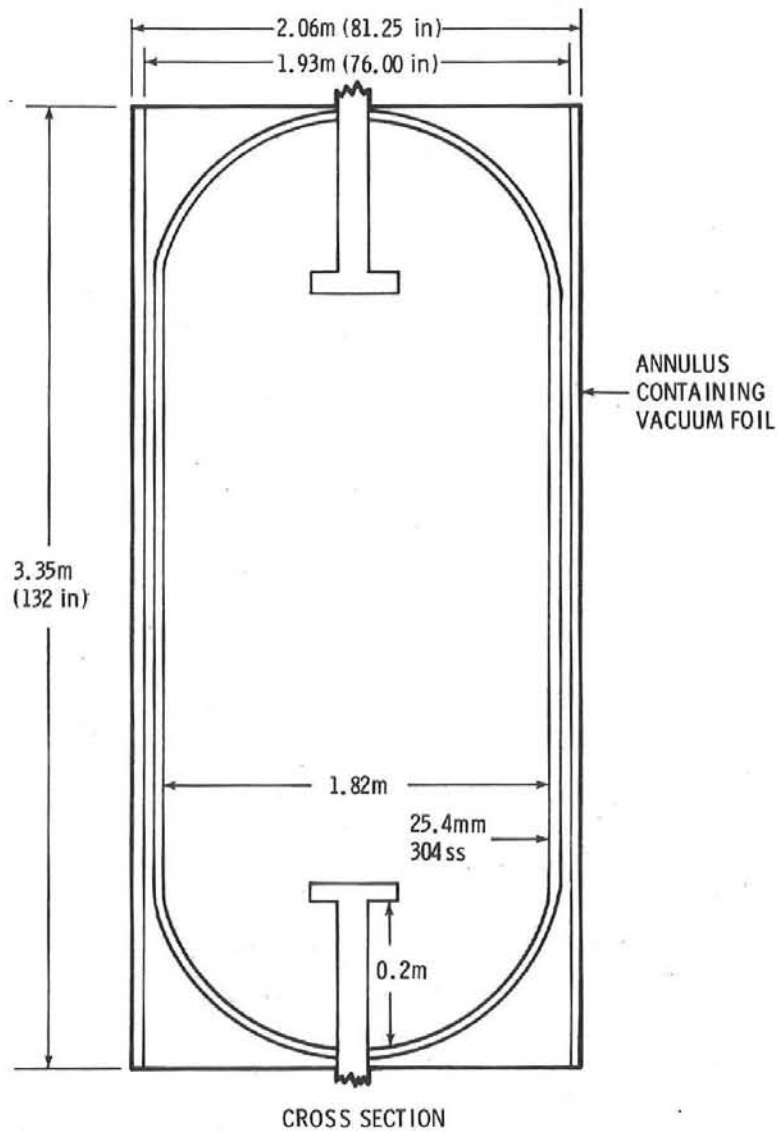


Figure 47. High Temperature Thermocline Storage Subsystem

In addition, the thick wall conducts heat around the thermocline so as to set up convection currents which will cause the thermocline to degrade. The thermal conductivity (k) of Therminol at 275°C (527°F) is  $7.6 \times 10^{-4}$  W/m-°C (.0631 BTU/ft-hr-°F) compared with 2640 W/m-°C (22 BTU/ft-hr-°F) for carbon steel (a ratio of approximately 360 to 1). The ratio of the horizontal area of Therminol in the tank to the horizontal area of the steel in the wall is also approximately 18 (actually 17.75). If film coefficients are ignored, one estimates that at least an order of magnitude more thermal energy is transferred around the thermocline through the steel walls than is transferred through the Therminol.

Insulation for the sides is vacuum foil enclosed in a 70 mm (2.5 in.) wide annulus as shown in Figure 47. This vacuum foil comprises 75 layers of .025 mm (.001 in.) aluminum attached to .15 mm (.006 in.) fiberglass.

Pressure inside the annulus is maintained at about 300 microns by a single stage vacuum pump. Computer calculations indicate that a heat transfer coefficient of  $5 \text{ W/m}^2\text{-}^\circ\text{C}$  through the wall is too low for actual values of heat lost. From literature on vacuum foil insulation the value for heat transfer for the vacuum foil should be in the neighborhood of  $.05 \text{ W/m}^2\text{-}^\circ\text{C}$  when the pressure in the annulus is 10 microns or less. Figure 48, prepared by Sandia, indicates that for this vacuum foil the heat transfer rate at 300 microns pressure in the annulus is about 80 times the heat transfer rate when the pressure in the annulus is 10 microns. Single stage vacuum pumps operating at maximum efficiency can maintain 10 microns in small volume systems with leak rates of  $10^{-4}$  cc/sec or less. In this case when the valve is closed to the pump, the pressure on the annulus changes as follows:

<u>Time</u> <u>(min)</u>	<u>Pressure</u> <u>(microns)</u>
0	50
2	100
5	200
10	250

The above data translate to an average leak rate of  $10^{-1}$  cc/sec over a 10-minute time period.

Another problem is that the 0.2 m thick layer of fluid (Figure 47) below the bottom diffuser is stagnant. Its temperature can be maintained only by taking heat from the fluid above it. A second thermocline is thus established at the level of the bottom diffuser. Other effects are unknown.

Thick steel legs are required to support the annulus which contains the insulation. These legs are not insulated from the foundation. We estimate that they can transfer out as much as  $.5 \times 10^6$  kJ/day.

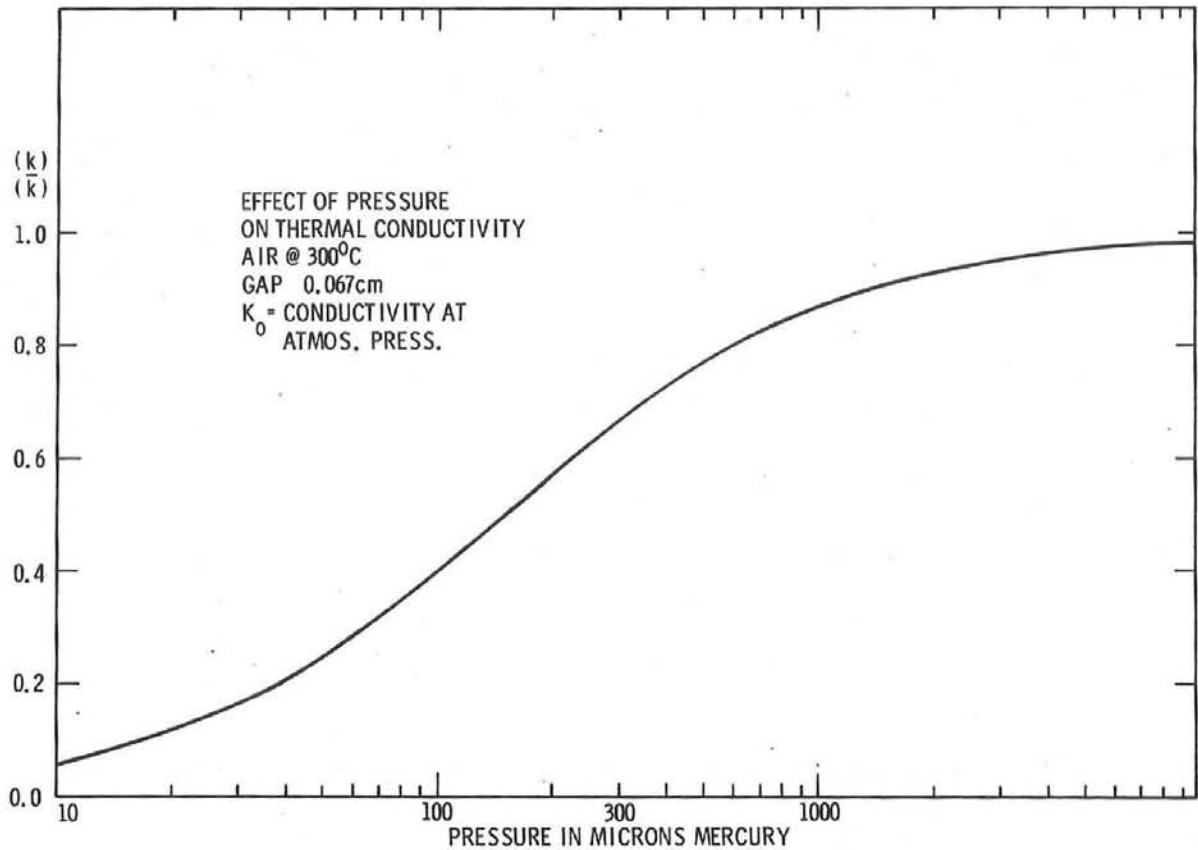


Figure 48. Effect of Pressure on Thermal Conductivity

In summary, the tank has the following problems:

1. The mass of the walls absorb up to 18% of theoretical thermal storage capacity when cold fluid is replaced by hot.
2. The thick wall will transfer an order of magnitude more energy around the thermocline than passes from hot to cold through the Therminol.
3. An adequate vacuum cannot be maintained in the annulus which contains the vacuum foil because the leak rate is too high. Losses through the wall are approximately an order of magnitude larger than they should be.
4. There is a second and unwanted thermocline on the level of the bottom diffuser.
5. The legs allow a significant heat loss, almost 10% per day, of theoretical maximum storage capacity.

In order to determine a cause of action with respect to thermocline, Sandia has constructed a scale model, Figure 49, and started studies just at the end of this reporting period. A computer program is being written which will take into account heat transfer through the walls as well as heating and cooling of walls as the thermocline changes position by conduction and convection of the fluid.

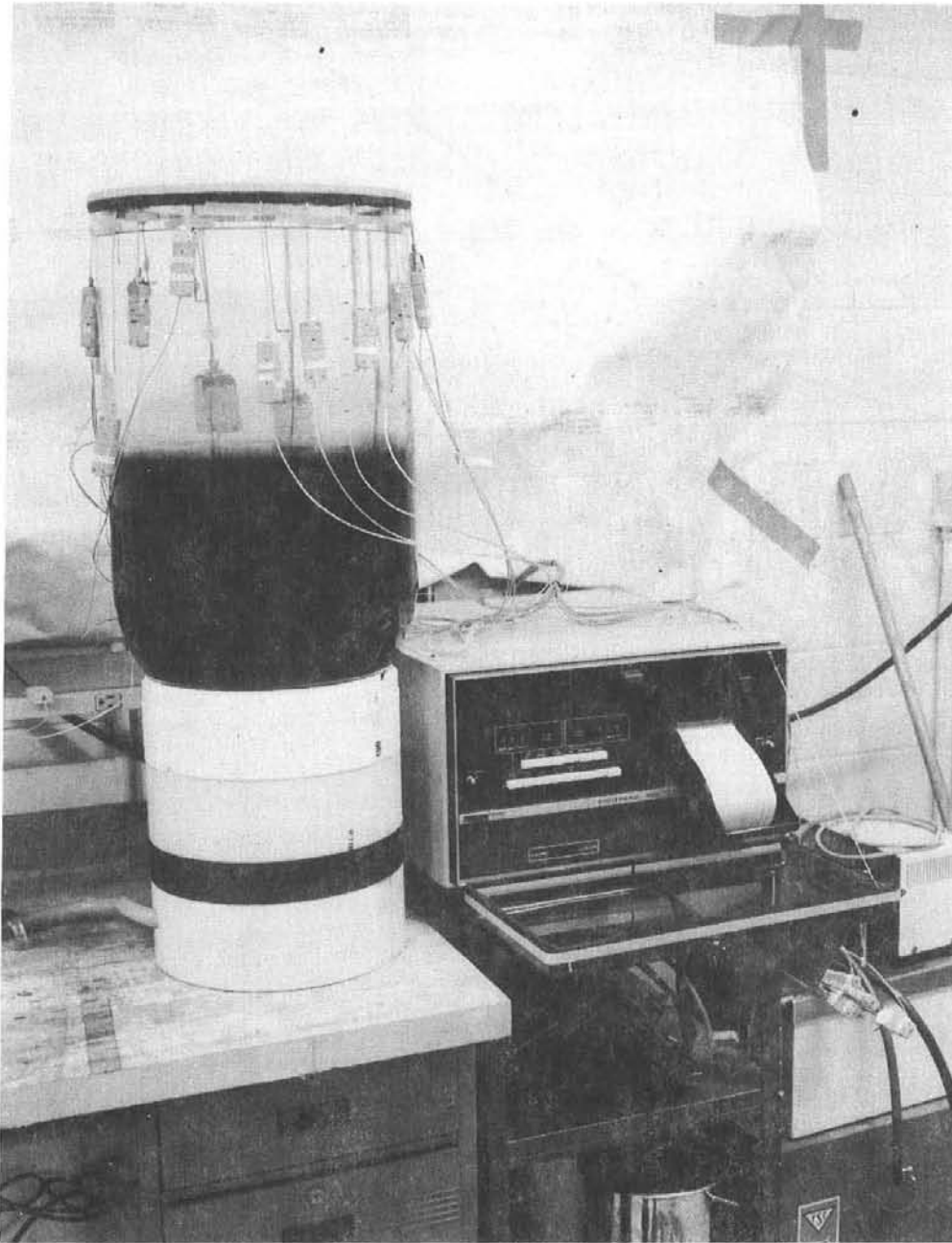


Figure 49. Thermocline Scale Model

Preparation continued during this period for expansion of the Solar Total Energy Test Facility, (Figure 2). Allison Engineering Company completed the engineering to perform the functions described in Task 5.0 of the previous semiannual report, SAND76-0662. Bids were solicited based on these designs. Jack Henderson Construction Co. was awarded the contract for the installation of the fluid loops. Mountain States Insulation was awarded the contract to insulate the tanks and piping. Construction will start about the middle of April.

Preliminary interface agreements have been established with the three contractors, General Atomic, Raytheon and Sheldahl for the new collector field subsystem.

## Task 6. Turbine/Generator Subsystem

Testing of the turbine system during October and early November could not be conducted at steady state power levels of 28 kWe or higher running from storage, due to inadequate Therminol fluid flow. Investigation indicated that the Therminol pump was cavitating. The top of the storage tank was removed and a loose pipe joint was found in the diffuser line above the liquid level. The joint was tightened, the tank reassembled and more Therminol added in mid-December. Later testing confirmed that this allowed sufficient flow for normal conditions, but that the Therminol could only be pumped to approximately 1.9 l/s (30 gal/min) vs. the 2.2 l/s (35 gal/min) attained previously.

Even though testing utilizing storage was limited, a series of tests were run during October utilizing the fuel-fired heater. The object of the tests was to determine the effects of turbine inlet pressure on energy conversion efficiency at full load. The condenser inlet/outlet coolant conditions were controlled at 88°C/77°C (190°F/170°F), 68°C/41°C (155°F/105°F) and 46°C/35°C (115°F/95°F), representing summer, winter and spring/fall conditions respectively. Changing the condenser coolant temperatures changes the condenser toluene pressure which changes the turbine nozzle pressure ratio (turbine inlet pressure/condenser pressure). Since the nozzles are most efficient at the design pressure ratio, it was felt that there would be an optimum turbine inlet pressure for each condenser condition. The test results, however, indicated that system efficiency was only a very weak function of turbine inlet pressure and that the most important factor in system efficiency is the condenser pressure, i. e., it was noted that the system efficiency was a very strong function of condenser pressure and that this pressure should be maintained as low as possible for the given condenser coolant temperature conditions.

This is shown in Figure 50 where the turbine inlet pressure was varied from 1450 to 1790 kPa (210 to 260 psia) at the winter condenser coolant conditions and the efficiency was found to vary only 0.6 percentage point which appears to be scatter. The general trend of cycle efficiency with condenser pressure is shown in Figure 51. The condenser has a vacuum pump system to maintain condenser pressure at the appropriate toluene saturation pressure by removing noncondensibles (such as air) as they outgas from within the system or leak into the system. The vacuum pump is controlled by a differential pressure switch which compares toluene saturation pressure in a sealed reference container in the condenser to the condenser vapor pressure.

During testing on October 28 at the summer condenser coolant conditions, the vacuum pump ran almost continuously and dumped liquid toluene. Under the hot condenser conditions and the cold ambient temperature of 4°C (40°F), the noncondensibles receiver tank was acting as a secondary condenser without adequate drain for the toluene. To correct this, the vacuum system differential pressure switch was adjusted to give a wider deadband. Unfortunately, this raised the condenser pressure excessively and dropped system efficiency about one percentage point. One possible problem is that the differential pressure switch sensing lines have different elevations and liquid may be condensing on the high side and affecting the setpoint of the switch with a liquid pressure head. The lines will be re-routed to test this theory.

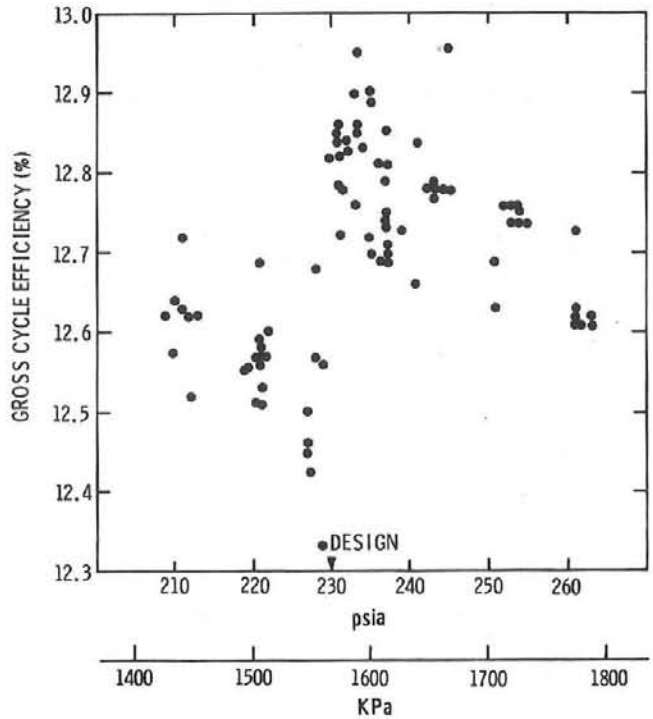
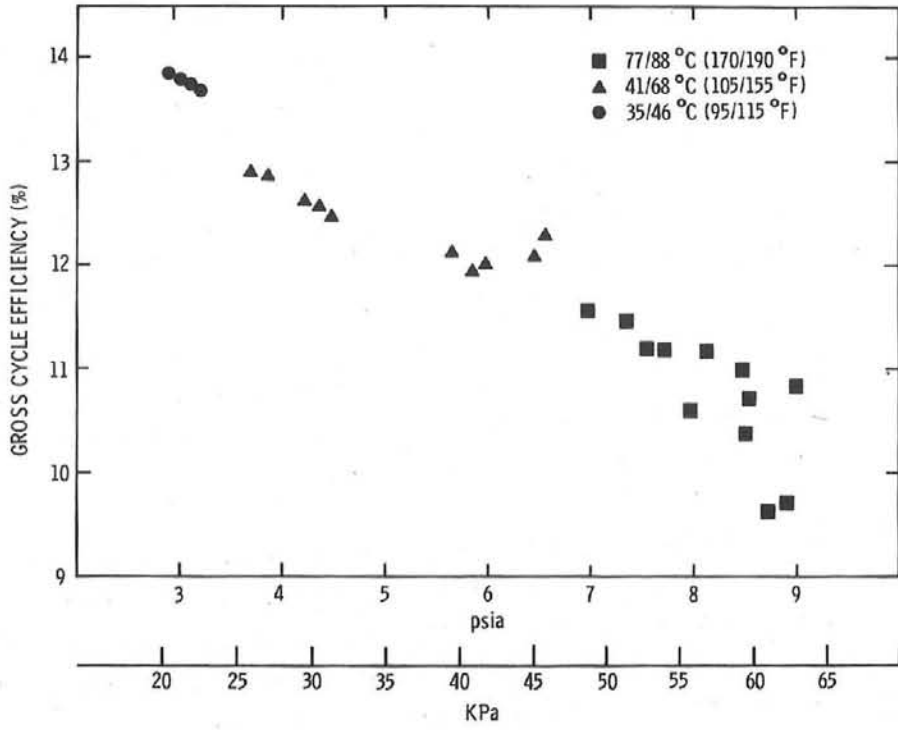


Figure 50. Gross Cycle Efficiency vs. Turbine Inlet Pressure (105°/155°F Condenser Coolant Temperatures)



Very little test activity took place during November or December due to the work load on the EG&G operating personnel. This work load was mainly concerned with the problems encountered with storage and the resulting teardown of the storage tank. The turbine bypass valve was removed during December for inspection to determine if it was leaking. Test data on the system indicated that there might be a sneak bypass between the high pressure inlet and the condenser. Discoloration on the valve seat indicated that the valve was leaking. The valve was lapped and reassembled, but a flange leaked when the valve and piping were replaced in the system. Replacement gaskets were ordered and were scheduled to arrive on January 3, but did not arrive until January 24. The gasket was replaced and the system became operational on February 1.

A series of tests were run during February to determine the turbine system response to a manual switchover from storage heat input to fossil fuel-fired heater input with the goal being to automate this process for use when the turbine system is integrated into the Building 832 operation. The tests were run by heating storage up the night before each test and allowing the piping and heater to cool overnight at temperatures of  $-7^{\circ}\text{C}$  to  $4^{\circ}\text{C}$  ( $\sim 20^{\circ}\text{F}$  to  $40^{\circ}\text{F}$ ). The turbine was operated from storage in the morning at various power levels from full load (32 kWe) to no load with the condenser cooling water controlled to summer conditions. The heater sequence was then initiated and as soon as a pilot flame was indicated the system mode switch was switched to circulate the boiler heat transfer fluid flow through the heater rather than storage. In all cases, the turbine operation could not be sustained, with shutdown occurring within one or two seconds after switching modes at full load and within approximately 30 seconds at no load.

Before tests could be run to switch from the heater to storage under similar test conditions (allowing storage piping to cool down overnight) the turbine indicated a low lube pressure condition and shut down on February 18. Investigation showed a high gearbox lube level due to toluene leaking into the gearbox with a resultant thinning of the lubricant. Diagnostic tests recommended by Sundstrand indicated that the turbine high speed shaft seal was the problem. The turbine/gearbox assembly was disassembled and the seal removed on March 1. The seal was found to have an uneven wear pattern on the carbon face and leaked profusely as a subassembly. Total run time on the seal was approximately 375 hours.

Sundstrand recommended a modification to the turbine wheel to add a conical washer under the bolt holding the wheel to the shaft. This more rigid assembly should reduce wheel flexure and contribute to longer seal life. Sundstrand provided an engineer, at their expense, to aid in check-out and reassembly of the turbine which was completed on March 15.

Off-design superheater exit temperature tests were conducted on March 16 and March 28. For these tests, the turbine system was run with the gas-fired heater at 32 kWe load and summer condenser conditions, varying the Therminol inlet temperature toluene superheater exit temperature and holding all other parameters constant. The results are shown in Figure 52. As can be seen in the figure, the turbine is relatively insensitive to the superheater out temperature allowing stable operation at temperatures  $< 288^{\circ}\text{C}$  ( $550^{\circ}\text{F}$ ).

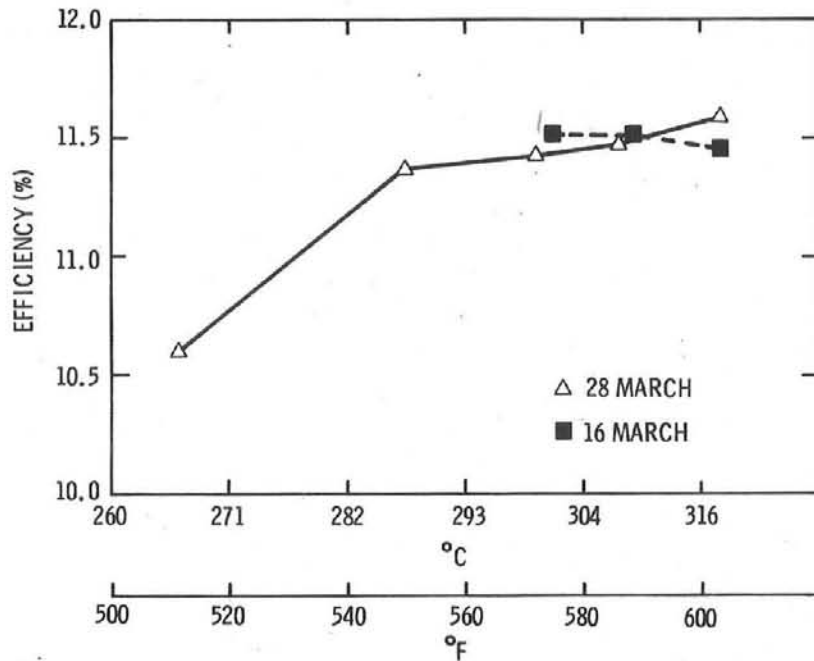


Figure 52. Turbine Efficiency vs. Toluene Superheater Out Temperature

Manual switchover testing from gas-fired heater to storage operation was conducted in late March. At 32 kWe electrical load and summer condenser conditions, the system ran for approximately 90 seconds after switchover before shutting down due to low boiler pressure. This was a worst case test, since the piping from storage had cooled overnight at temperatures of 4°C (40°F) or less (winter-type temperatures), which would be an unlikely combination with the summer condenser conditions. The test was rerun, with the turbine operating with winter condenser conditions and the switchover was completed successfully. Various methods of solving the problem of switching from storage to gas-fired heater operation are under consideration.

#### Task 7. Heating and Cooling Subsystems

In the Solar Total Energy System Test Facility the energy rejected by the turbo/generator system is at higher temperatures than that rejected in conventional electrical generating processes. This rejected energy is used to heat and cool the 1100 m<sup>2</sup> Solar Projects Building.

During this reporting period construction was initiated and essentially completed on the heating and cooling fluid transfer system between the turbine condenser and the heating and cooling system in the Solar Projects Building.

Contractor fluid flow and leak testing have been completed. All Sandia-designed instrumentation and control consoles have been installed and connected to the heating and cooling fluid transfer system so that full control capability is available. Operational mode checkout testing by Sandia has been initiated.

The solar building modifications contract to change the project building's loads to loads more typical of a total energy system were satisfactorily completed during the reporting period. Building electrical loads after modification were monitored for a week and were from 25 to 30-kW.

Task 8. Collector Module Test Facility

Activities during this period were concerned primarily with expansion of the Collector Module Test Facility (Figure 53). A small amount of progress was made to improve the accuracy and precision with which we measure flow rates and temperatures. Tests were continued on arrays of photovoltaic generators. The results of these tests are documented by the Photovoltaic Systems Definition Project, Definition Division. Raytheon conducted a test to evaluate the compatibility of Therminol with the materials of their proposed receiver (see Task 4.0).

5



Figure 53. Collector Module Test Facility

## 8.1 Development and Modification

As reported in the previous semiannual report, (SAND76-0662), plans were developed for the expansion of the Collector Module Test Facility, the purposes of which are:

- To obtain data on collectors and collector components purchased by Sandia or ERDA,
- To obtain data on collectors and collector components which are involved in a project in which Sandia or ERDA has a vital interest.

The Collector Module Test Facility now has the following fluid capabilities:

Loop 1 - Therminol to 315°C (600°F), 0.51 MPa (75 psi)

Loop 3 - Water to 332°C (630°F), 18.3 MPa (2650 psi)

Loops 1 and 3 will normally be used for collectors and collector components. Loop 2 will normally be used for photovoltaic generators. Test Loops 1 and 3 will use an HP 2116 minicomputer to acquire, manipulate, and reduce data. A second 100 channel A/D converter will be added to increase data acquisition capability.

Loop 2 which will generate water to 135°C (275°F) at .51 MPa (75 psi) is under construction and is expected to be complete by the end of May 1977. Test Loop 2 for photovoltaic generators has an HP 9640A minicomputer to acquire, manipulate, and reduce data. This data acquisition system is capable of acquiring 155 data points per photovoltaic array. It is anticipated that the usual test will consist of two arrays.

Test Loops 2 and 3, which use water (or water and ethylene glycol), are protected from the elements (particularly freezing) by 4.5 x 6 m insulated buildings (Figure 53), which can be heated to about 5°C in the winter.

The controls for the loops, the computers, and other data acquisition equipment are housed in an 84 m<sup>2</sup> (900 ft<sup>2</sup>) building which also has a small amount of office space and work area.

Three piers with top surfaces flush with the ground are available for mounting test specimens for Test Loop 2. These are configured to accommodate the mounting arrangement in current use for the photovoltaic generators.

Three piers with top surfaces flush with the ground are available for mounting test specimens on Test Loop 3. These are configured to accommodate the Sheldahl SLATS Collector.

Special equipment to calibrate flow meters is being developed. This consists of a container mounted on a load cell to make it possible to weigh the fluid passing through a flow meter during a time interval (Figure 54).

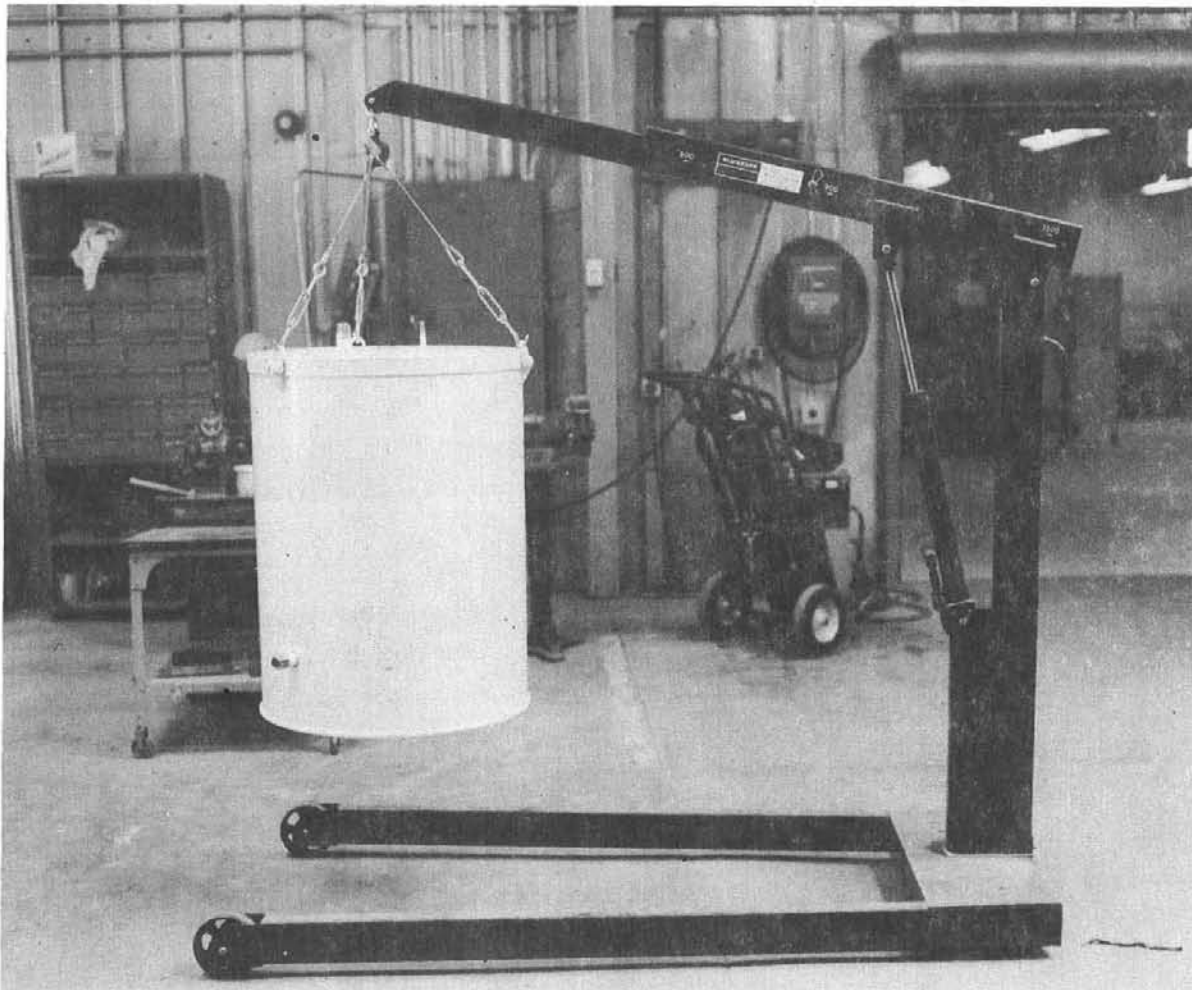


Figure 54. Flow Meter Calibration Container

Still to be installed are:

1. Conduits to carry instrumentation leads from the test item to the instrumentation building.
2. A panic button which will enable the operator to shut off all electric power to all loops in the event of an emergency such as a fire or liquid spill.
3. Some minor utilities.

The above work is scheduled for completion before June 1, 1977.

Equipment to enhance the accuracy and precision of the change in bulk temperature of the fluid as it passes through the receiver of a collector under test is being evaluated. This temperature measurement problem comprises two distinct elements. The first is the actual measurement of the temperature and the second is the location of the measuring devices so that they sense bulk temperature and not merely a local temperature.

To solve the first part of the problem, Sandia has ordered equipment from Foxboro which determines temperature difference from the opposing output of two thermocouples. The accuracy and precision of the thermocouples and electronic equipment will be checked in the Sandia Standards Laboratory over a range of temperatures and temperature differences.

The second problem is more challenging. Asymmetric heating of a receiver combined with the poor heat transfer characteristics of Therminol 66 results in a temperature gradient across the receiver, the predicted shape of which is shown in Figure 55. Moving the thermocouple tip across the receiver diameter has resulted in observed temperature changes of as much as  $2^{\circ}\text{C}$  ( $3.6^{\circ}\text{F}$ ) with all other conditions remaining the same. For a small collector under test, ( $30\text{ m}^2$  or less), the change in temperature across the receiver diameter can easily equal a significant proportion of the change in bulk temperatures across the length of the receiver.

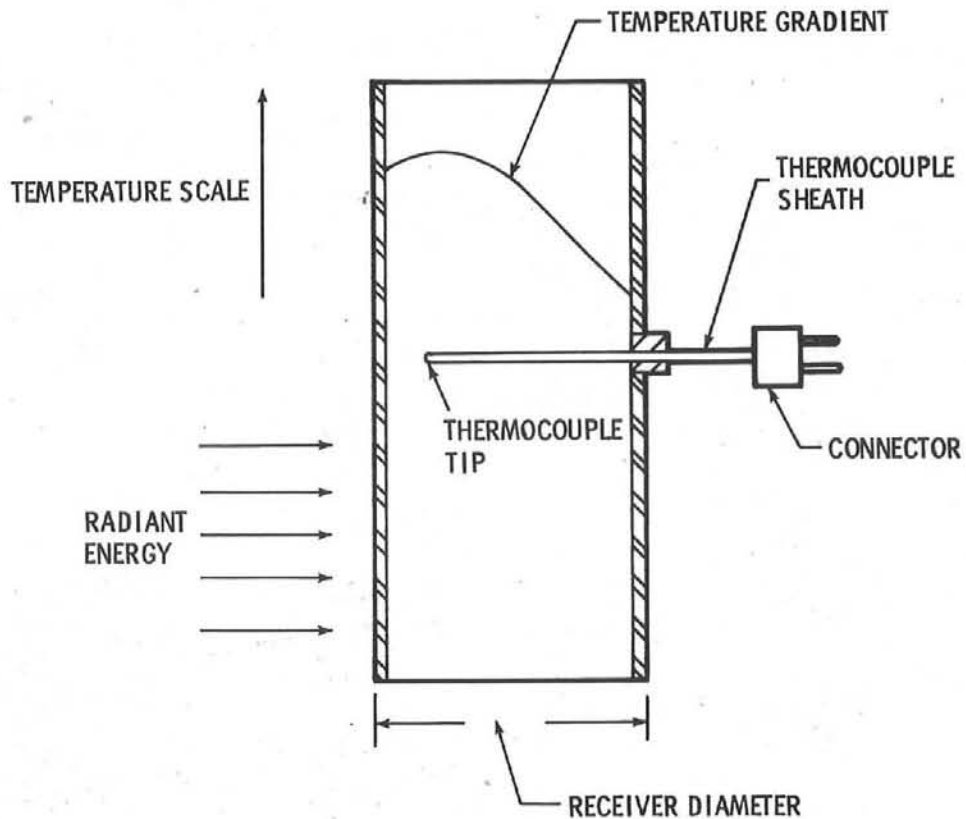


Figure 55. Predicted Temperature Gradient in an Asymmetrically Heated Receiver Carrying Therminol

The amount of energy collected is determined by measuring mass rate of flow and change in bulk temperature. A small error in either parameter can have a significant effect on the calculated efficiency of the collector.

At the beginning of this reporting period Sandia initiated studies to find a turbulence generator, static mixer, or combination of both which would be compatible with small collectors to be tested and would not significantly disturb other test parameters.

## 8.2 Operations

The Kirtland Operation of EG&G, an ERDA contractor, was assigned the task to design and install the instrumentation housing and associated electronics. As of the middle of December 1976, some preliminary work had been done in foundations (Figure 56). All testing was being done on Loop 1 (Figure 57).



Figure 56. Test Loop Foundation Work

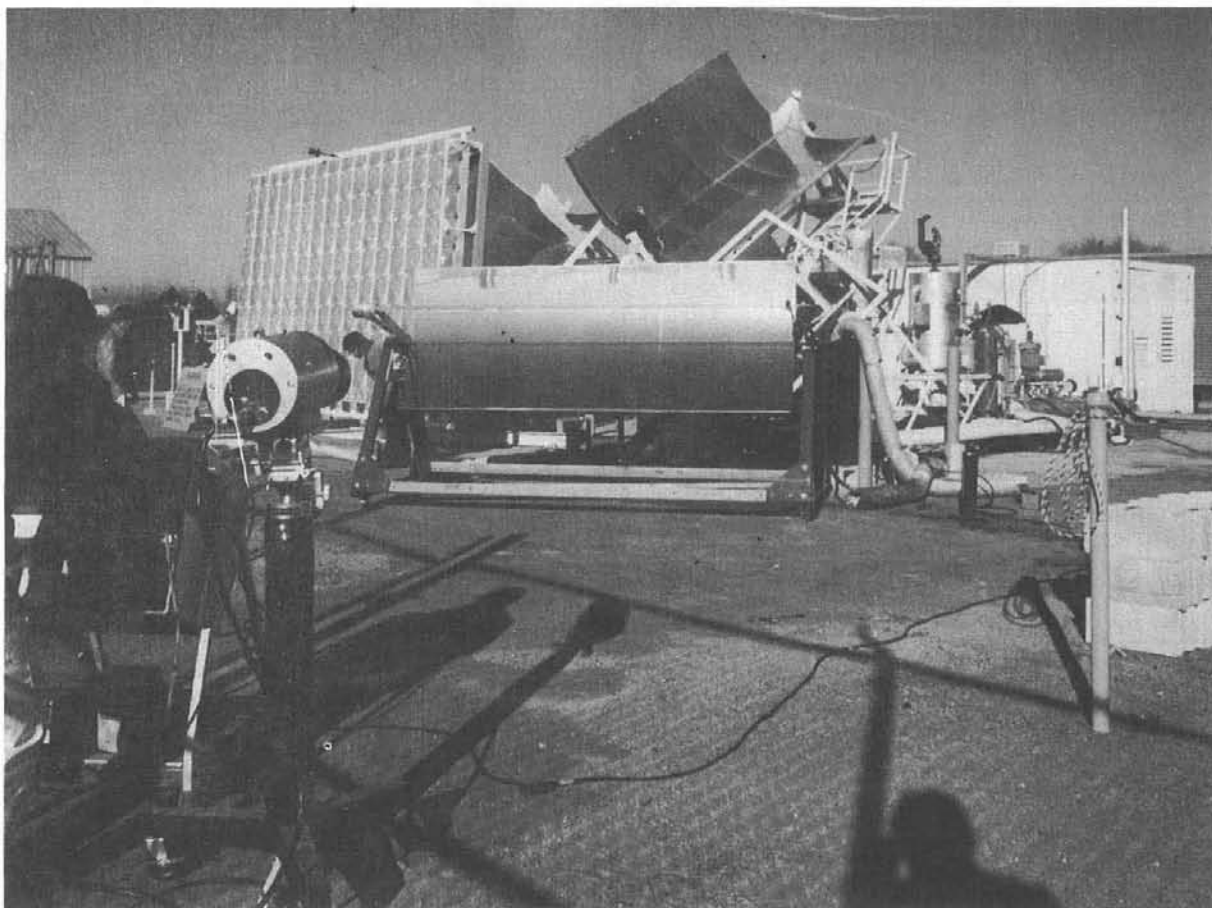


Figure 57. Test Modules on Loop No. 1

On December 16, 1976, authorization was given by Sandia management to procure a building. By January 31, 1977, EG&G had the building in place and started installation of the wiring. Sandia's Plant Engineering revised the utility plan and let contracts to supply power, water and drain to the test loops and to the instrumentation building.

In January 1976 the fluid loop designed and fabricated by Barber-Nichols, Denver, Colorado, to supply high pressure, high temperature water to the Sheldahl receiver arrived. Sheldahl installed the SLATS receiver (Figure 58).

By March 22, 1977, all building was essentially complete, Figure 53.

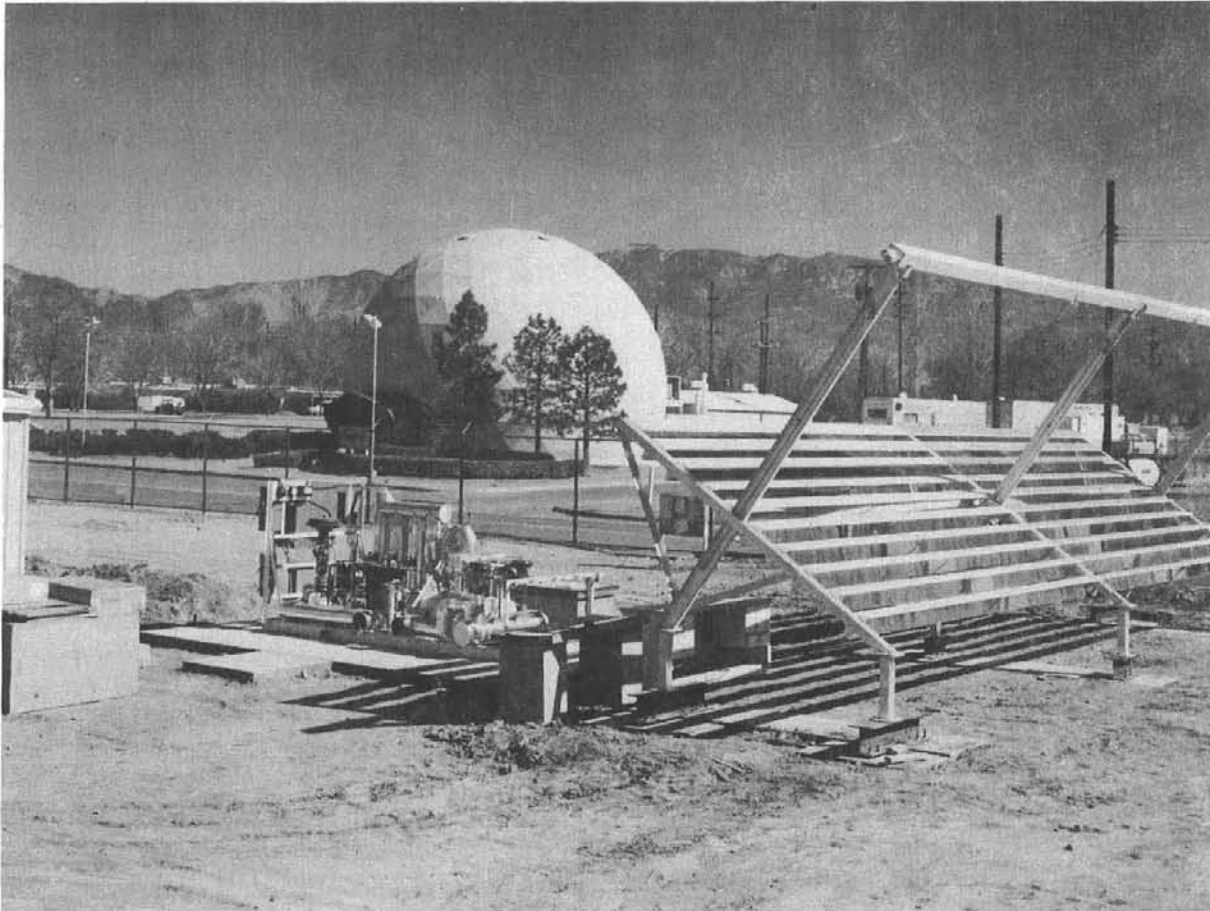


Figure 58. Sheldahl Collector Module on Barber-Nichols Test Loop

A pressure safety analyses report was prepared by the contractor of each individual component (the fluid loop, the high pressure piping to connect the fluid loop to the receiver and the receiver) and reviewed by Sandia. This review uncovered two possible weaknesses:

1. The receiver consists of two parallel lengths of pipe connected at the east end by a "U" joint. The supplier was unable to provide complete details on the method used to fabricate the "U" joint. It was assumed by Sandia that the "U" joint was bent to shape from straight pipe and that the bend radius caused thinning in excess of that allowed by ANSI Code B31. 1. Sandia designed and installed a deflector to control anything which would be released if the "U" joint failed. In fairness to the supplier, his quality control records indicate a competence and thoroughness which make it most likely that the "U" joint was fabricated so as to meet or exceed all ANSI codes.

2. The material of the flanges of the flow meters was 304 stainless steel instead of carbon steel per ASTM A-105 as specified. The stainless steel flanges are capable of only 13 MPa (1875 psi) maximum allowable working pressure (MAWP) at 343°C (650°F) instead of the required 18.3 MPa (2650 psi). Fortunately, the nature of the saturation pressure-temperature curve for water (Figure 31) is such that the system is derated only slightly in temperature to 312°C (595°F). In the meantime, the supplier is rushing to produce new flow meters with flanges of the correct material.

The fluid loop was proof pressure tested by Barber-Nichols prior to shipment at 27.5 MPa (4,000 psi) and 338°C (640°F). The remainder of the system was proxy pressure tested at 27.5 MPa and ambient temperature on April 11, 1977, at Sandia.

On April 18, 1977, Sheldahl obtained the first data point, 46% efficiency with an input temperature of 135°C, a flow rate of 30 liters/second and a pressure of 4.2 MPa. This first effort at testing revealed the need for considerable adjustment of equipment. More accurate results will be included in the next semiannual report.

In October 1976 a simulated Raytheon receiver was tested on Sandia's 1.2 m (4 ft) x 1.8 m (6 ft) N-S parabolic reflector, Figure 59. The test was to determine whether there might be incompatibility between Therminol 66 and Zirconium copper, which is the intended material for the receivers of the parabolic dishes to be installed by Raytheon at Sandia in 1977. No incompatibility was detected.

In December 1976 Sandia tested for Acurex Aerotherm a 1.2 x 4.7 m (4 ft x 10 ft) parabolic trough collector with an Alzac reflector surface, Figure 60, which uses water to 93°C (200°F) as the heat transfer medium. Acurex decided not to add antifreeze to the water to avoid disturbing heat transfer characteristics. Initial tests indicated the need for a modified receiver tube, which was installed.

Further testing was interrupted by freezing temperature and intermittent cloudiness. It was decided to prevent freezing by circulating water at 15°C (60°F) through the receiver at night. On the night of December 22, 1976, however, the temperature dropped to -23°C (-10°F). The system froze in spite of the circulating heated water.

The collector was returned to Acurex in January 1977. It was modified in accordance with information acquired by the test. Acurex reports efficiencies of 65 to 70% following these modifications based on tests at its plant.

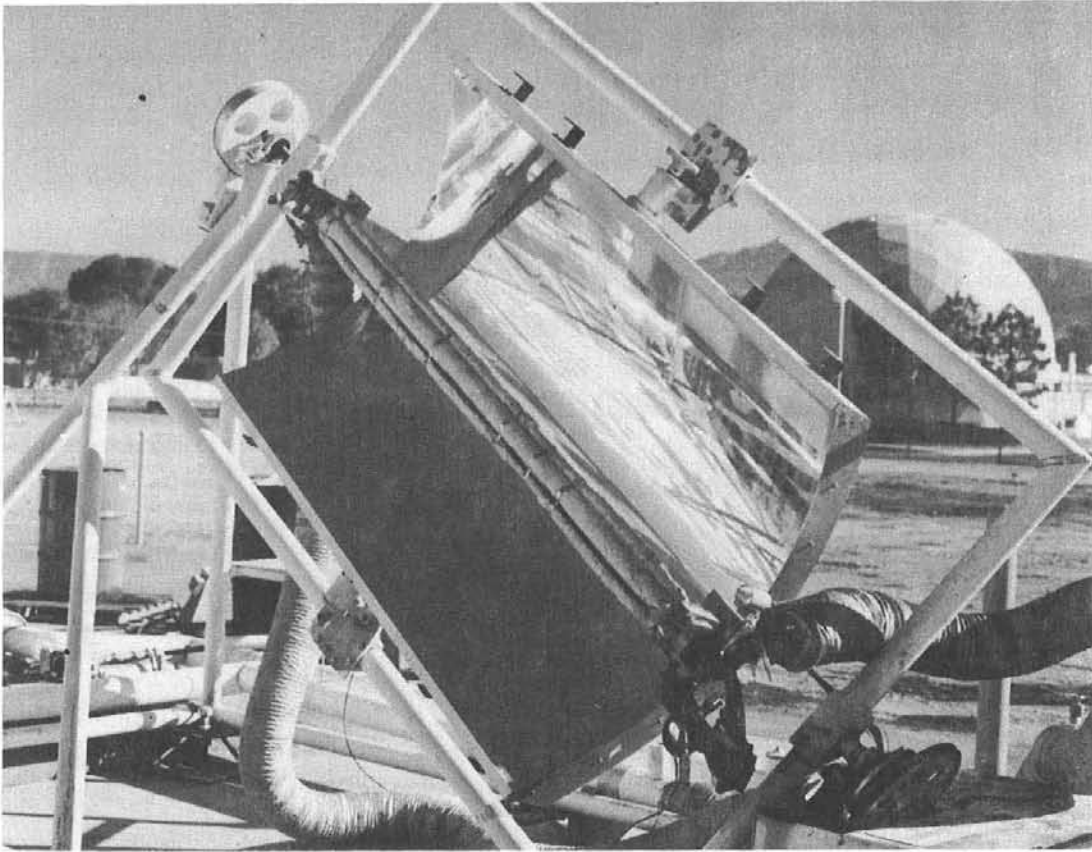


Figure 59. Simulated Raytheon Receiver Under Test on Sandia Collector

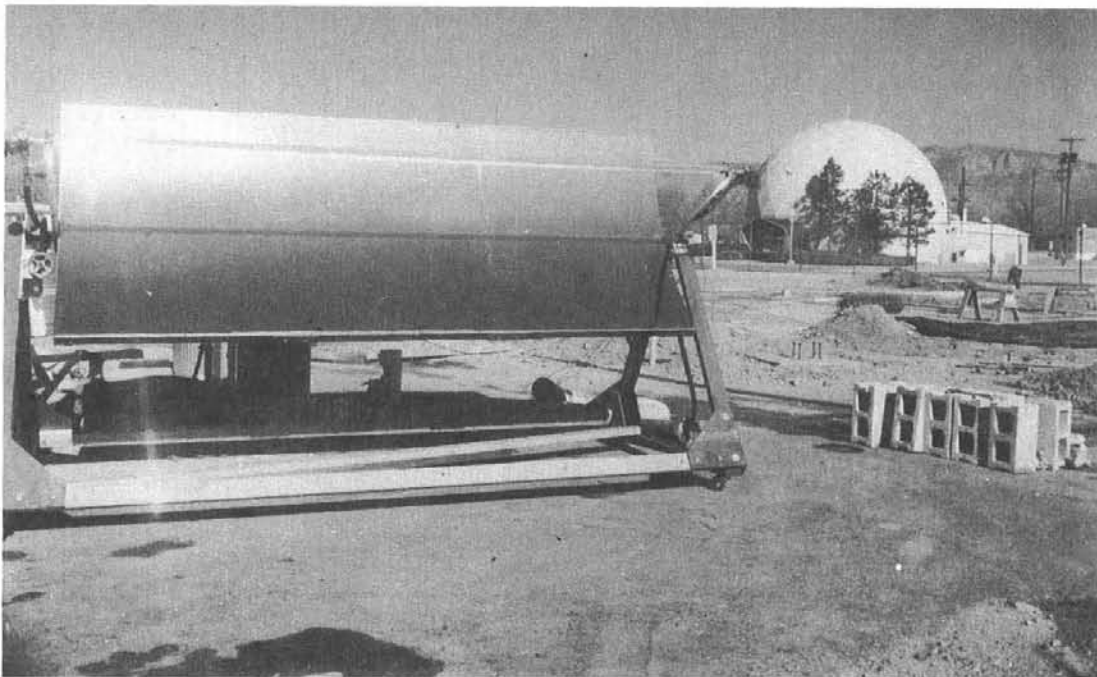


Figure 60. Acurex-Aerotherm Collector

In January 1977 the water on Loop 1 was replaced with Therminol 66. A week was spent circulating Therminol at 140°C (300°F) to boil off all water left from the previous test. At the end of this period a large slug of water (apparently from melting ice) entered the heater tank of the fluid loop, turned to steam, and caused all three safety valves to be activated. This fact is mentioned because it illustrates two points. First, water is difficult to use as a heat transfer fluid in climates where freezing temperatures are expected. Second, it is not profitable to switch water and heat transfer oils in test systems.

Following the above incident with the water, the fluid loop was used to calibrate a three-way self-activating Taylor-Sybron valve for the ERDA/New Mexico irrigation project.

Figure 61 shows the test schedule for the remainder of CY1977.

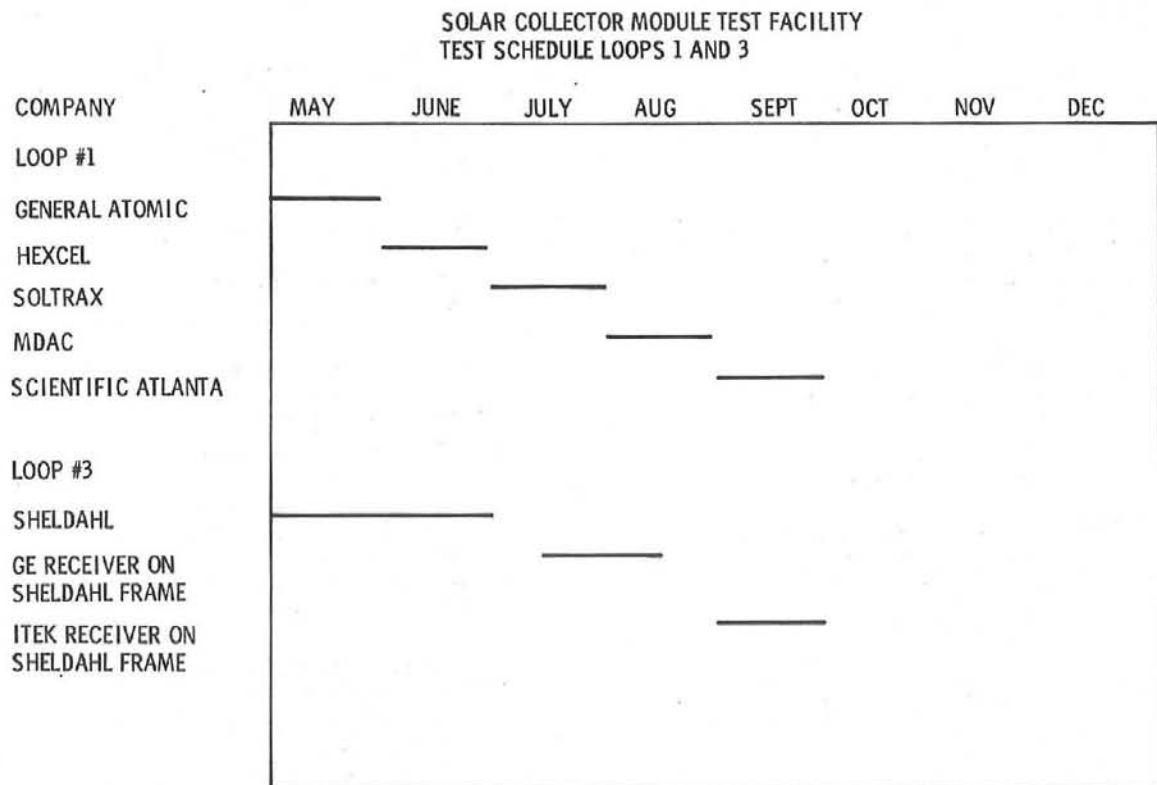


Figure 61. CY1977 CMTF Test Schedule

DISTRIBUTION:  
TID-4500-R65, UC-62 (298)

American Gas Association  
1515 Wilson Boulevard  
Arlington, VA 22209  
Attn: P. Susey

Argonne National Laboratory (3)  
9700 South Cass Ave.  
Argonne, IL 60439  
Attn: M. L. Kyle  
Office of the Director  
S. Zwerdling  
Director of Solar Energy Programs  
A. Michaels  
National Science Div.

Battelle Memorial Institute  
Pacific Northwest Laboratory  
P. O. Box 999  
Richland, WA 99352  
Attn: K. Drumheller

Brookhaven National Laboratory  
Associated Universities, Inc.  
Upton, LI, NY 11973  
Attn: J. Blewett

University of Delaware  
Institute of Energy Conversion  
Newark, DE 19711  
Attn: K. W. Boer

Edison Electric Institute  
90 Park Avenue  
New York, NY 10016  
Attn: L. O. Elsaesser  
Director of Research

US Energy Research and Development Adm. (17)  
Solar Energy Division  
20 Massachusetts Ave.  
Washington, DC 20545  
Attn: H. Marvin  
R. Blieden  
G. Kaplan (10)  
S. Gronich  
J. Rannels  
L. McLamed  
C. J. Swet  
S. Sergeant

US Energy Research and Development Adm. (5)  
Albuquerque Operations Office  
P.O. Box 5400  
Albuquerque, NM 87115  
Attn: D. L. Krenz  
D. K. Nowlin (3)  
J. R. Roder

Envirodynamics, Inc.  
1 North Park East  
Dallas, TX 75231  
Attn: J. E. Guthrie

Energy Institute  
1700 Las Lomas  
Albuquerque, NM 87131  
Attn: T. T. Shisman

Environmental Factors and Public Utilities Div.  
Department of Housing and Urban Development  
Washington, DC 20410  
Attn: A. R. Siegel, Director

University of Idaho  
Moscow, ID 83843  
Attn: H. Silha

Deputy to the Science Advisor  
U. S. Department of Interior  
Room 5204  
Washington, DC 20204  
Attn: M. Prochnik

Intertechnology Corporation  
Box 340  
Warrenton, VA 22186  
Attn: G. C. Szego, President

Lone Star Gas Company  
901 S. Harwood St.  
Dallas, TX 75201  
Attn: L. H. Sutherland

University of California  
Lawrence Livermore Laboratory  
P. O. Box 808  
Livermore, CA 94550  
Attn: W. C. Dickinson

Congressional Research Service  
Library of Congress  
Washington, DC 20540  
Attn: H. Bullis  
Science Policy Division

Midwest Research Institute  
425 Volker Blvd.  
Kansas City, MO 64110  
Attn: J. O. Bradley

New Mexico Solar Energy Association  
P.O. Box 2004  
Santa Fe, NM 87501

New Mexico State University  
Las Cruces, NM 88001  
Attn: R. L. San Martin

DISTRIBUTION: (cont)

University of New Mexico  
Department of Mechanical Engineering  
Albuquerque, NM 87113  
Attn: W. A. Cross  
For: M. W. Wilden

Northern Natural Gas Co.  
2223 Dodge St.  
Omaha, NB 68102  
Attn: J. M. De La Castro

Oak Ridge National Laboratory (2)  
P. O. Box Y  
Oak Ridge, TN 37830  
Attn: J. Johnson  
R. Pearlstein

Office of Science and Technology  
Executive Office of the President  
Washington, DC 20506  
Attn: R. Balzhizer

Office of Technology Assessment  
Old Immigration Building, Rm 722  
119 D. Street, NE  
Washington, DC 20002  
Attn: R. Larsen

Jet Propulsion Laboratory  
Bldg 277 Rm 201  
4800 Oak Grove Dr.  
Pasadena, CA 91103  
Attn: V. C. Truscello

Omaha Public Power District  
1623 Harney  
Omaha, NB 68102  
Attn: A. R. Spangler

The Pentagon  
Room 3E114, Mail Stop 103  
Washington, DC 20540  
Attn: G. Dorough  
Deputy Director for Research  
and Advanced Technology

Raytheon, Inc.  
Missile System Division  
Spencer Laboratories  
Wayside Avenue  
Burlington, MA 01803  
Attn: L. Paradis

Southern California Gas Co.  
P. O. Box 3249  
Terminal Annex  
Los Angeles, CA 90051  
Attn: S. Cunningham

Southern Union Gas Company  
Fidelity Union Tower Building  
Room 1537  
1507 Pacific Avenue  
Dallas, TX 75201  
Attn: J. O. Carnes

Gas Company of New Mexico  
723 Silver SW  
Albuquerque, NM 87103  
Attn: B. D. Daugherty

Sundstrand Electric Power  
4747 Harrison Avenue  
Rockford, IL 61101  
Attn: A. W. Adam

Carroll V. Kroeger, Sr.  
Director, Tennessee Energy Office  
Suite 250  
Capitol Hill Bldg.  
Nashville, TN 37219

Watt Engineering Ltd  
RR 1, Box 183 1/2  
Cedaredge, CO 81413  
Attn: A. D. Watt

Texas Electric Service Co.  
P. O. Box 970  
Fort Worth, TX 76101  
Attn: J. A. Harris  
Marketing Services Manager

W. G. Newton  
General Manager  
South Plains Electric Coop. Inc.  
P. O. Drawer 1830  
Lubbock, TX 79408

Messr Bernard Devin  
Chef de Projet Solaire  
Cen Saclay  
B. P. No. 2  
91190 GIF SUF YVETTE

Larry Smith  
HLO Smith  
ICI  
United States Inc.  
P. O. Box 6008  
Chatanooga, TN 37401

Gus Hutchison  
Solar Kinetics Inc.  
147 Parkhouse St.  
P. O. Box 10764  
Dallas, TX 75207

DISTRIBUTION: (cont)

Gerald Katz  
8116 Appleton Ave.  
Milwaukee, WI 53218

Del Manufacturing Co.  
905 Monterey Pass Road  
Monterey Park, CA 91754  
Attn: M. M. Delgado

Soltrax, Inc.  
720 Rankin Rd., NE  
Albuquerque, NM 87107  
Attn: C. A. Coonce  
Vice President, Research

Honorable Manuel Lujan, Jr.  
1323 Longworth Building  
Washington, DC 20515

Honorable Harold Runnels  
1535 Longworth Building  
Washington, DC 20515

Honorable Pete V. Domenici  
4103 New Senate Building  
Washington, DC 20510

Honorable Harrison H. Schmitt  
1909 Wyoming NE  
Albuquerque, NM 87112

Richard Waterman  
Solar Intel  
P. O. Box 38  
Riverton, CT 06065

Steve Tipaldi  
General Delivery Capitala  
Capitala, CA 95060

Pat Lynch  
318 Rackley Bldg.  
Pennsylvania State University  
University Park, PA 16002

Mitchell Knight  
372 Bluff View Drive  
Largo, FL 33540

D. J. McCann  
Energy Research Center  
Department of Chemical Engineering  
University of Sydney  
Australia 2006

Krishan D. Mahnan  
Head, Mech. Eng. Dept.  
College of Agricultural Eng.  
Punjab Agricultural University  
Ludhiana, Punjab, INDIA

Bill Laughran  
Hi G Research & Eng.  
244 Woodland Avenue  
Bloomfield, CT 06002

Ed Diamond  
Manager, Advanced Concepts  
Grumman Corporation  
4175 Veterans Memorial Highway  
Ronkonkoma, NY 11779

A. J. Poche  
General Electric Co.  
P. O. Box 8661  
Philadelphia, PA 19101

B. P. Gupta  
MS MNI7-T789  
Honeywell, Inc.  
2600 Ridgeway Parkway  
Minneapolis, MN 55413

Darwin Vexler  
Chemical Projects Associates, Inc.  
30 Rockefeller Plaza  
New York, NY 10020

National Aeronautics Space Adm.  
Lewis Laboratory  
21000 Brook Park Road  
Cleveland, OH 44135  
Attn: R. Dusche, Mail Stop 500-204

American Technological University  
P. O. Box 1416  
Killeen, TX 76541  
Attn: J. Kincel, Director  
Solar Total Energy Program

Sun Gas Co.  
2 No. Pk. E  
P. O. Box 20  
Dallas, TX 75231  
Attn: R. Clarke

Sun Search Inc.  
669 Boston Post Road  
Guilford, CT 06437  
Attn: M. Barber, Jr.

Sheldahl Inc.  
21405 Hamburg Avenue  
Lakeville, MN 55044  
Attn: J. Menke

Barber-Nichols Engineering Co.  
6325 W. 55th Avenue  
Arvada, CO 80002  
Attn: B. Barber

DISTRIBUTION: (cont)

Solar Dynamics Inc.  
200 Jefferson NE  
Albuquerque, NM 87108  
Attn: R. Bell

Stanford Research Institute  
Menlo Park, CA 94025  
Attn: A. J. Slemmons

Commanding General  
White Sands Missile Range, NM 88002  
Attn: STEWS-TE-NT  
M. Squires

1100 C. D. Broyles  
Attn: J. D. Kennedy, 1110  
G. E. Hansche, 1120

1260 K. J. Touryan  
1262 H. C. Hardee  
1280 T. B. Lane  
1284 R. T. Othmer  
1300 D. B. Shuster  
1330 R. C. Maydew  
1333 S. McAlees, Jr.  
1354 G. W. Gobeli  
2300 J. C. King  
2320 K. L. Gillespie  
Attn: C. M. Gabriel, 2323  
L. W. Schulz, 2324

2323 S. B. Martin  
2530 M. K. Parsons  
3700 L. S. Conterno  
3720 L. E. Fuller (3)  
Attn: E. G. Dyllo, 3721

5000 A. Narath  
Attn: J. K. Galt, 5100

5110 F. L. Vook  
5130 G. A. Samara  
5150 J. E. Schirber  
5200 E. H. Beckner  
5231 J. H. Renken  
5420 J. V. Walker  
5700 J. H. Scott  
5710 G. E. Brandvold  
5712 J. A. Leonard (200)  
5713 J. V. Otts  
5714 R. P. Stromberg  
5715 R. H. Braasch  
5719 D. G. Schueler  
5730 H. M. Stoller  
5735 M. M. Newsom  
5740 V. L. Dugan  
5800 R. S. Claassen  
Attn: R. L. Schwoebel, 5820  
5830 M. J. Davis  
Attn: D. M. Mattox, 5834  
5840 H. J. Saxton  
Attn: J. N. Sweet, 5842  
F. P. Gerstle, 5844  
R. J. Eagan, 5845  
E. K. Beauchamp, 5846

8100 L. Gutierrez  
Attn: A. C. Skinroad, 8132  
8180 C. S. Selvage  
8313 R. W. Mar  
Attn: T. T. Bramlette, 8313  
9300 W. A. Gardner  
9330 A. J. Clark, Jr.  
9340 W. E. Caldes  
Attn: J. L. Mortley, 9344  
9400 H. E. Lenander  
9410 R. L. Brin  
Attn: R. K. Petersen, 9412  
9515 J. T. Hillman  
9700 R. E. Hopper  
Attn: H. H. Pastorius, 9740  
R. W. Hunnicutt, 9750  
9742 M. H. Wempe  
6011 G. C. Newlin  
8266 E. A. Aas  
3141 C. A. Pepmueller (Actg) (5)  
3151 W. L. Garner (3)  
For ERDA/TIC (Unlimited Release)